RECENT "THEORY" RESULTS ON CEνNS

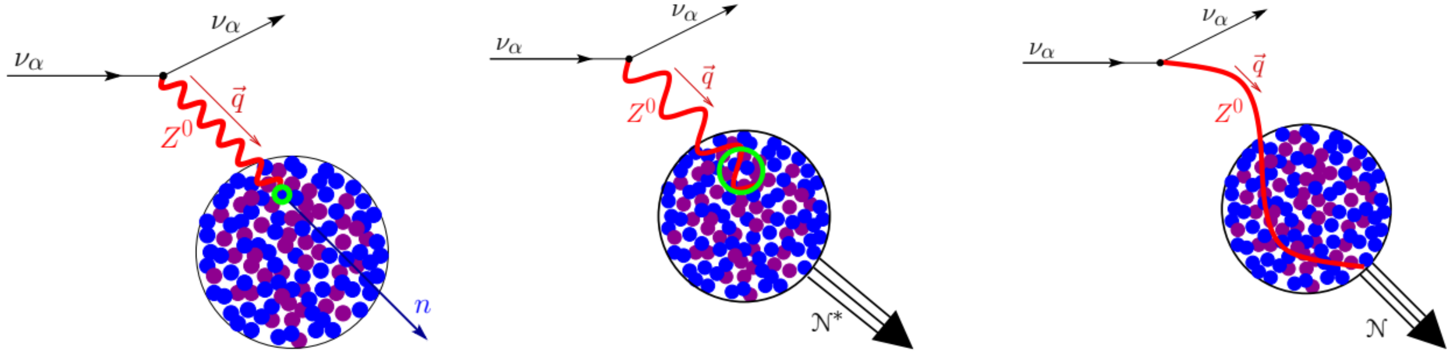

For a recent review see Europhysics Letters, Volume 143, Number 3, 2023 (EPL 143 34001), arXiv:2307.08842v2

Matteo Cadeddu
matteo.cadeddu@ca.infn.it

NOW 2024
Neutrino Oscillation Workshop

In collaboration with
M. Atzori Corona, N. Cargioli, F. Dordei, C. Giunti, C. Ternes, Y. Li

Coherent elastic neutrino nucleus scattering (aka CEνNS)

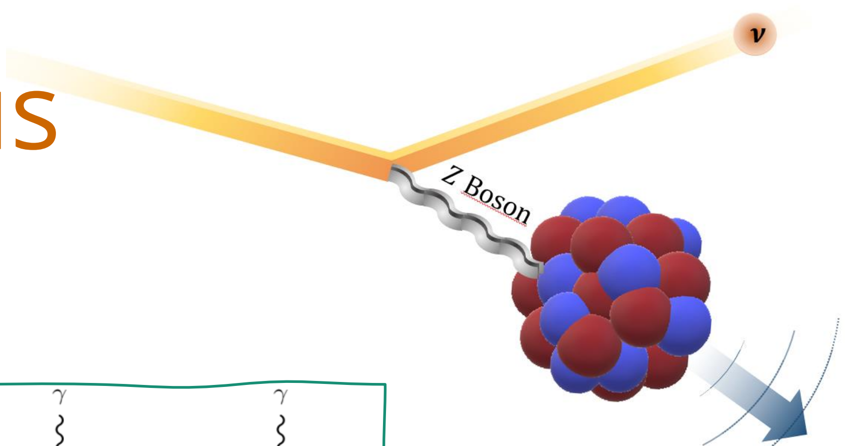

+ A pure weak neutral current process

$$\boxed{\frac{d\sigma_{\nu_\ell\text{-}\mathcal{N}}}{dT_{\rm nr}}(E,T_{\rm nr}) = \frac{G_{\rm F}^2 M}{\pi}\left(1-\frac{MT_{\rm nr}}{2E^2}\right)(Q^V_{\ell,\rm SM})^2}$$

+ Weak charge of the nucleus

$$Q^V_{\ell,\rm SM} = \Big[\underbrace{g_V^p(\nu_\ell)\,Z F_Z\left(|\vec{q}|^2\right)}_{\text{protons}} + \underbrace{g_V^n N F_N\left(|\vec{q}|^2\right)}_{\text{neutrons}}\Big]$$

In general, in a weak neutral current process which involves nuclei, one deals with **nuclear form factors** that are different for protons and neutrons and cannot be disentangled from the neutrino-nucleon couplings!

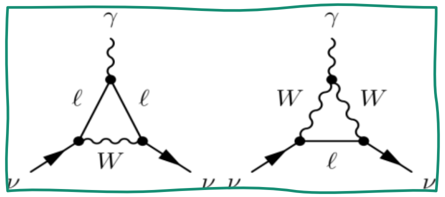

J. Erler and S. Su. *Prog. Part. Nucl. Phys.* 71 (2013). arXiv:1303.5522 & PDG2023 and **M. Atzori Corona et al. arXiv:2402.16709**

+ Neutrino-nucleon tree-level couplings

$$g_V^p = \frac{1}{2} - 2\sin^2(\vartheta_W) \cong \mathbf{0.02274}$$

$$g_V^n = -\frac{1}{2} = -0.5$$

+ Radiative corrections are expressed in terms of WW, ZZ boxes and the neutrino charge radius diagram → Flavour dependence

$$g_V^p(\nu_e) \simeq 0.0381,\ g_V^p(\nu_\mu) \simeq 0.0299 \quad g_V^n \simeq -0.5117$$

Nuclear physics, but since $g_V^n \approx -0.51 \gg g_V^p(\nu_\ell) \approx 0.03$ neutrons contribute the most

$$\boxed{\frac{d\sigma}{dE_r} \propto N^2}$$

What we can learn from CEνNS

M. Cadeddu et al., JHEP 01 (2021) 116, arXiv:2008.05022

O. G. Miranda et al., JHEP 05 (2020) 130, arXiv:2003.12050

M. Atzori Corona et al., JHEP 05 109 (2022), arXiv:2202.11002

C. Giunti, *PRD* 101 (2020) 3, 035039, arXiv:1909.00466

D. K. Papoulias and T. S. Kosmas, PRD 97, 033003 arxiv:1711.09773

D. A. Sierra et al., PRD 98, 075018 (2018) arXiv:1806.07424

L. J. Flores et al., JHEP 06 (2020) 045, 2002.12342

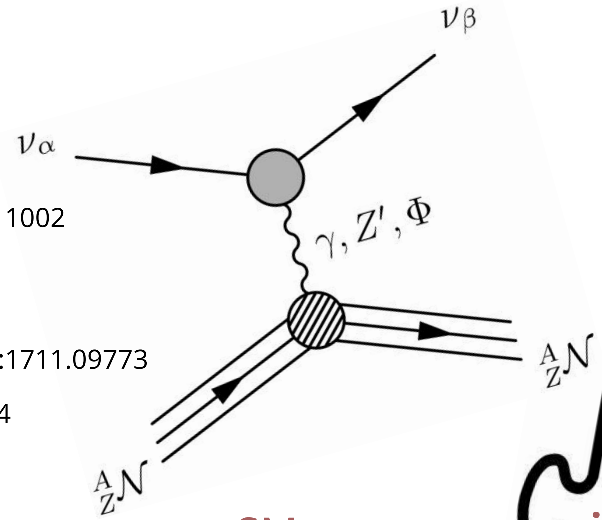

O. G. Miranda et al., JHEP 05 (2020) 130, arXiv:2003.12050

B. Dutta et al., Phys. Rev. Lett. 123, 061801 (2019)

O. G. Miranda et al., JHEP 07 (2019) 103, arXiv: 1905.03750

D. Aristizabal Sierra et al., Phys. Rev. D 98, 075018 (2018)

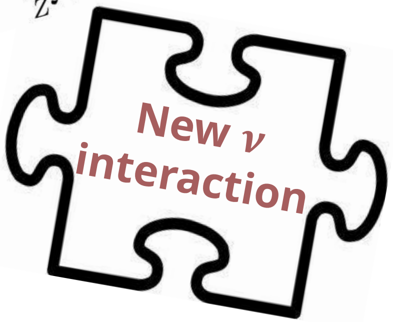

Neutrino energy

Mass of the nucleus

SM vector proton coupling

SM vector neutron coupling

$$\frac{d\sigma^{CE\nu NS}(E_\nu, E_r)}{dE_r} \cong \frac{G_F^2\, m_N}{\pi}\left(1-\frac{m_N E_r}{2E_\nu^2}\right)\left[g_V^p\left(\sin^2(\vartheta_W)\right) Z\, F_Z(|\vec{q}|^2) + g_V^n\, N\, F_N(|\vec{q}|^2)\right]^2 + \dots$$

Weinberg angle

Proton Form Factor

Neutron Form Factor

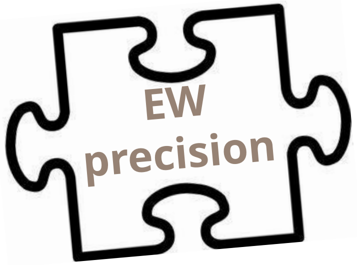

D. Papoulias et al., PLB 800 (2020) 135133, arXiv:1903.03722

Coloma et al., JHEP 08 (2020) 08, 030, arXiv:2006.08624

D. A. Sierra et al., JHEP 1906:141 (2019) arXiv: 1902.07398

B. Canas et al., PRD 101, 035012 (2020), arXiv:1911.09831

K. Patton, J. Engel, G. C. McLaughlin, and N. Schunck, Phys. Rev. C 86, 024612 (2012).

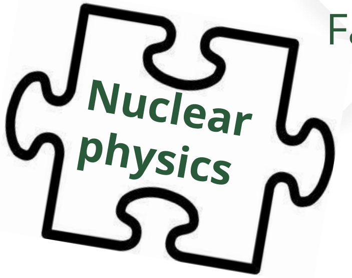

CEνNS players

$$\pi^+ \to \mu^+ + \nu_\mu$$ Prompt component

$$\mu^+ \to e^+ + \bar{\nu}_\mu + \nu_e$$ Delayed component

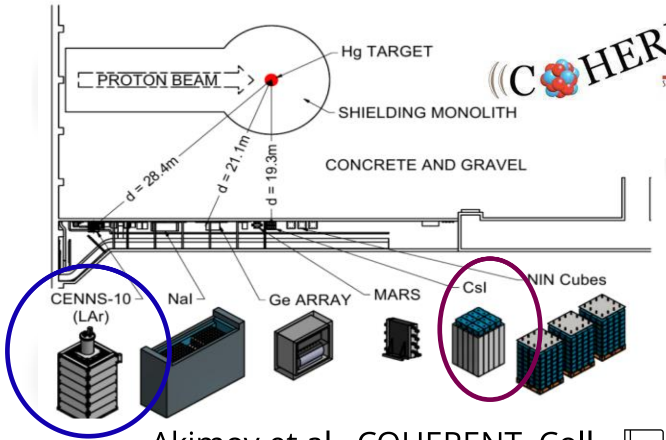

COHERENT CsI

D. Akimov et al. **Science** 357.6356 (2017)

+ Updated in Akimov et al., PRL 129, 081801 (2022)

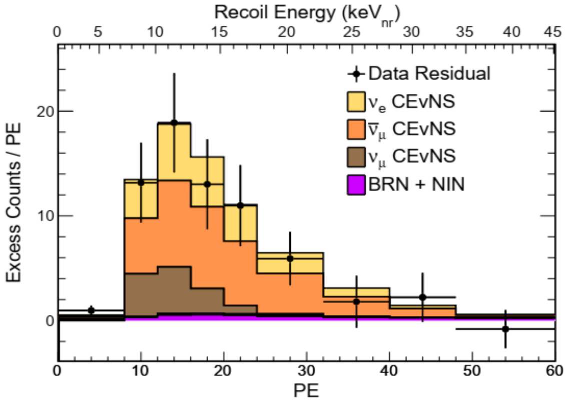

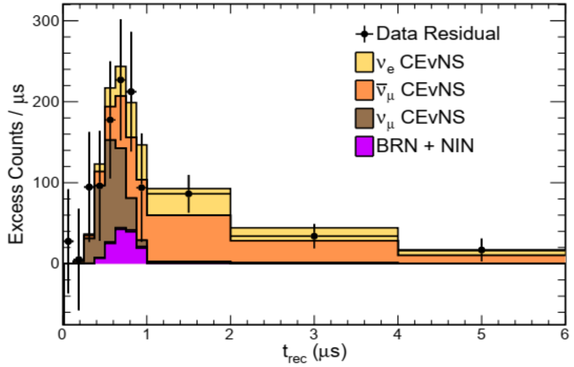

COHERENT Ar

Akimov et al., COHERENT Coll. PRL 126, 01002 (2021)

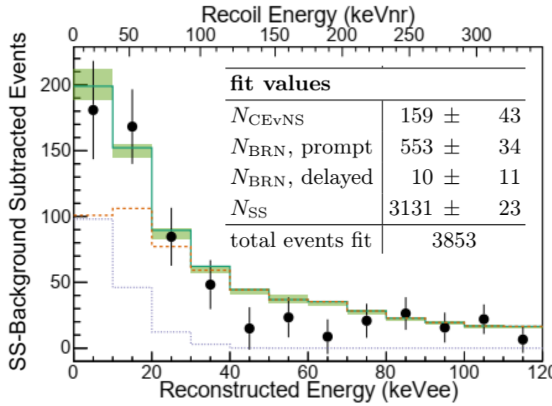

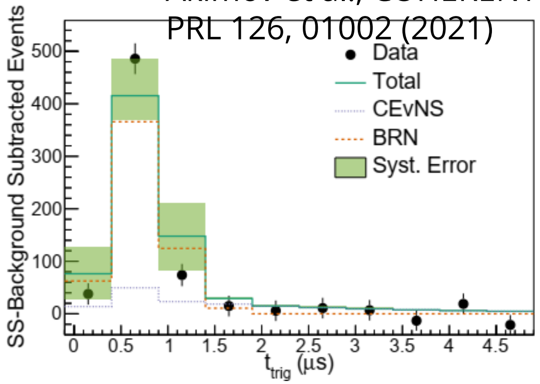

NCC- 1701 (Dresden-II)

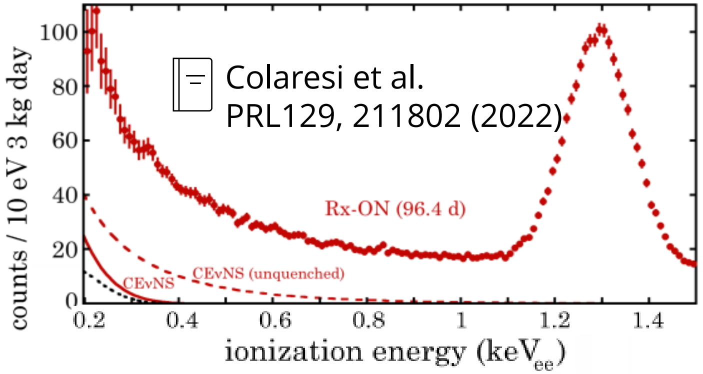

+ 3 kg germanium detector @DRESDEN reactor. A strong preference for the presence of CEvNS is found.

NEW COHERENT Ge-Mini result on germanium
arXiv:2406.13806 Null Hypothesis rejected at 3.9σ

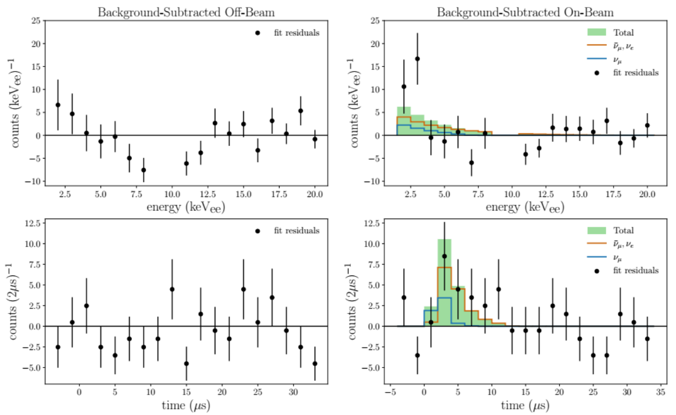

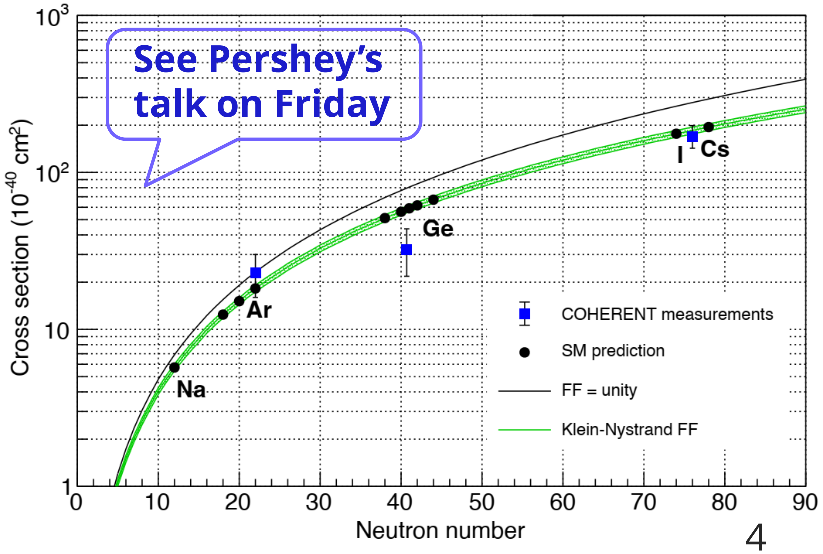

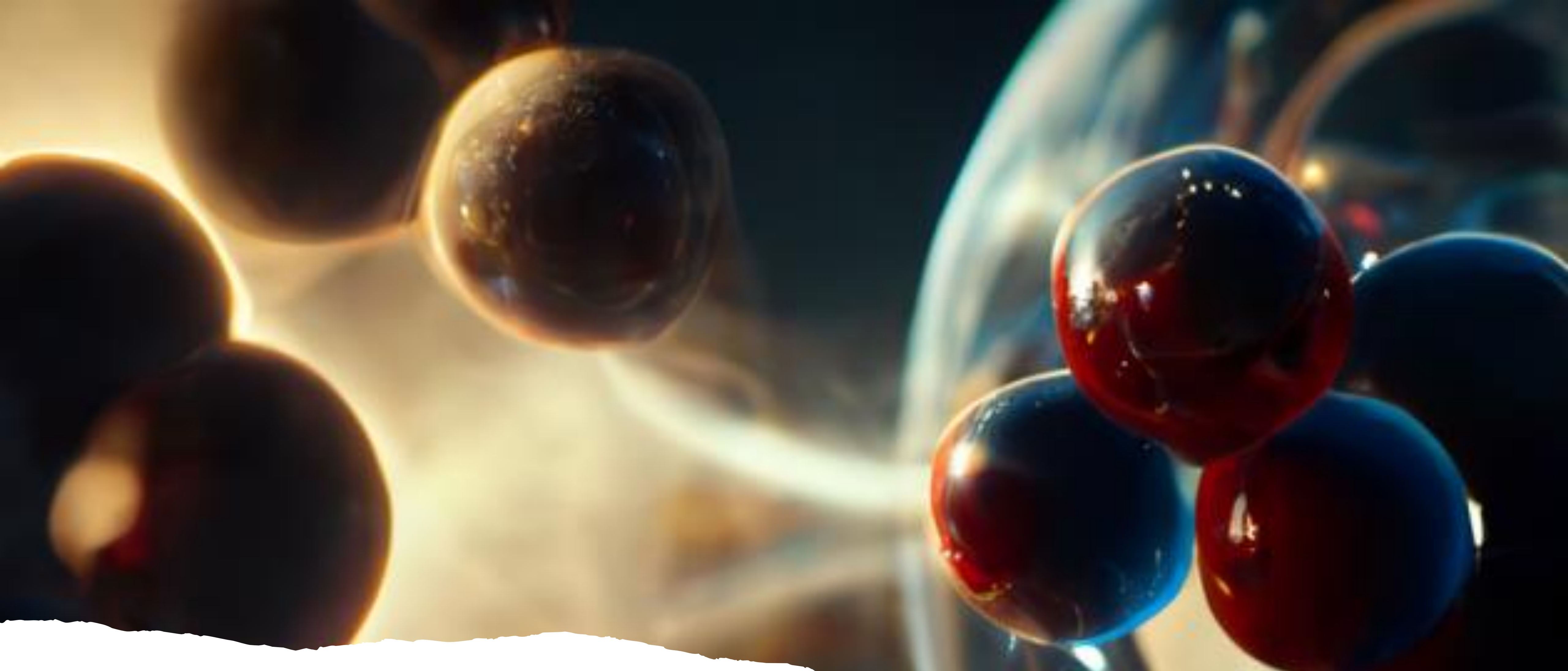

Standard Model physics

M. Atzori Corona et al. Refined determination of the weak mixing angle at low energy, arXiv:2405.09416 (2024)

Neutron form factor dependence in CEνNS cross section

$$\frac{d\sigma^{CE\nu NS}(E_\nu, E_r)}{dE_r} \cong \frac{G_F^2\, m_N}{\pi}\left(1 - \frac{m_N E_r}{2E_\nu^2}\right)\left[g_V^p\left(\sin^2(\vartheta_W)\right) Z\, F_Z(|\vec{q}|^2) + g_V^n\, N\, F_N(|\vec{q}|^2)\right]^2$$

Neutron form factor (R_n) to be fitted

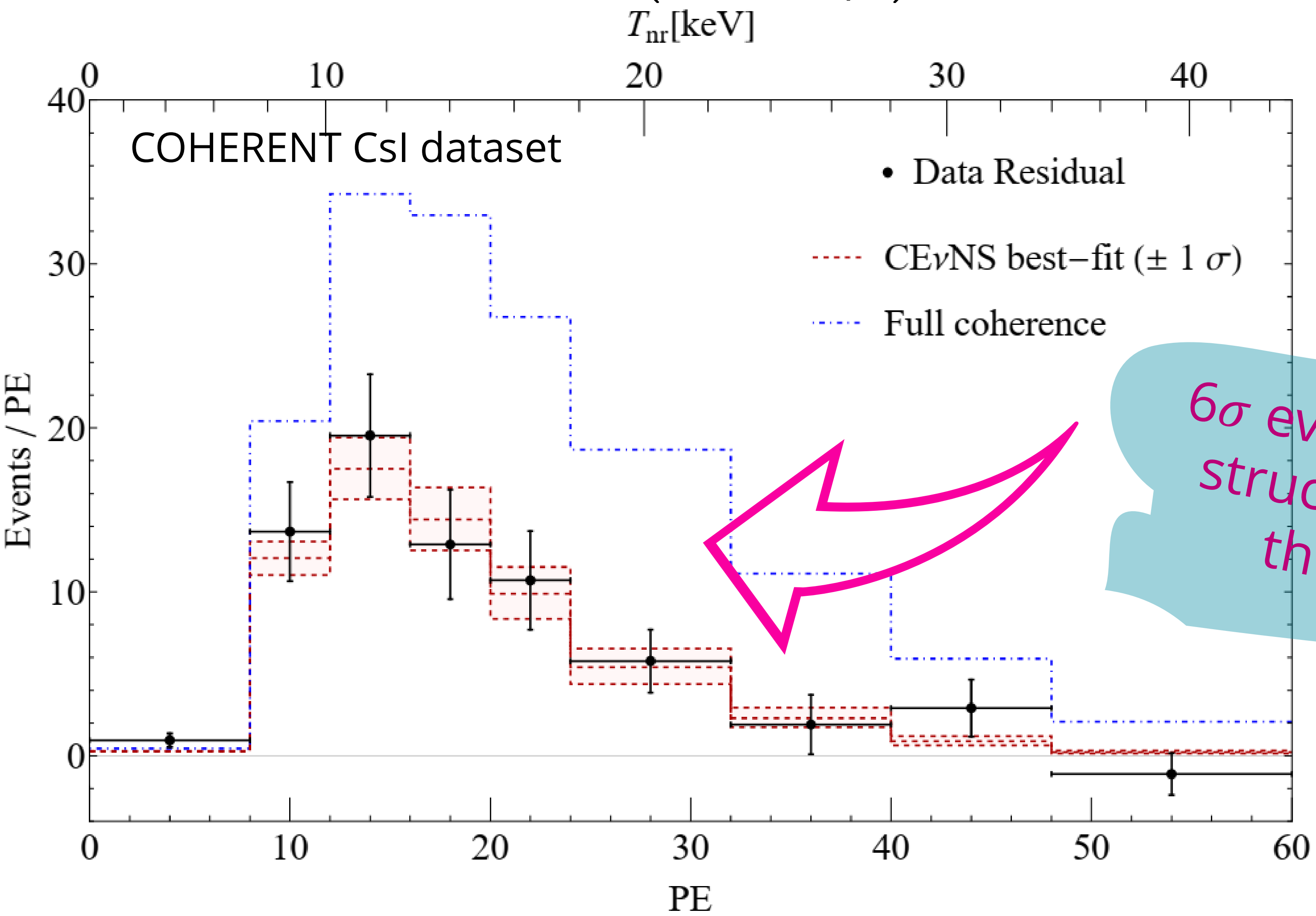

6σ evidence of the nuclear structure suppression of the full coherence!

See also:

Rossi et al. PRD 109, 095044 (2024) arXiv:2311.17168

De Romeri et al. JHEP04(2023)035 arXiv:2211.11905

D. Papoulias et al., PLB 800 (2020) 135133, arXiv:1903.03722

M. Atzori Corona et al., EPJC 83 (2023) 7, 683. ArXiv:2303.09360

The CsI neutron skin fixing $\sin^2(\vartheta_W)$

If we fix the value of $\sin^2\vartheta_W$ at the SM prediction ($0.23863(5)$) then we obtain (1D fit):

M. Atzori Corona et al., EPJC 83 (2023) 7, 683
arXiv:2303.09360

$R_n\ (\mathrm{CsI}) = 5.47 \pm 0.38$ fm

~7% precision

Neutron skin: R_n (CsI)- R_p (CsI)

$\Delta R_{np}(\mathrm{CsI}) = 0.69 \pm 0.38$ fm

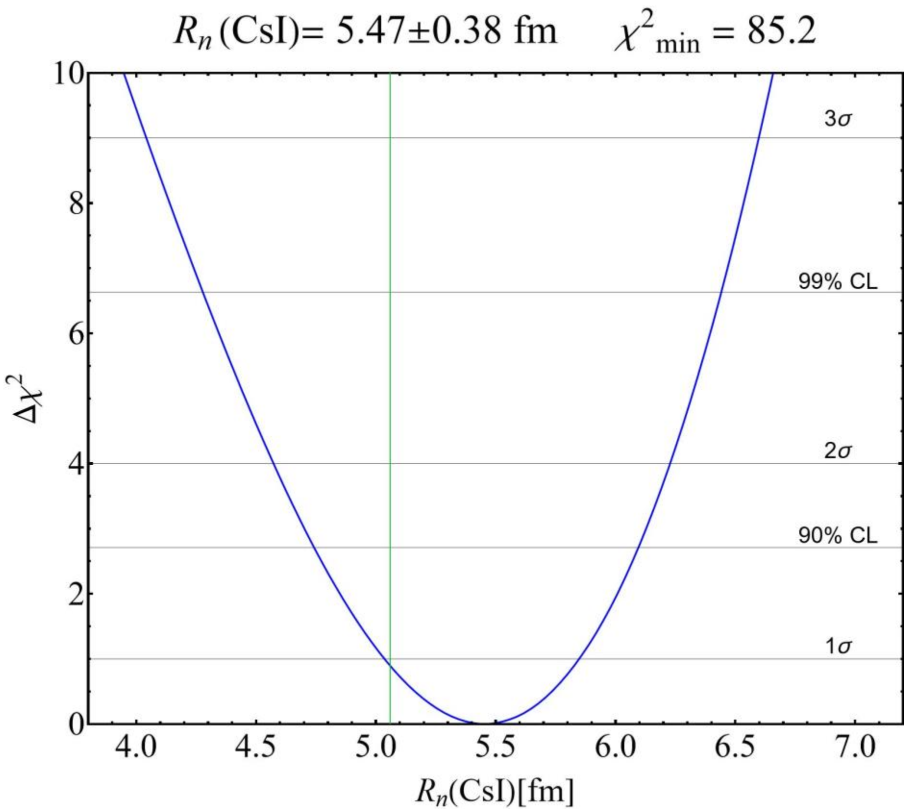

Theoretical values of the neutron skin of Cs and I obtained with nuclear mean field models. The value is compatible with all the models…

$0.12 < \Delta R_{np}^{CsI} < 0.24$ fm

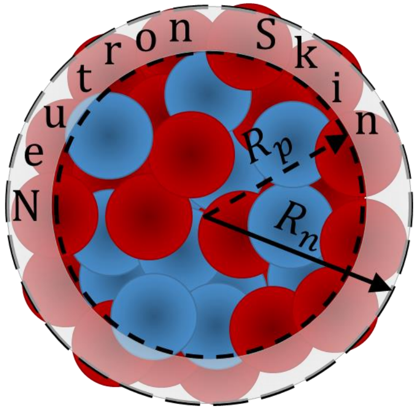

Model	^{127}I						^{133}Cs					
	$R_p^{\rm point}$	R_p	$R_n^{\rm point}$	R_n	$\Delta R_{np}^{\rm point}$	ΔR_{np}	$R_p^{\rm point}$	R_p	$R_n^{\rm point}$	R_n	$\Delta R_{np}^{\rm point}$	ΔR_{np}
SHF SkI3 [81]	4.68	4.75	4.85	4.92	0.17	0.17	4.74	4.81	4.91	4.98	0.18	0.18
SHF SkI4 [81]	4.67	4.74	4.81	4.88	0.14	0.14	4.73	4.80	4.88	4.95	0.15	0.14
SHF Sly4 [82]	4.71	4.78	4.84	4.91	0.13	0.13	4.78	4.85	4.90	4.98	0.13	0.13
SHF Sly5 [82]	4.70	4.77	4.83	4.90	0.13	0.13	4.77	4.84	4.90	4.97	0.13	0.13
SHF Sly6 [82]	4.70	4.77	4.83	4.90	0.13	0.13	4.77	4.84	4.89	4.97	0.13	0.13
SHF Sly4d [83]	4.71	4.79	4.84	4.91	0.13	0.12	4.78	4.85	4.90	4.97	0.12	0.12
SHF SV-bas [84]	4.68	4.76	4.80	4.88	0.12	0.12	4.74	4.82	4.87	4.94	0.13	0.12
SHF UNEDF0 [85]	4.69	4.76	4.83	4.91	0.14	0.14	4.76	4.83	4.92	4.99	0.16	0.15
SHF UNEDF1 [86]	4.68	4.76	4.83	4.91	0.15	0.15	4.76	4.83	4.90	4.98	0.15	0.15
SHF SkM* [87]	4.71	4.78	4.84	4.91	0.13	0.13	4.76	4.84	4.90	4.97	0.13	0.13
SHF SkP [88]	4.72	4.80	4.84	4.91	0.12	0.12	4.79	4.86	4.91	4.98	0.12	0.12
RMF DD-ME2 [89]	4.67	4.75	4.82	4.89	0.15	0.15	4.74	4.81	4.89	4.96	0.15	0.15
RMF DD-PC1 [90]	4.68	4.75	4.83	4.90	0.15	0.15	4.74	4.82	4.90	4.97	0.16	0.15
RMF NL1 [91]	4.70	4.78	4.94	5.01	0.23	0.23	4.76	4.84	5.01	5.08	0.25	0.24
RMF NL3 [92]	4.69	4.77	4.89	4.96	0.20	0.19	4.75	4.82	4.95	5.03	0.21	0.20
RMF NL-Z2 [93]	4.73	4.80	4.94	5.01	0.21	0.21	4.79	4.86	5.01	5.08	0.22	0.22
RMF NL-SH [94]	4.68	4.75	4.86	4.94	0.19	0.18	4.74	4.81	4.93	5.00	0.19	0.19

Weak mixing angle from CEνNS only

$$\frac{d\sigma^{CE\nu NS}(E_\nu, E_r)}{dE_r} \cong \frac{G_F^2\, m_N}{\pi}\left(1 - \frac{m_N E_r}{2E_\nu^2}\right)\left[g_V^p\left(\sin^2(\vartheta_W)\right) Z\, F_Z(|\vec{q}|^2) + g_V^n\, N\, F_N(|\vec{q}|^2)\right]^2$$

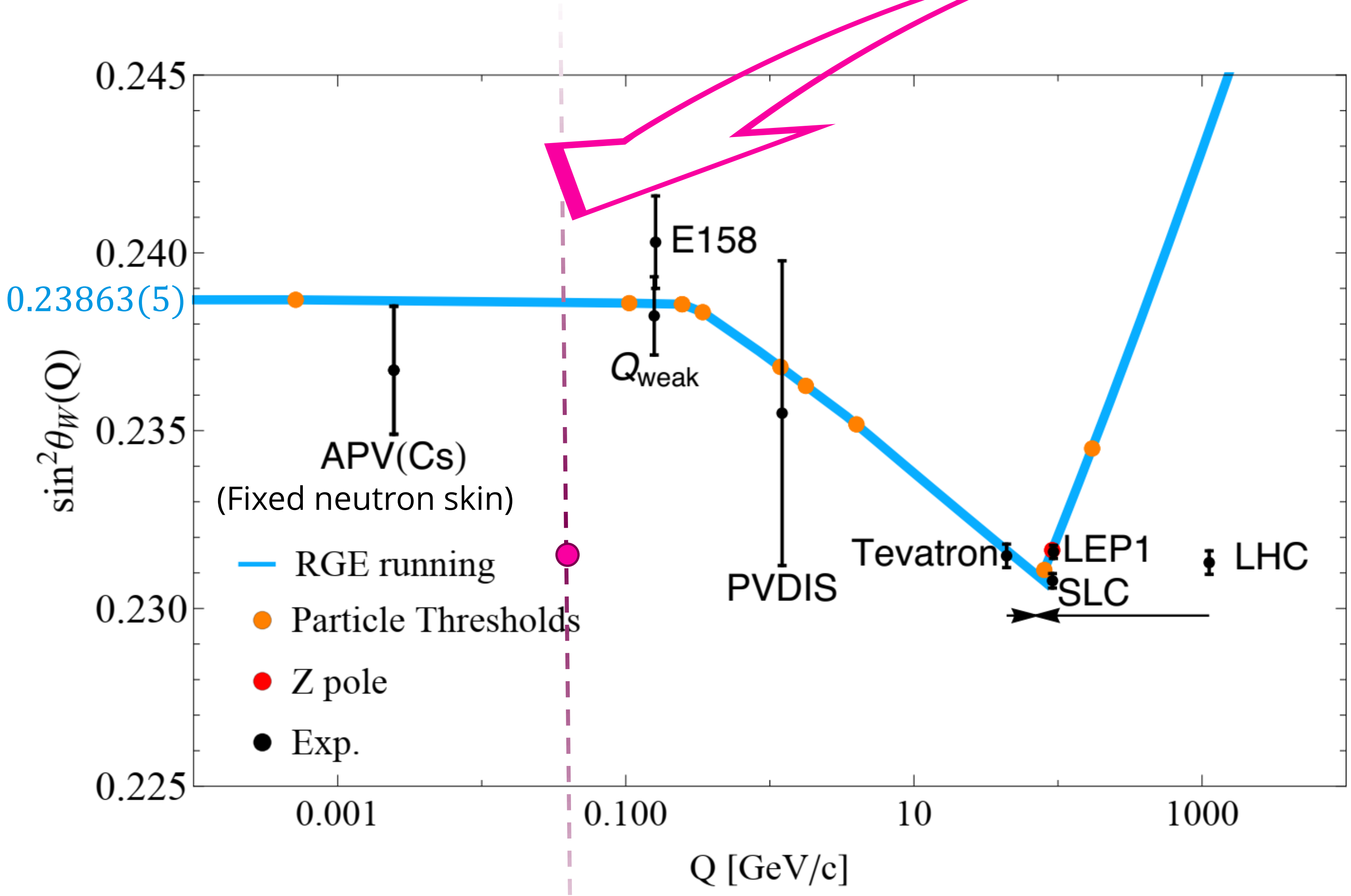

If we fix the value of the neutron radius of Cs and I and we fit for the weak mixing angle only we obtain:

$$\sin^2\vartheta_W = 0.231^{+0.027}_{-0.024}$$

The precision on the weak mixing angle using CEνNS is poor because of the neutrino-proton coupling suppression!

M. Atzori Corona et al., EPJC 83 (2023) 7, 683. ArXiv:2303.09360

Electroweak probes available

+ We can combine many electroweak processes to extract R_n(Cs) and $\sin^2\vartheta_W$.

➢ Atomic Parity Violation (APV): atomic electrons interacting with nuclei- **Cesium (Cs)** and **lead (Pb)** available.

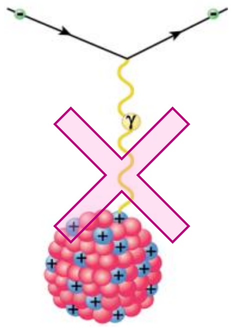

Mediated by photons. Sensitive to the charge (proton) distribution

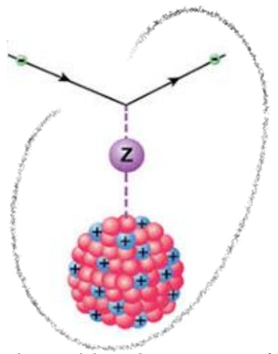

Mediated by the Z. Mostly sensitive to the weak (neutron) distribution.

M. Cadeddu and F. Dordei, PRD 99, 033010 (2019), arXiv:1808.10202

+ Atomic Parity Violation APV(Cs) and CEνNS depends both on the **weak charge** and thus on R_n(Cs) and $\sin^2\vartheta_W$

+ We can combine APV(Cs) and COHERENT(CsI) to obtain a fully data driven measurement of the WMA in the low energy regime!

$$Q_W^{SM} \approx Z\left(1 - 4\sin^2\theta_W^{SM}\right) - N$$

➢ Parity Violation Electron Scattering (PVES): polarized electron scattering on nuclei- **PREX(Pb)** & CREX(Ca)

➢ Coherent elastic neutrino-nucleus scattering (CEνNS)- **Cesium-iodide (CsI),** argon (Ar) and germanium (Ge) available.

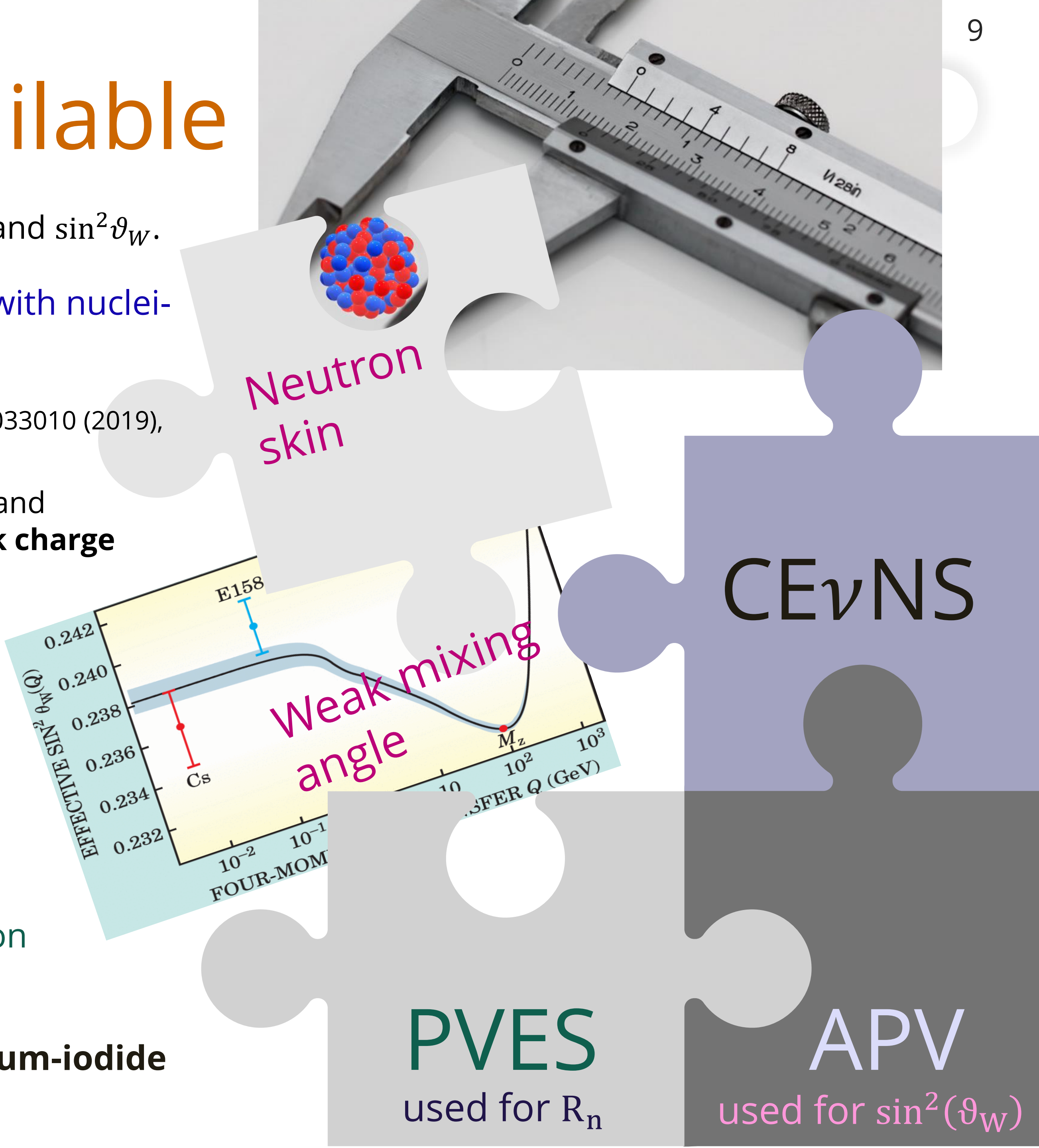

Electroweak only fit

- We perform a fit using Electroweak (EW) only information removing the R_n(Cs) input from CSRe
- APV(Cs) 21
- COHERENT CsI
- APV(Pb)+PREX-II

M. Atzori Corona et al. PRC 105, 055503 (2022), Arxiv: 2112.09717,

- APV has been measured also using lead.
- Moreover PREX-II has measured the Pb neutron skin with Parity Violation Electron Scattering (PVES).

We can profit from a very nice correlation between R_n(Cs) and R_n(Pb) within many theoretical nuclear models to translate R_n(Pb) to R_n(Cs)

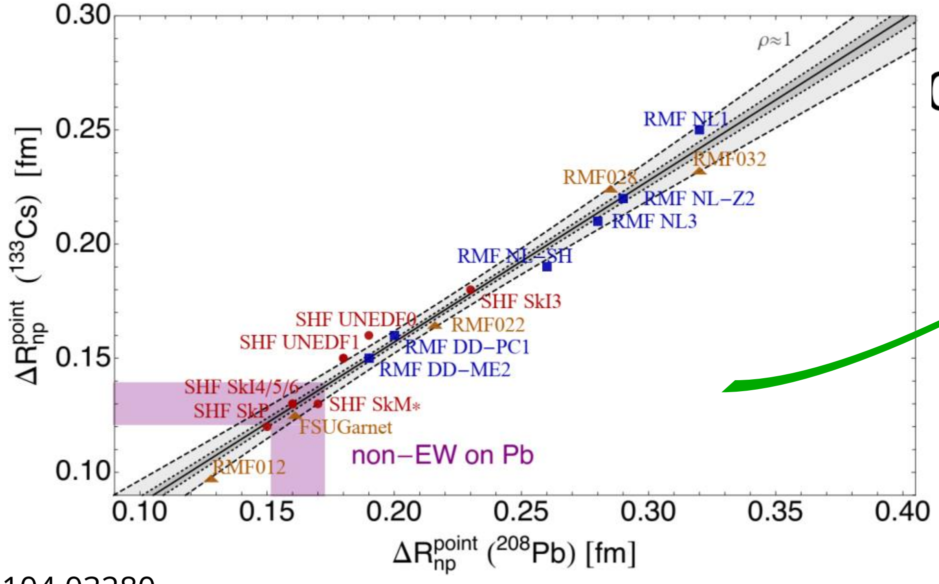

M. Cadeddu et al. PRD **104**, 011701 (2021), arXiv:2104.03280

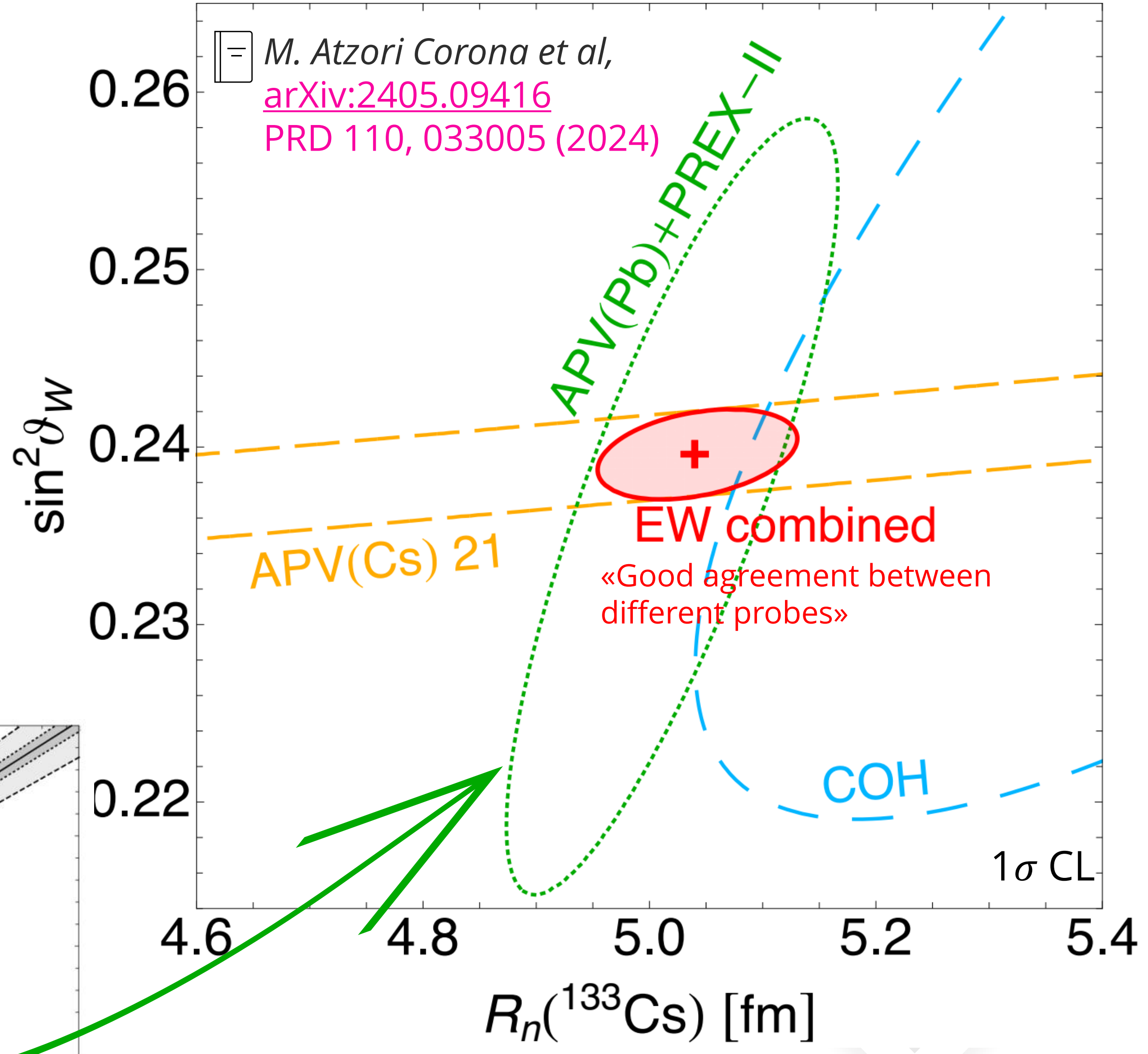

- ✓ Pros: only electroweak probes used
- ❖ Cons: we should trust the theoretical nuclear models for the translation of R_n(Pb) to R_n(Cs)

Conclusions for $\sin^2\vartheta_W$

A very nice agreement between the EW fit and that R_n(Cs) from proton scattering is achieved!

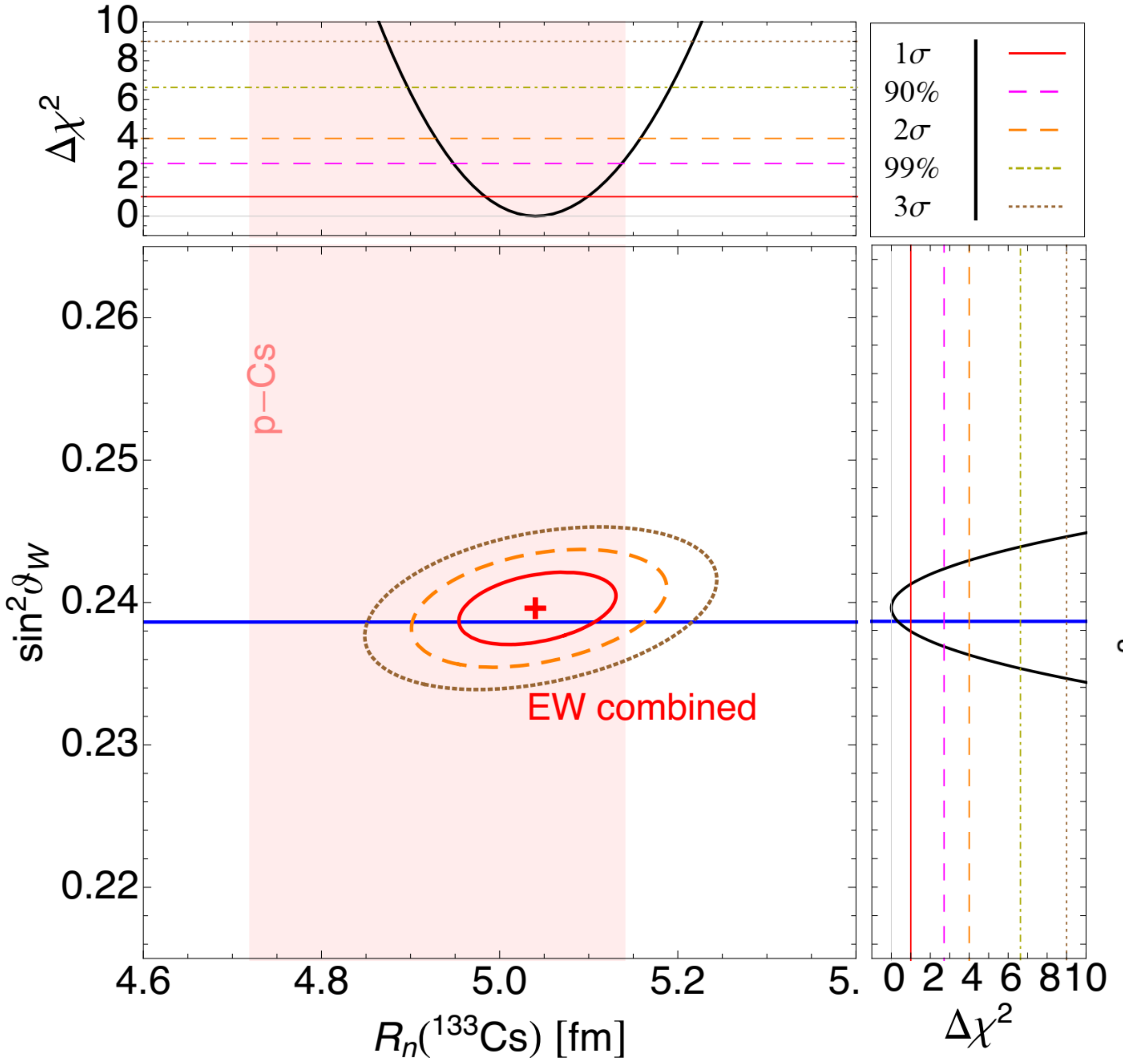

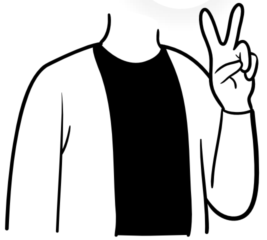

$$\sin^2\vartheta_W = \begin{cases} \boxed{0.2396 \pm 0.0017\,(\text{EW combined})} \\ \boxed{0.2396^{+0.0020}_{-0.0019}\,(\text{APV(Cs)} + \text{COH} + \text{CSRe})} \end{cases}$$

✓ same central values different uncertainties.

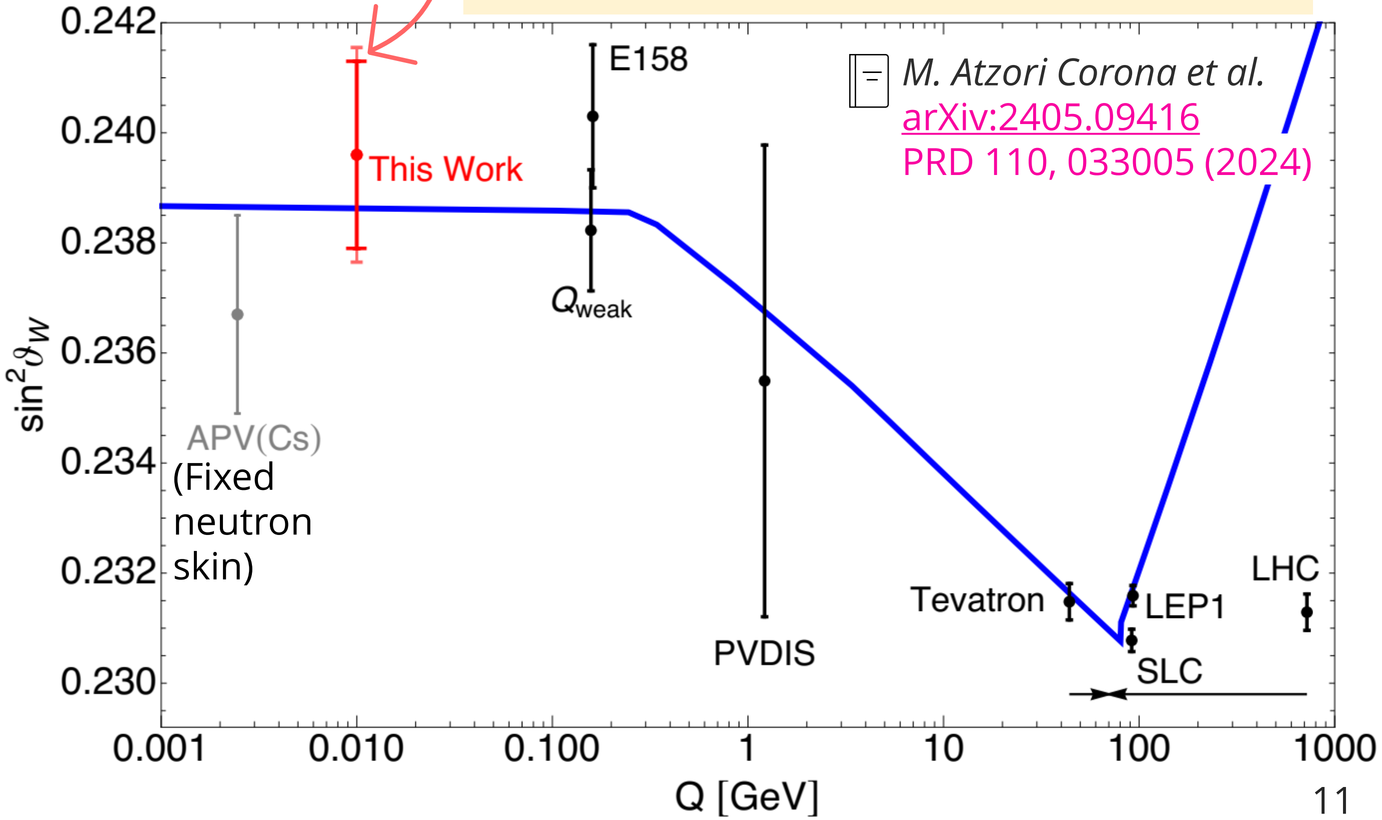

M. Atzori Corona et al.
arXiv:2405.09416
PRD 110, 033005 (2024)

Conclusions for R_n(Cs)

	$\sin^2\vartheta_W$	$R_n(^{133}\mathrm{Cs})$[fm]	
APV(Cs)+COH+CSRe	$0.2396^{+0.0020}_{-0.0019}$	5.04 ± 0.19	3.8%
EW combined	0.2396 ± 0.0017	5.04 ± 0.06	1.2%

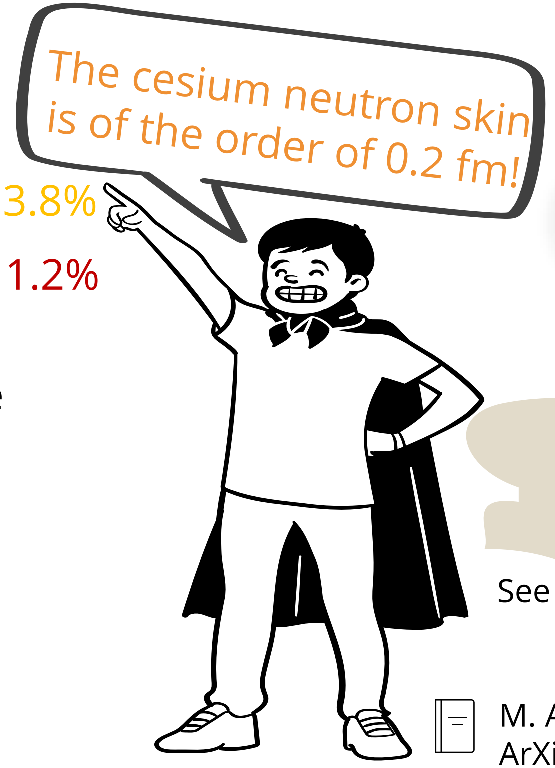

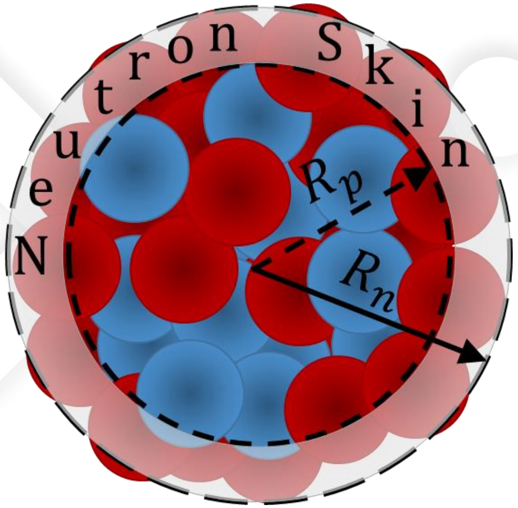

The neutron radius (or skin) of ^{133}Cs tends to be «large» but we cannot conclude more than this.

✓ **We need** precise CEνNS measurements on this!

The COHERENT program for R_n(Cs) for is exciting!

See D. Akimov et al., arXiv:2204.04575 (2022)

M. Atzori Corona et al., EPJC 83 (2023) 7, 683. ArXiv:2303.09360

✓ With COH-CryoCsI-I we can reach same R_n(CsI) precison of the current EW combined fit (3.7%) and with COH-CryoCsI-II a better precision of the EW combined fit (0.5%)

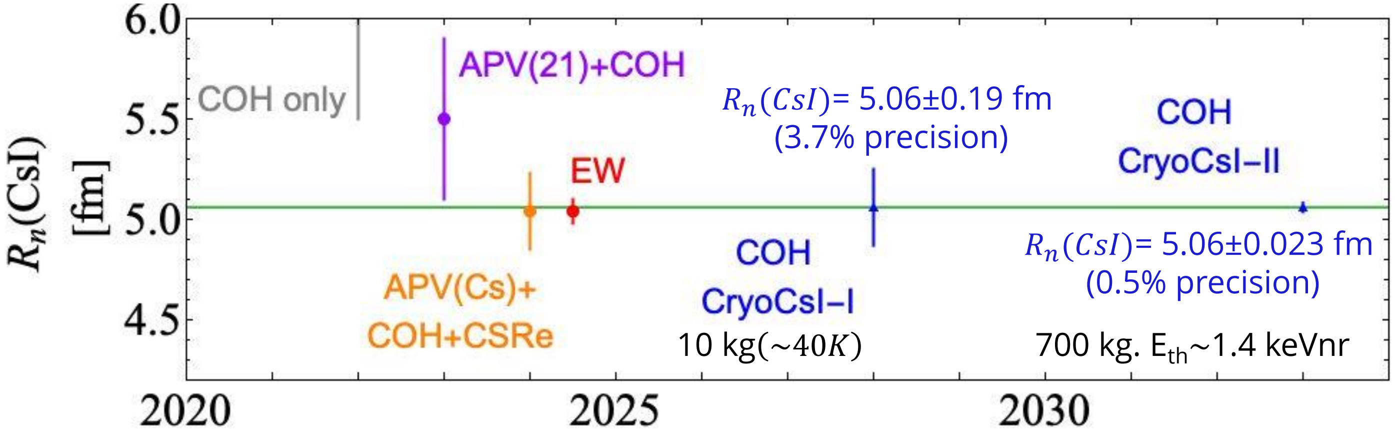

Conclusions for R_n(Cs) and $\sin^2\vartheta_W$:

«STANDARD MODEL RULEZ!»

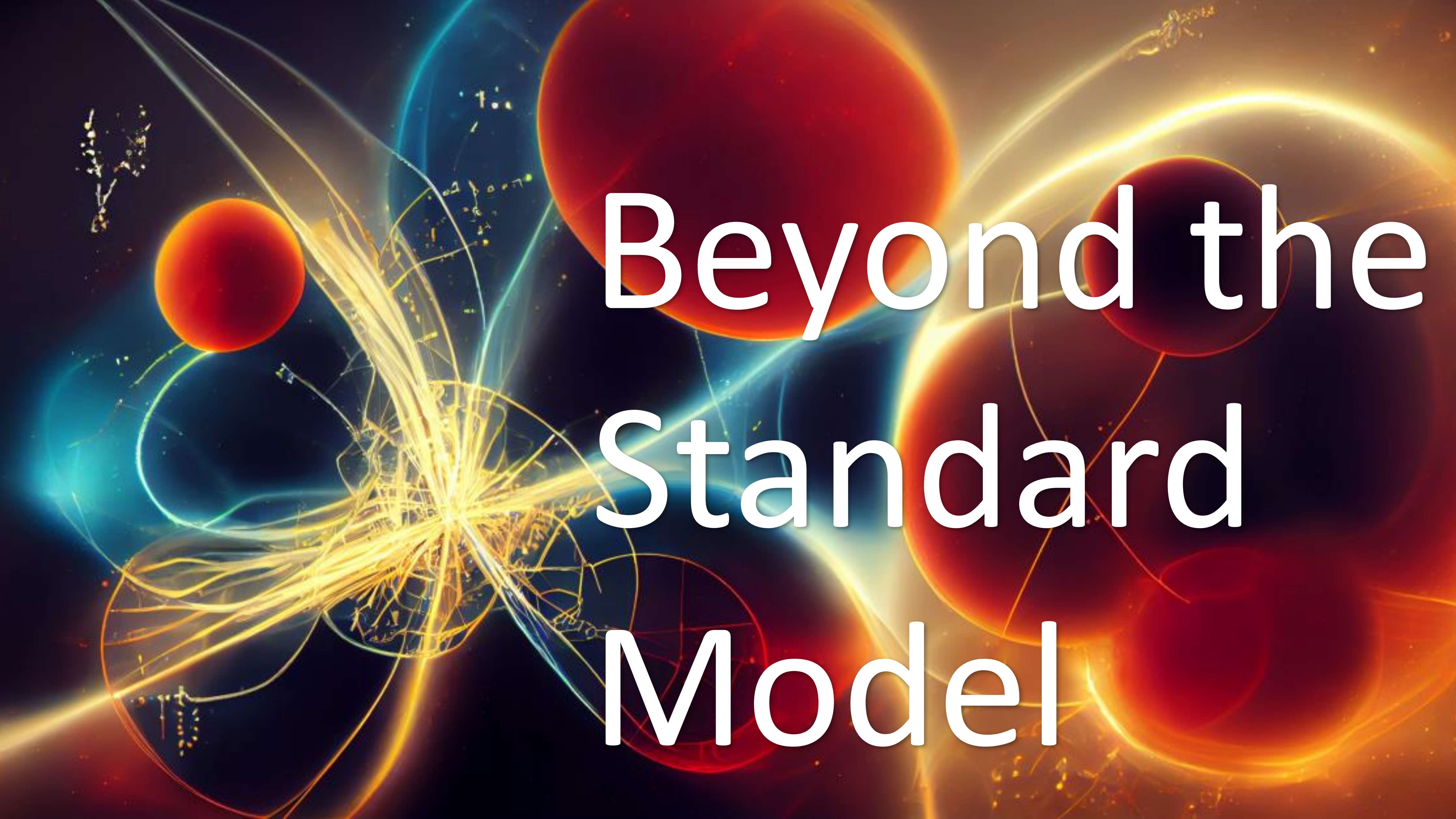
Beyond the Standard Model

Light mediators from SM U(1)' extensions: vector-boson case

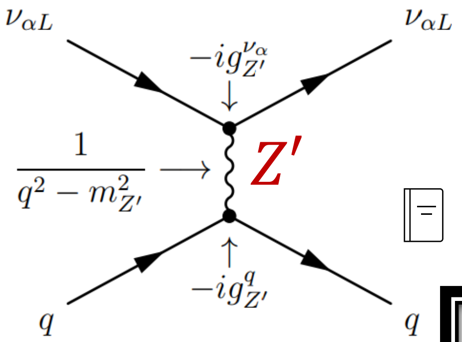

$$\mathcal{L}_{Z'}^{V} = -Z'_\mu \left[\sum_{\ell=e,\mu,\tau} g_{Z'}^{\nu_\ell V}\, \overline{\nu_{\ell L}} \gamma^\mu \nu_{\ell L} + \sum_{q=u,d} g_{Z'}^{qV}\, \bar{q} \gamma^\mu q \right]$$

M. Atzori Corona et al. JHEP 05 (2022)109, arXiv:2202.11002

- Search for anomaly free extensions of the SM (connection with Dark Sectors, Hidden Sectors..)
- Light mediators ~ MeV – few GeVs

Rev.Mod.Phys. 81 (2009) 1199-1228

$$SU(2)_{\mathrm{L}} \otimes U(1)_Y \otimes SU(3)_{\mathrm{c}} \rightarrow SU(2)_{\mathrm{L}} \otimes U(1)_Y \otimes SU(3)_{\mathrm{c}} \otimes U(1)'$$

- The effect of the new mediator is quantified by additional terms in the weak charge of the nucleus

$$Q^V_{\ell,\mathrm{SM+V}} = Q^V_{\ell,\mathrm{SM}} + \frac{\boxed{g_{Z'}^2}\boxed{Q'_\ell}}{\sqrt{2}G_F\,(|\vec{q}|^2 + \boxed{M_{Z'}^2})} \left[(2\boxed{Q'_u} + \boxed{Q'_d})\, Z F_Z(|\vec{q}|^2) + (\boxed{Q'_u} + 2\boxed{Q'_d})\, N F_N(|\vec{q}|^2) \right]$$

The universal model is not anomaly free

These models are anomaly free if the SM is extended with right-handed neutrinos

Anomaly-free

The coupling of the new vector boson with the quarks is generated by kinetic mixing of Z' with the photon at the one-loop level

Model	Q'_u	Q'_d	Q'_e	Q'_μ	Q'_τ
universal	1	1	1	1	1
$B-L$	$1/3$	$1/3$	-1	-1	-1
$B-3L_e$	$1/3$	$1/3$	-3	0	0
$B-3L_\mu$	$1/3$	$1/3$	0	-3	0
$B-2L_e-L_\mu$	$1/3$	$1/3$	-2	-1	0
$B-L_e-2L_\mu$	$1/3$	$1/3$	-1	-2	0
$B_y+L_\mu+L_\tau$	$1/3$	$1/3$	0	1	1
L_e-L_μ	0	0	1	-1	0
L_e-L_τ	0	0	1	0	-1
$L_\mu-L_\tau$	0	0	0	1	-1

See also:
Miranda et al. Phys. Rev. D 101, 073005 (2020)
Coloma et al. JHEP 01 (2021) 114

Constraints on light mediators from COHERENT data

For more constraints: M. Atzori Corona et al. JHEP 05 (2022)109, arXiv:2202.11002

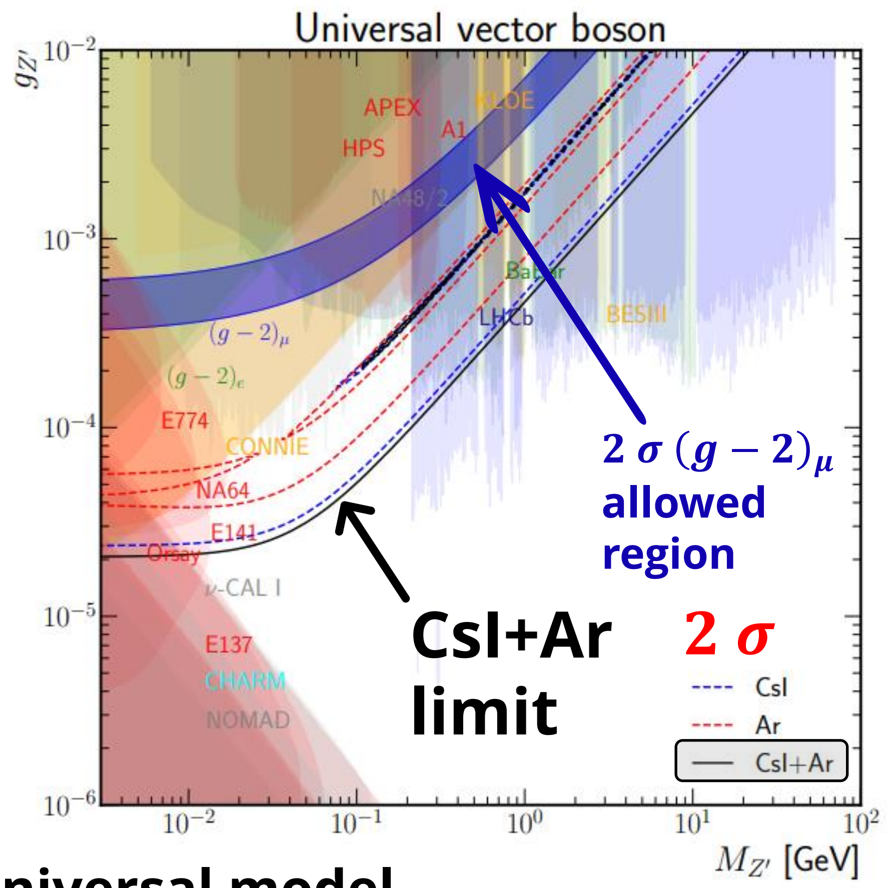

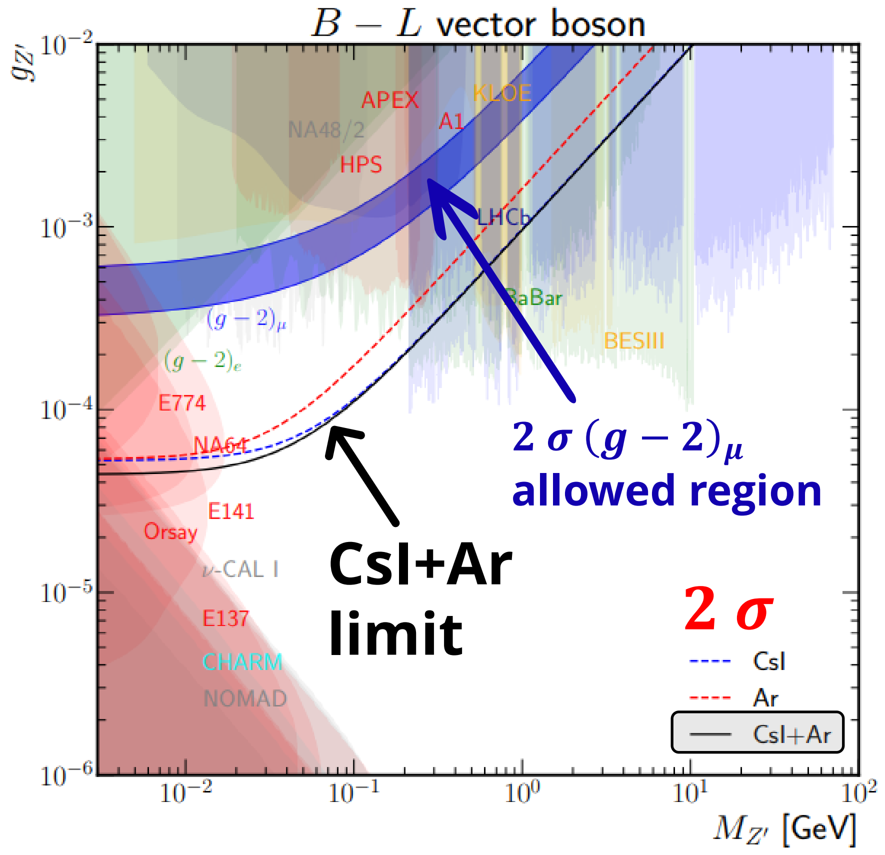

Universal model

- **Same coupling** to all SM fermions
- Improved constraints for 20<$M_{Z'}$<200 MeV and 2×10^{-5}<$g_{Z'}<10^{-4}$
- $(g-2)_\mu$ excluded

B-L

- **Quark charge** $Q_q=1/3$; **Lepton charge** $Q_\ell=-1$
- Improved constraints for 10<$M_{Z'}$<200 MeV and 5×10^{-5}<$g_{Z'}<3\times10^{-4}$
- $(g-2)_\mu$ excluded

Constraints on light mediators from COHERENT data

For more constraints: M. Atzori Corona et al. JHEP 05 (2022)109, arXiv:2202.11002

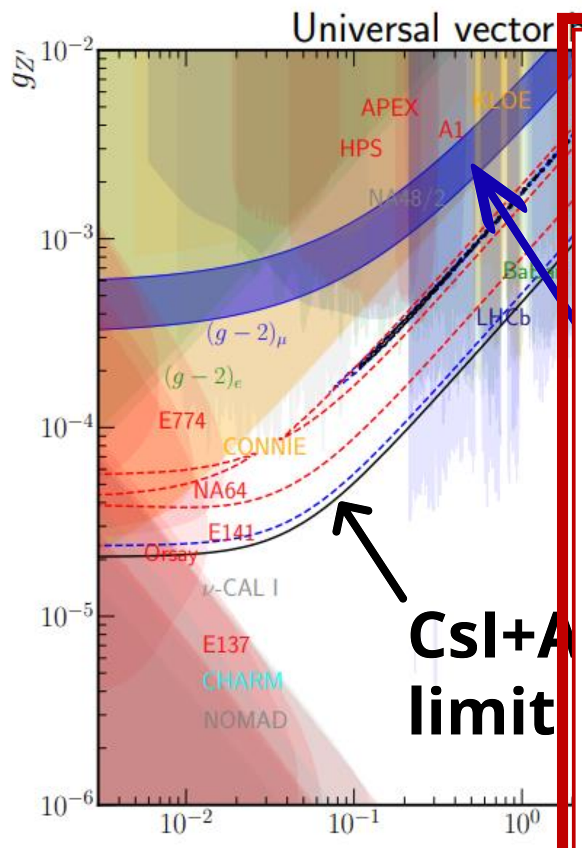

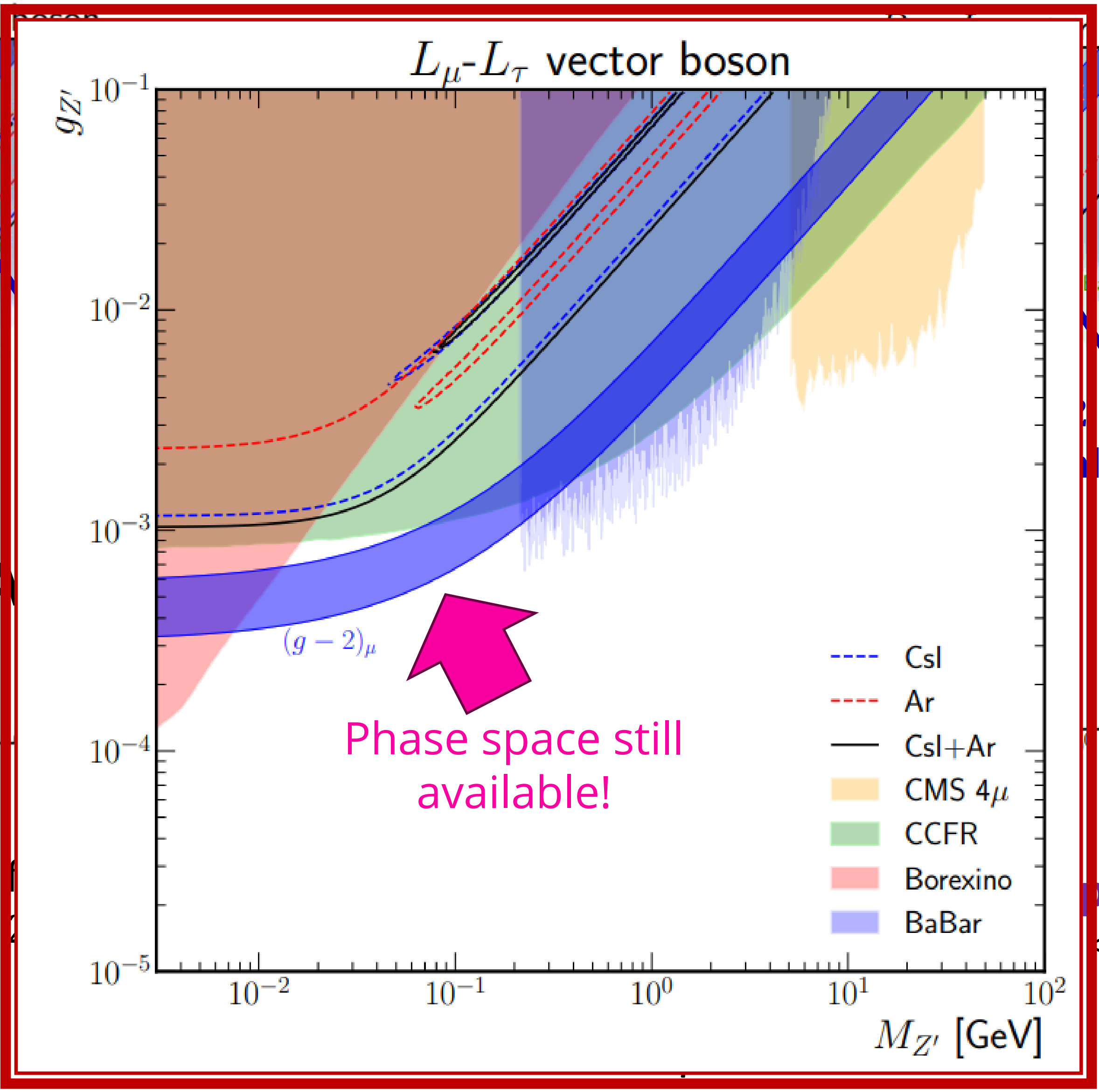

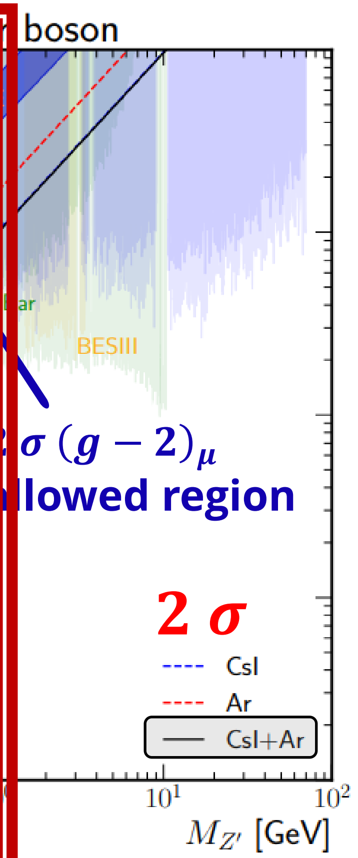

Universal model

- **Same coupling** to all SM f
- Improved constraints for and $2\times10^{-5}<g_{Z'}<10^{-4}$
- $(g-2)_\mu$ excluded

pton charge $Q_\ell=-1$

$<M_{Z'}<$200 MeV and

Limits on ν magnetic moment and millicharge

In the SM the channel due to neutrino-electron scattering is negligible with respect to that of CEvNS, however the contribution due to the magnetic moment and the millicharge grows as 1/T. Dark matter-searching experiments such as LZ, XENONnT that observe solar neutrinos are sensitive to these quantities

M. Atzori Corona et al. PRD **107**, 053001 (2023), arXiv:2207.05036

$$\frac{d\sigma^{\mathrm{MM}}_{\nu_\ell}}{dT_{\mathrm{e}}}(E,T_{\mathrm{e}}) = Z^{\mathrm{Xe}}_{\mathrm{eff}}(T_{\mathrm{e}})\frac{\pi\alpha^2}{m_e^2}\left(\frac{1}{T_{\mathrm{e}}}-\frac{1}{E}\right)\left|\frac{\mu_{\nu_\ell}}{\mu_{\mathrm{B}}}\right|^2$$

$$\left.\frac{d\sigma_{\nu_\ell}}{dT_{\mathrm{e}}}\right|^{\mathrm{EC}}_{\mathrm{EPA}} = \frac{2\alpha}{\pi}\frac{\sigma_\gamma(T_e)}{T_e}\log\left[\frac{E_\nu}{m_\nu}\right]q^2_{\nu_\ell}$$

For the «neutrino charge radius» see Dordei's talk on saturday

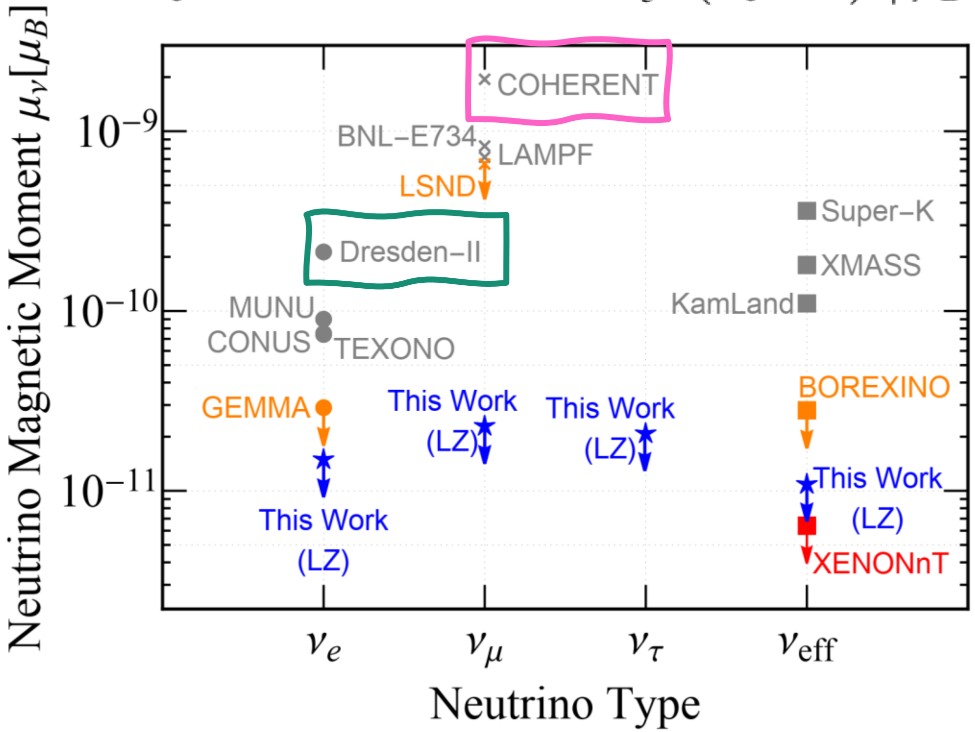

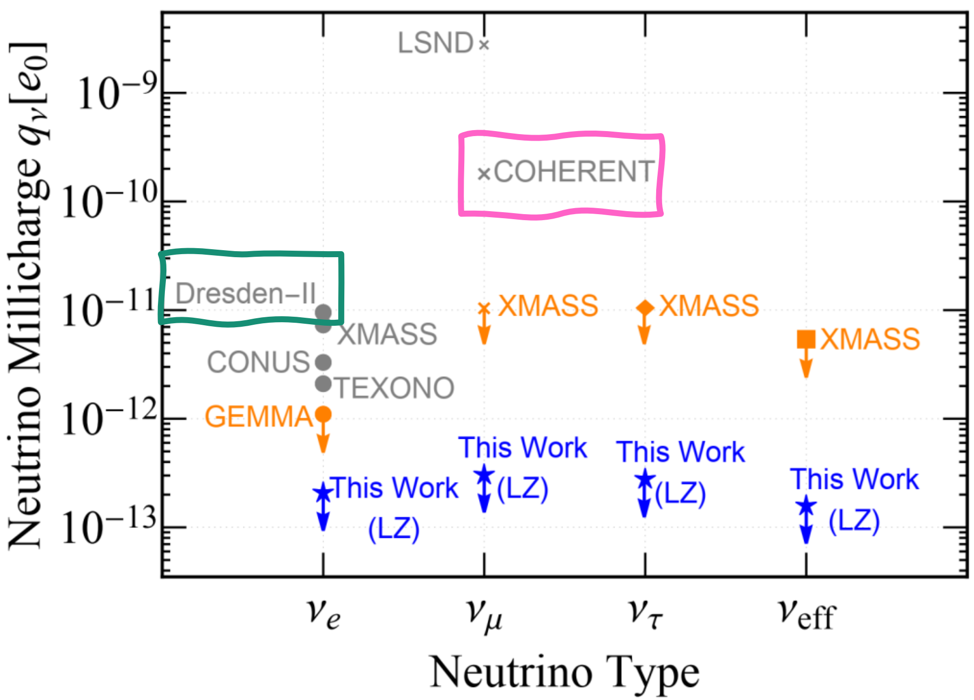

$$\mu_\nu = \frac{3e_0G_F}{8\sqrt{2}\pi^2}m_\nu \simeq 3.2\times10^{-19}\left(\frac{m_\nu}{\mathrm{eV}}\right)\mu_B$$

➢ CEvNS limits from COHERENT and Dresden-II detectors competitive. Dresden-II profits from the very low threshold, however the CEvNS signal in Dresden-II is debated…

Migdal contribution in reactor CEvNS experiments

Atzori Corona et al. PLB 852 (2024) 138627, arXiv:2307.12911

SuperCDMS Coll. Arxiv:2202.07043

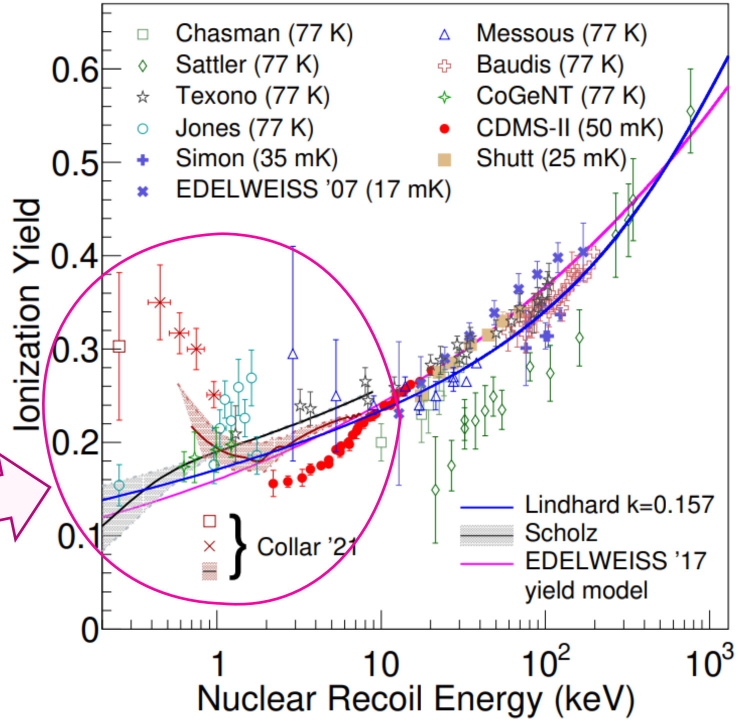

- The first observation of CEvNS at reactors by Dresden-II [PRL129 211802 (2022)] relies on an unexpected enhancement at low energies [PRD 103, 122003] of the measured quenching factor (QF) with respect to the Lindhard prediction (k=0.157).
- The QF quantifies the reduction of the ionization yield produced by a nuclear recoil with respect to an electron recoil of the same energy.
- Since the Dresden-II result implies an extra observable ionization signal produced after the nuclear recoil, some authors [PRD 104, 015005 , PRD 106, L031702] have cleverly interpreted this enhancement as due to the so called Migdal effect

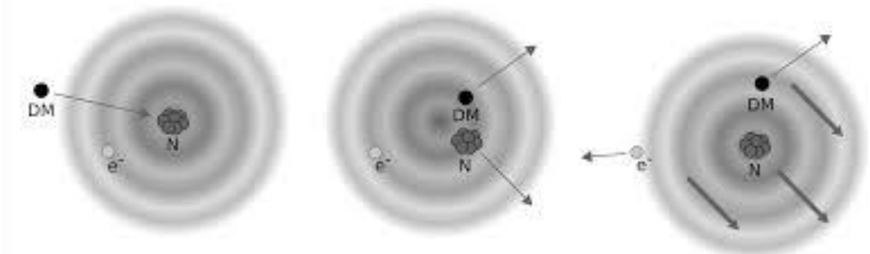

✓ The Migdal contribution to the standard CEνNS signal calculated with the Lindhard quenching factor is completely negligible for observed energies below $\sim$0.3 keV where the signal is detectable, and thus unable to provide any contribution to CEνNS searches in this energy regime.

✓ A different explanation is thus required!

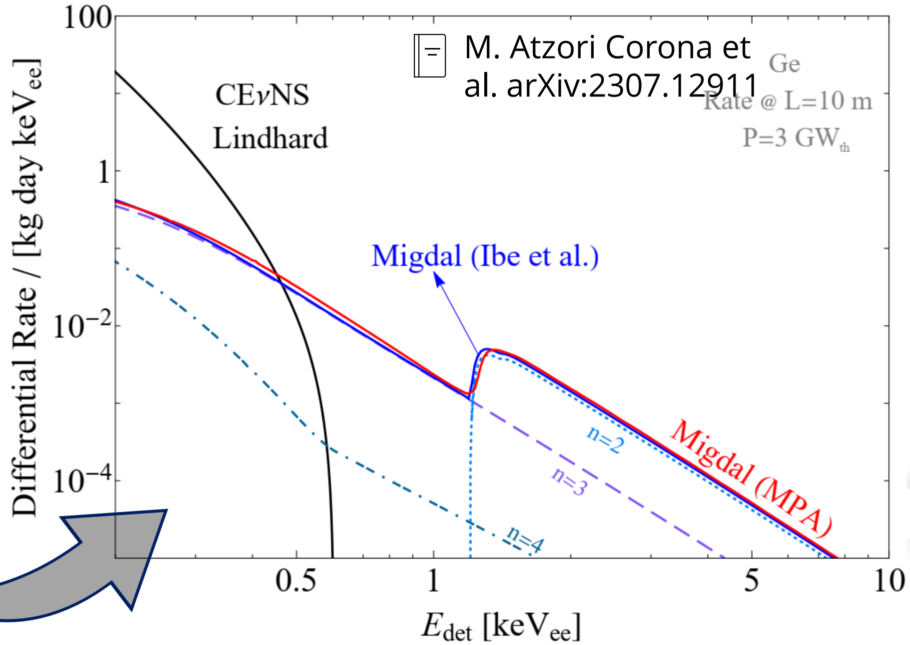

Conclusions

- CEνNS is a powerful tool for measuring both SM and BSM physics.
- Combination with other electroweak probes is fundamental in order to break some degeneracies!
- Many CEνNS experiments are expected to produce results soon!

The future is bright!


THANK YOU FOR YOUR ATTENTION!

BACKUP

Cs neutron skin from proton-elastic scattering

New measurement from **proton-cesium elastic scattering at low momentum transfer** using an in-ring reaction technique at the **Cooler Storage Ring** (**CSRe**) at the Heavy Ion Research Facility in Lanzhou, which can be included in the derivation of $\sin^2\vartheta_W$. The authors employed this value to re-extract the COHERENT $\sin^2\vartheta_W$ value by fitting the CEνNS CsI dataset, finding $\sin^2\vartheta_W$ = 0.227 ± 0.028.

New direct measurement of the cesium-133 neutron skin, $\Delta\boldsymbol{R_{np}}(\mathbf{Cs}) = \mathbf{0.12 \pm 0.21}$ **fm** available!

+ Experiments with hadronic probes are more precise BUT result interpretation of hadronic probe experiments is difficult due to the complexity of strong-force interactions.

Hovever, this is the first **DIRECT** determination of R_n(Cs)!

Huang et al. arXiv:2403.03566v2

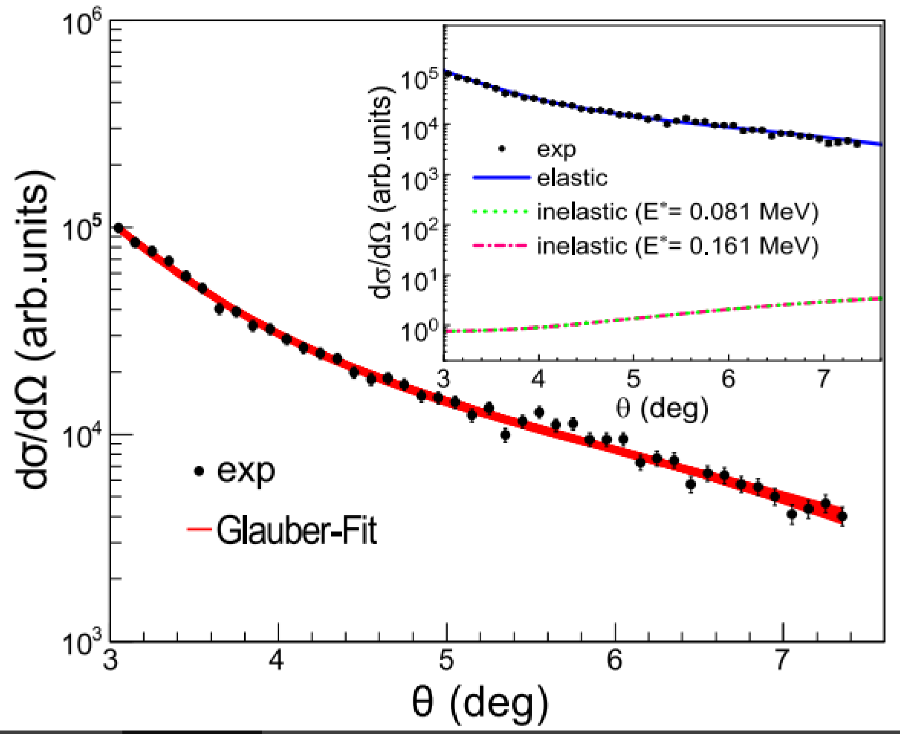

"Cesium neutron radius determination with hadronic probes has been historically experimentally challenging due to the low melting point and spontaneous ignition in air."

First results: fit using R_n(Cs) from CSRe

+ We combine APV(Cs) and COHERENT CsI adding a prior on R_n(Cs)= 4.94 ± 0.21 fm coming from the **Cooler Storage Ring** (**CSRe**)

$\sin^2 \vartheta_W$	$R_n(^{133}\mathrm{Cs})$[fm]
$0.2396^{+0.0020}_{-0.0019}$	5.04 ± 0.19

Big improvement with respect to our previous result (arXiv:2303:09360):

$$\sin^2 \vartheta_W = 0.2423^{+0.0032}_{-0.0029}, \quad R_n(\mathrm{CsI}) = 5.5^{+0.4}_{-0.4}\ \mathrm{fm}$$

✓ Pros: For the first time a direct measurement on R_n(Cs) is used

❖ Cons: CSRe R_n(Cs) still comes from hadronic probes...

Can we use electroweak only inputs?

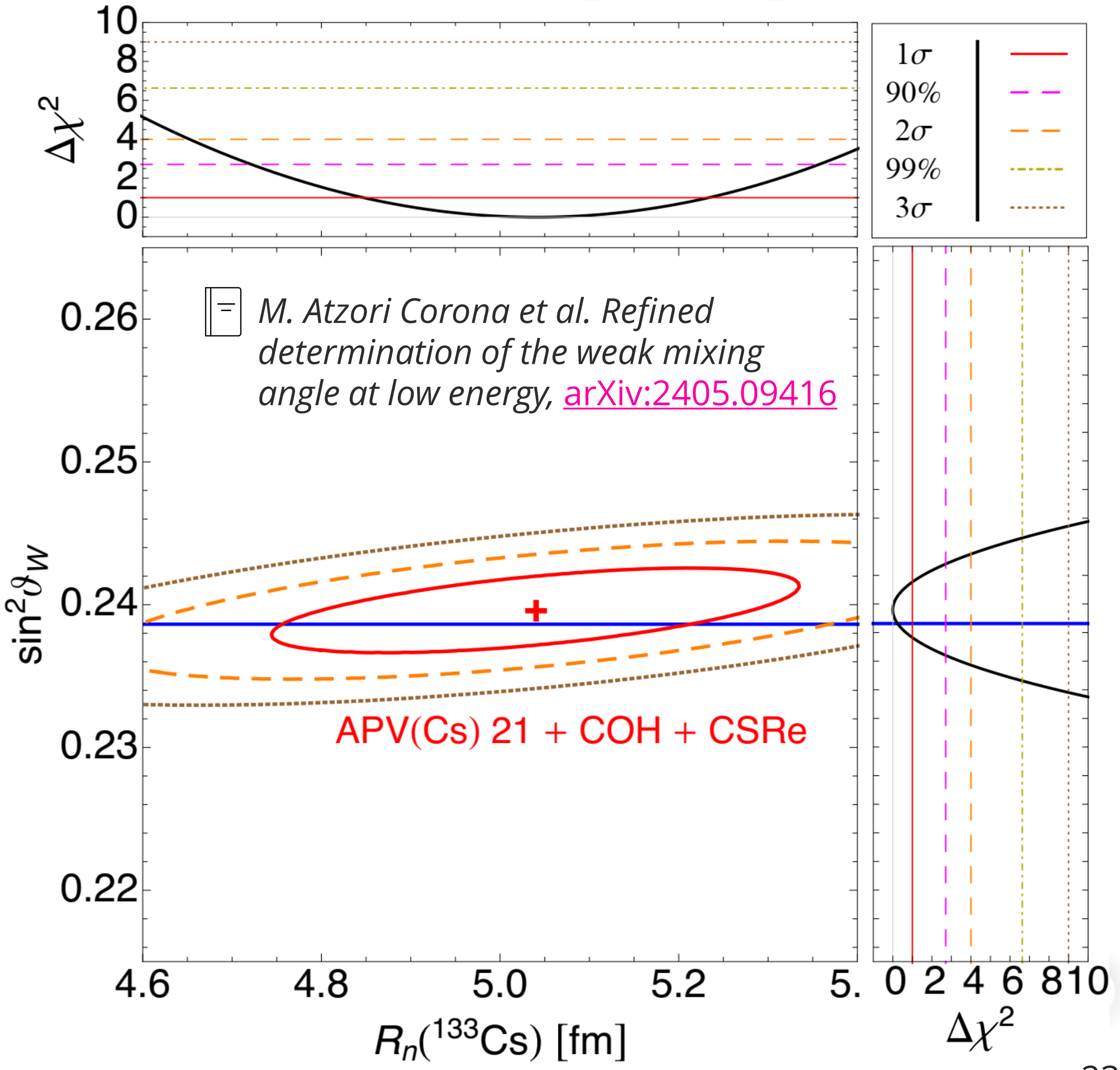

Dresden-II result

+ 3 kg ultra-low noise germanium detector 10 m away from a reactor
+ the background comes from the elastic scattering of epithermal neutrons and the electron capture in ^{71}Ge.
+ The Quenching Factor describes the suppression of the ionization yield produced by a nuclear recoil compared to an electron recoil.

Electron-equivalent energy:

$$T_e = f_Q(T_{nr})\, T_{nr}$$

➢ Dresden-II Ge quenching factor models

- Fef: iron filtered neutron beam
- YBe: photo-neutron source

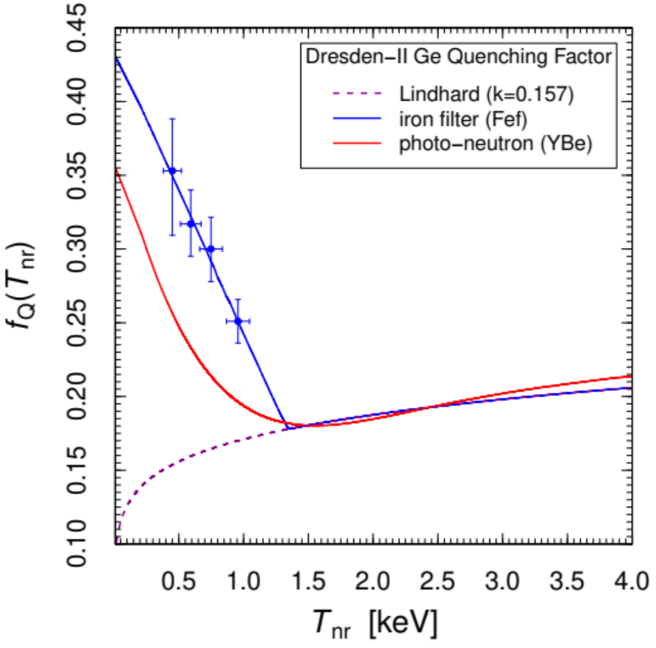

Colaresi et al. arXiv:2202.09672v1

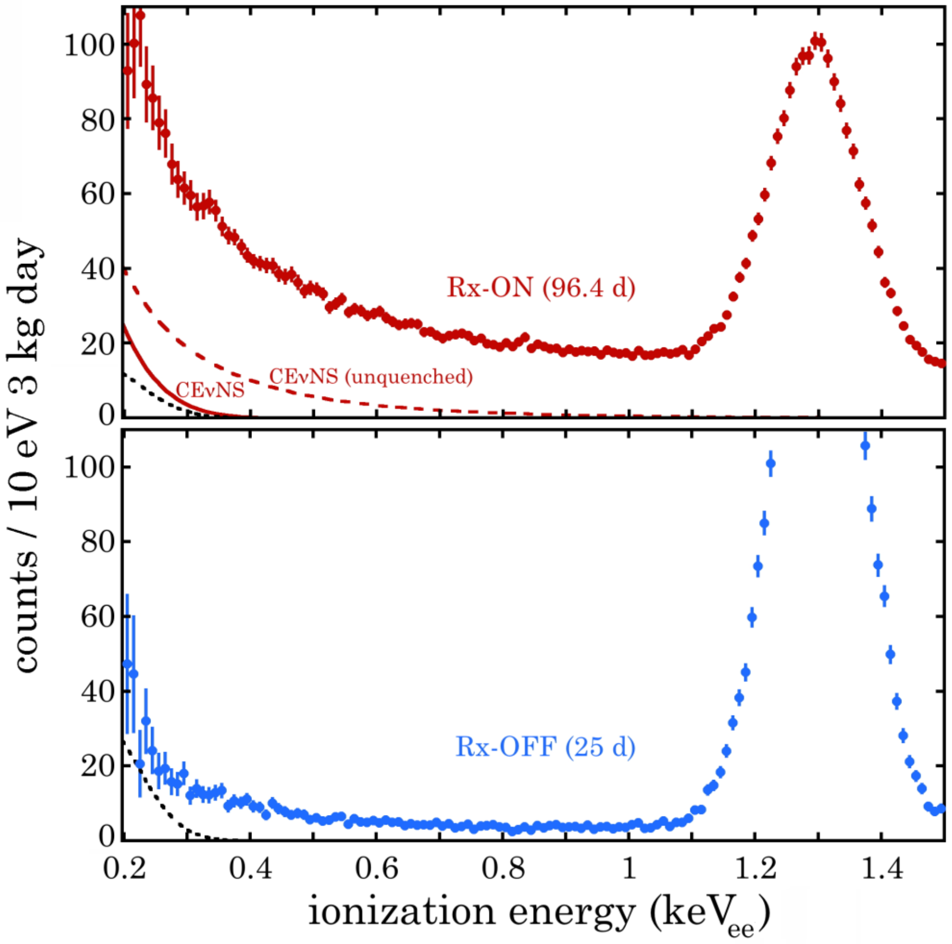

+ Ultra-low energy threshold

$$\boxed{0.2 < T_e < 1.5\ \mathrm{keV_{ee}}}$$

➢ This feature makes reactor neutrinos very sensitive to possible ν electromagnetic properties (millicharge, magnetic moment) since the related cross section goes like 1/T

Migdal contribution

$$\left(\frac{d\sigma_{\bar{\nu}_e\text{-}\mathcal{N}}}{dT_{\rm nr}}\right)^{\text{Ibe } et\ al.}_{\text{Migdal}} = \frac{G_F^2 M}{\pi}\left(1-\frac{MT_{\rm nr}}{2E_\nu^2}\right) Q_W^2 \times |Z_{\rm ion}(q_e)|^2 ,$$

Where Z_{ion} is the ionization rate of an individual electron in the target

$$|Z_{\rm ion}(q_e)|^2 = \frac{1}{2\pi}\sum_{n,\ell}\int dT_e \frac{d}{dT_e} p^c_{q_e}(n\ell \to T_e)$$

p^c are the ionization probabilities for an atomic electron with quantum numbers n and ℓ that is ionized with a final energy T_e.

- The formalism developed in PRD 102, 121303 relates the **photoabsorption cross section σ_γ** to the Migdal dipole matrix element without requiring any many-body calculation.
- ➢ Photoabsorption cross section is experimentally known, such that the Migdal rate suffers from very small uncertainties

$$\left(\frac{d^2\sigma_{\bar{\nu}_e\text{-}\mathcal{N}}}{dT_{\rm nr}dE_r}\right)^{\rm MPA}_{\rm Migdal} = \frac{G_F^2 M}{\pi}\left(1-\frac{MT_{\rm nr}}{2E_\nu^2}\right) Q_W^2 \times \frac{1}{2\pi^2\alpha_{\rm EM}}\frac{m_e^2}{M}\frac{T_{\rm nr}}{E_r}\sigma_\gamma^{\rm Ge}(E_r),$$

✓ The Migdal contribution to the standard CEνNS signal calculated with the Lindhard quenching factor is completely negligible for observed energies below ~0.3 keV where the signal is detectable, and thus unable to provide any contribution to CEνNS searches in this energy regime.

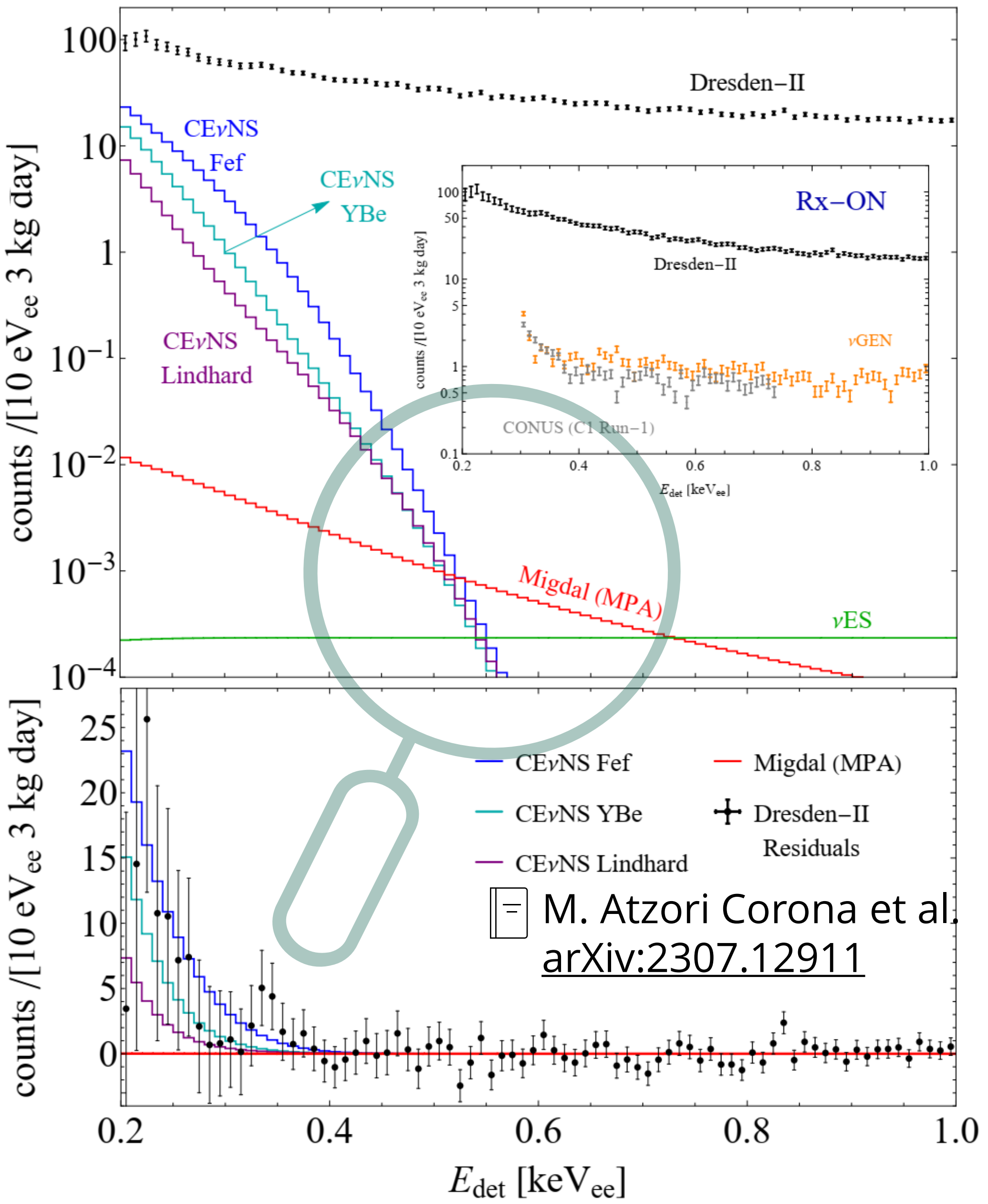

M. Atzori Corona et al. arXiv:2307.12911

✓ A different explanation is thus required!

WIMPS: the future and the CEvNS background

A solar/atmospheric neutrino can mimic a WIMP signal almost perfectly

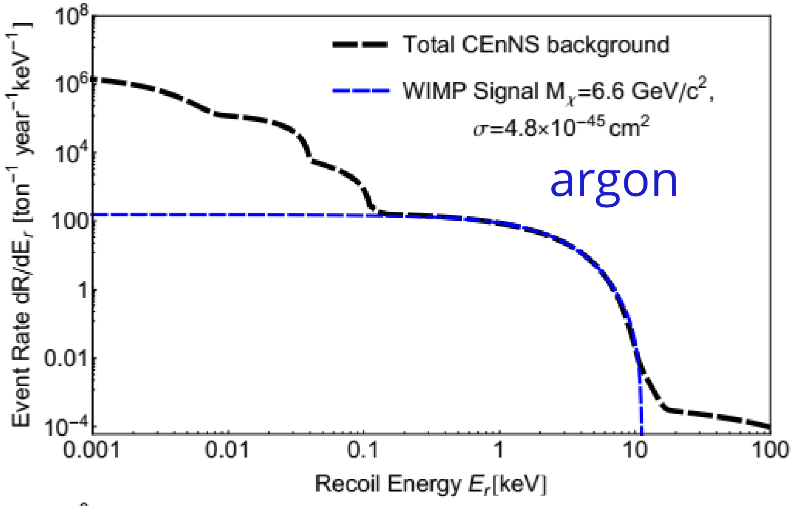

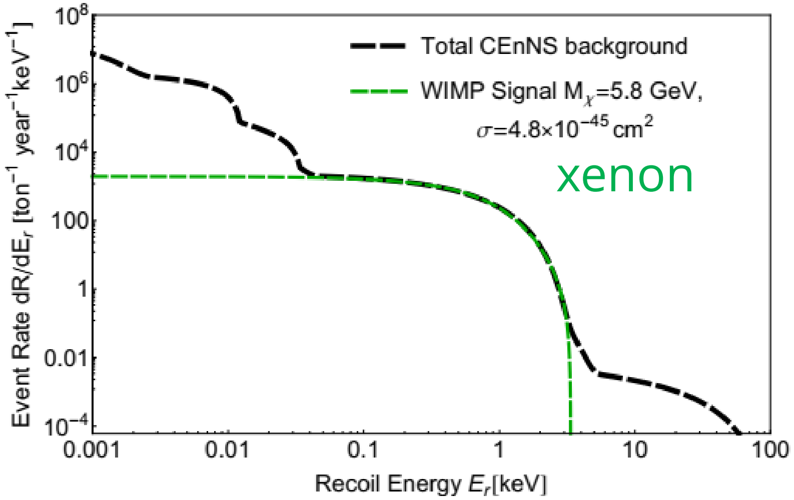

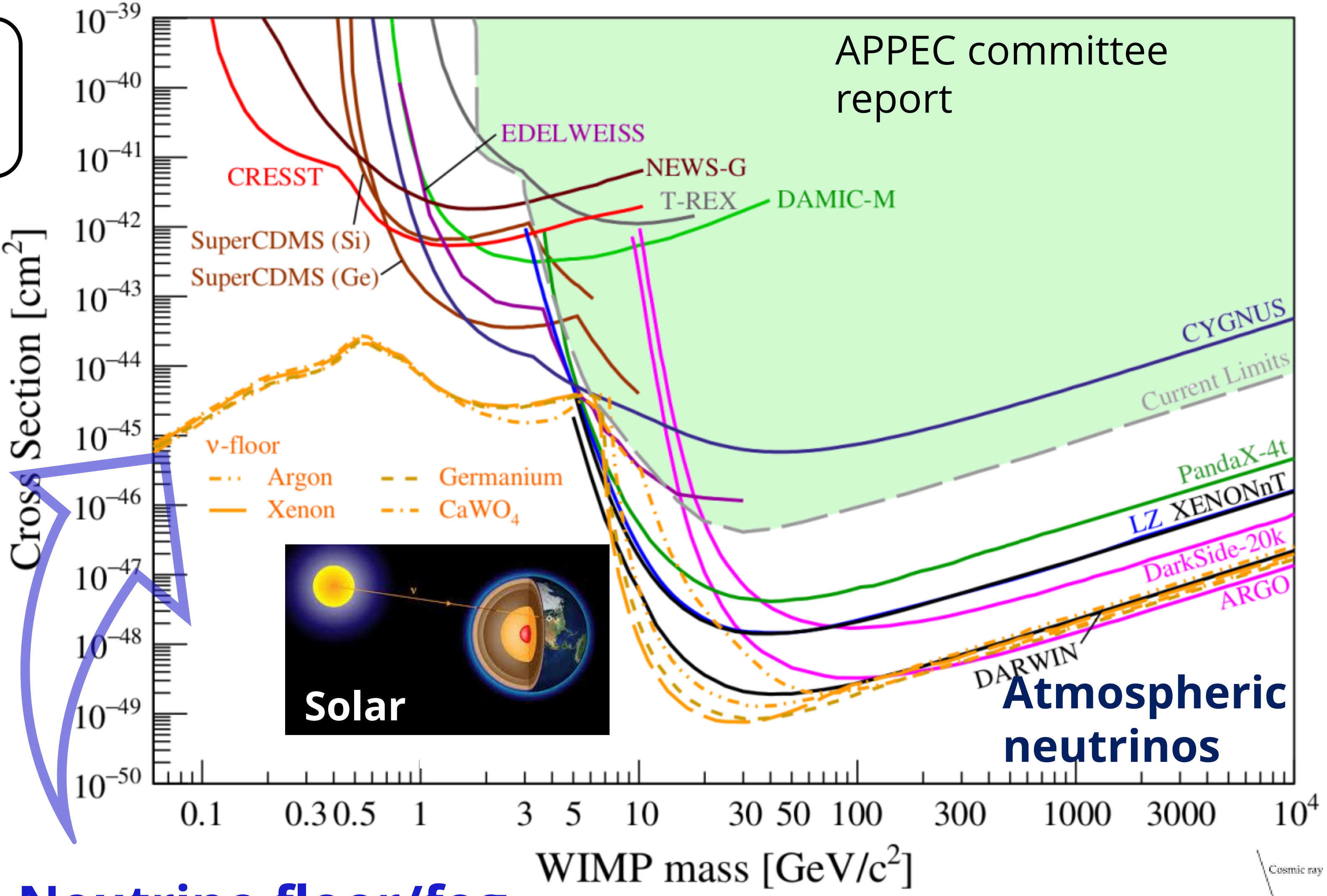

Neutrino floor/fog

CEνNS produces recoils very similar to those produced by dark matter, thus limiting sensitivity

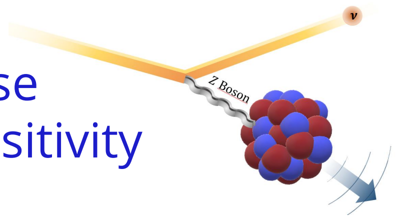

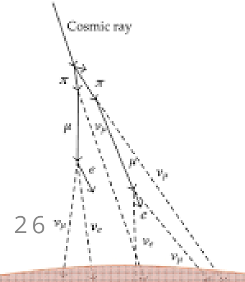

Similarities between neutrino and WIMP spectra

A WIMP signal could almost perfectly be mimicked by solar neutrino backgrounds

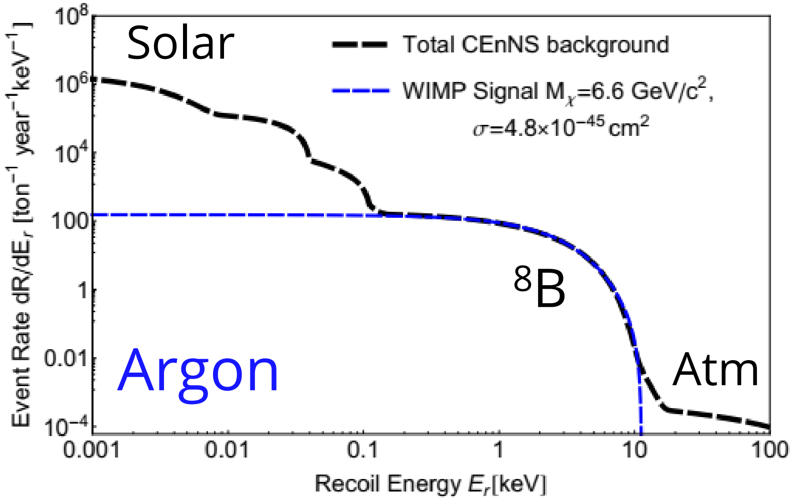

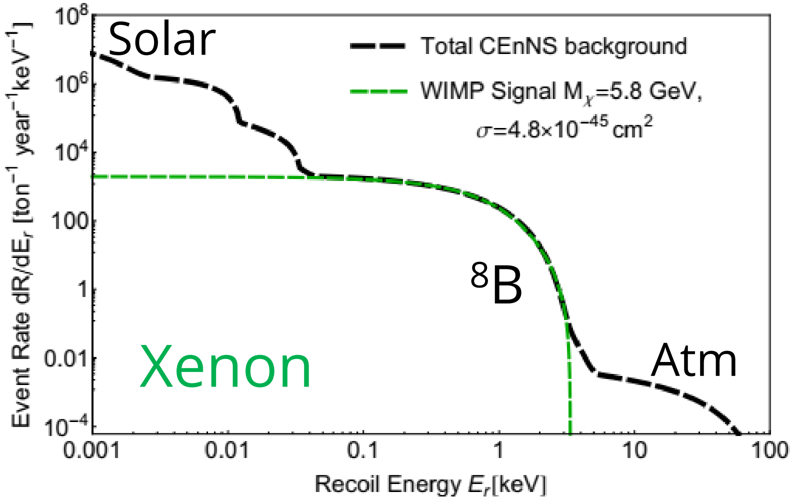

Same number of WIMP and background neutrino events but **different shape**!

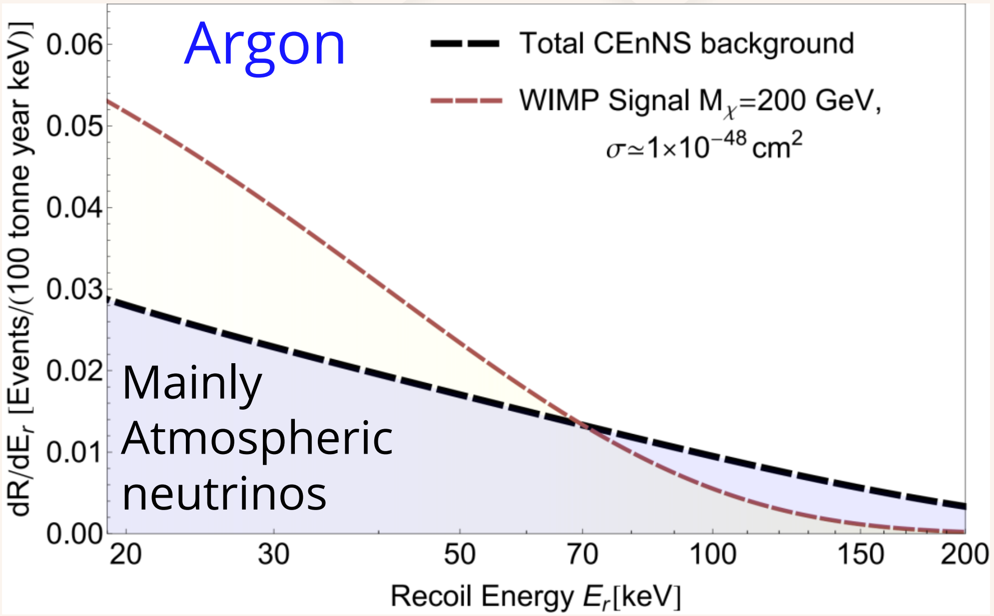

A likelihood analysis which makes use of the shape information *would help in disentangling WIMP from atmospheric neutrinos*!

Neutrino floor/fog

Can we overcome the neutrino floor at high masses?

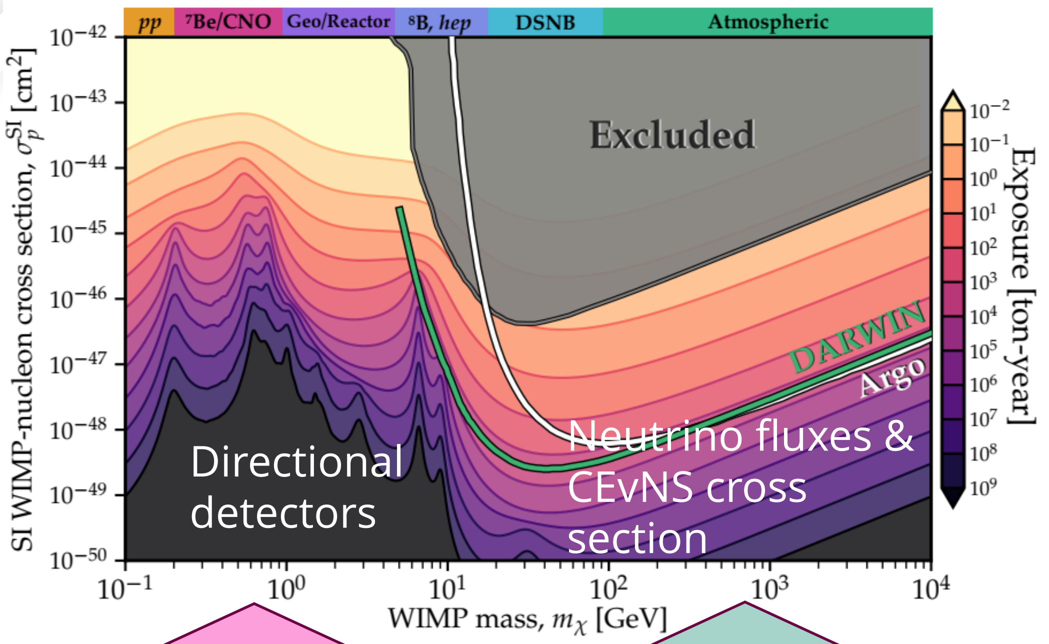

WIMPs and solar ν's come from different directions: possibility of distinguishing them with directional detectors

Background caused by atmospheric ν's (mainly isotropic) - directionality helps only little. Better to reduce the systematics on the neutrino flux and CEνNS cross-section.

- **Neutrino floor**: Theoretical lower limit on detectability of WIMPs.
- **Neutrino fog**: surpassable nature of the neutrino floor with sufficient statistical data.
- Old methods: Rely on arbitrary experimental exposure and energy threshold choices.

<u>Define neutrino floor as boundary of neutrino fog (calculation free from assumptions)</u>

➢ **New definition**: Derivative of experimental discovery limit with respect to exposure, minimizing influence of syst. uncertainties.

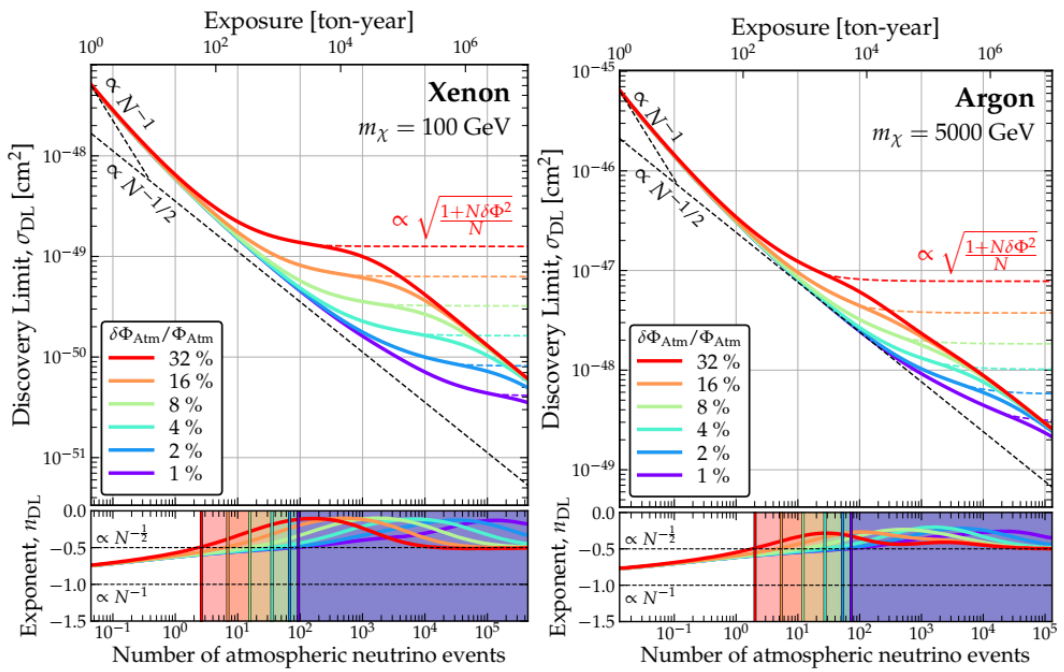

arXiv:2002.07499

SI discovery limits at m_W = 100 GeV for Xe and m_W = 5000 GeV for Ar target as a function of CEνNS events N, and the fractional uncertainty on the atmospheric flux

The strategy

APV (Cs)

+ Sensitive to the weak mixing angle
+ Similarly sensitive to the neutron skin

COHERENT (CsI)

+ CEνNS is sensitive to the neutron skin
+ But less sensitive to the weak mixing angle

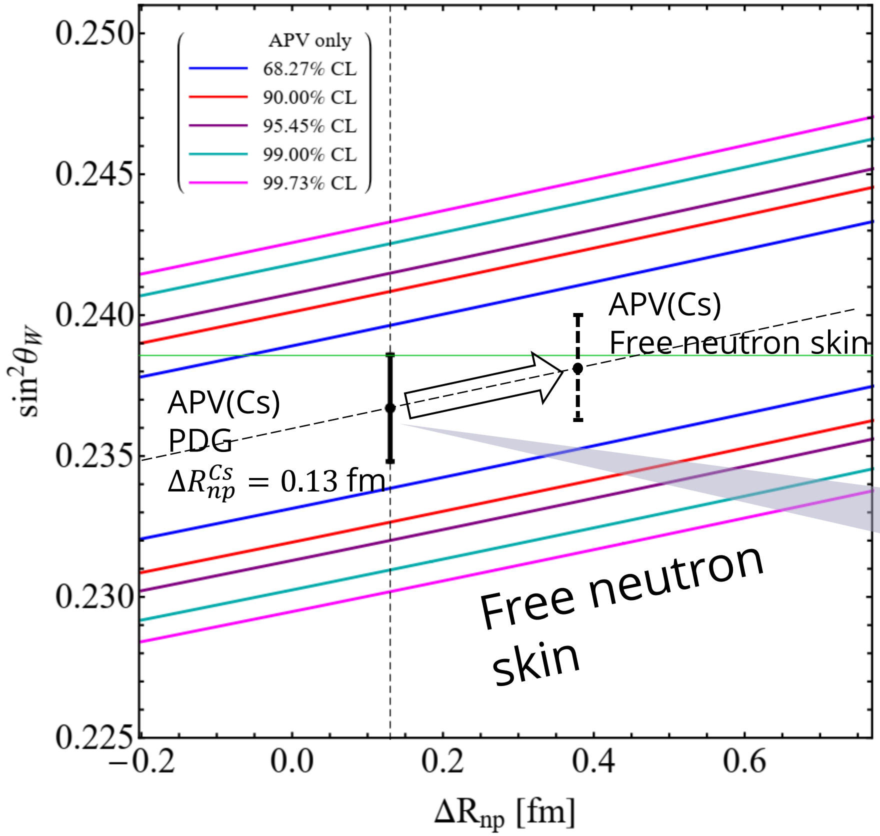

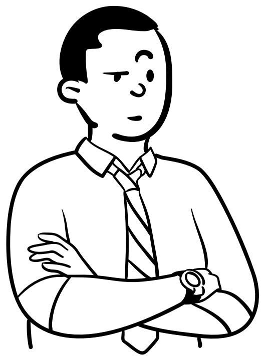

APV(Cs) PDG corresponds to $\Delta R_{np}^{Cs}(\mathrm{Extr.}) = 0.13$ fm

Extrapolated from antiprotonic atoms…

$$\sin^2\vartheta_W(\mathrm{COH-CsI}) = 0.231^{+0.027}_{-0.024}(1\sigma)^{+0.046}_{-0.039}(90\%\mathrm{CL})^{+0.058}_{-0.047}(2\sigma)$$

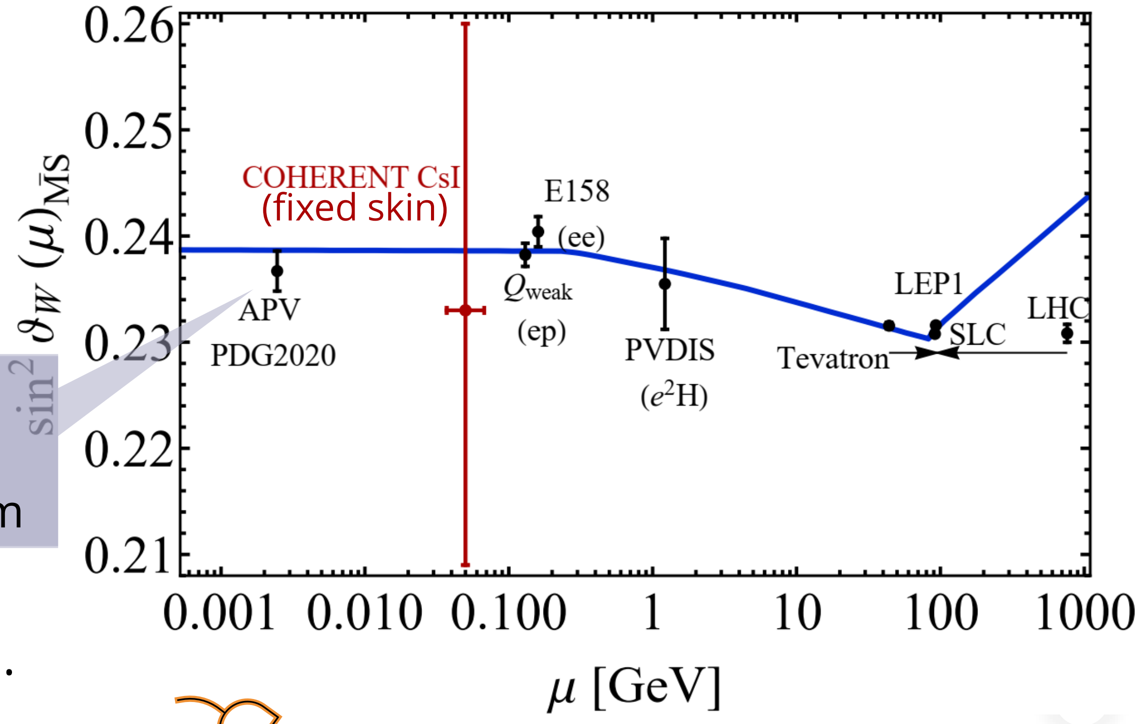

Why not combining them?

Neutrino charge radius

- In the SM the effective vertex reduces to $\gamma_\mu F(q^2)$ since the contribution $q_\mu \gamma^\mu q_\mu / q^2$ vanishes in the coupling with a conserved current

$$\Lambda_\mu(q) = (\gamma_\mu - q_\mu \gamma^\mu q_\mu / q^2) F(q^2)$$

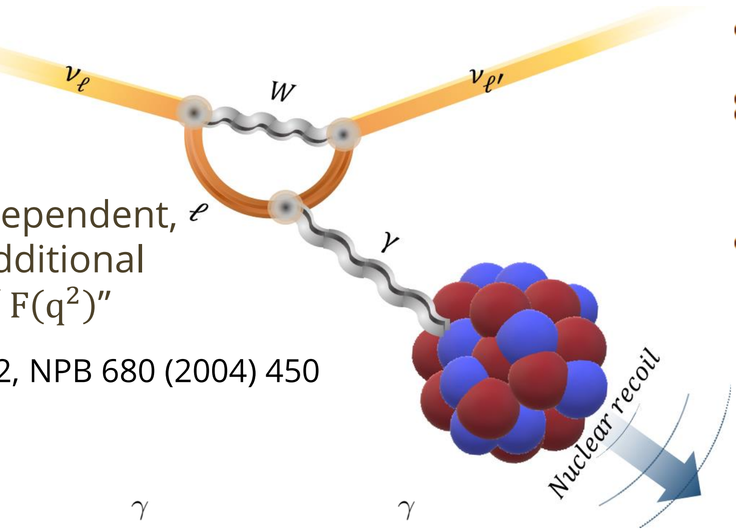

"A charge radius that is gauge-independent, finite is achieved by including additional diagrams in the calculation of $F(q^2)$"

Bernabeu et al, PRD 62 (2000) 113012, NPB 680 (2004) 450

- In the Standard Model

$$\langle r^2_{\nu_l} \rangle_{SM} = -\frac{G_F}{2\sqrt{2}\pi^2}\left[3 - 2\log\left(\frac{m_e^2}{m_W^2}\right)\right]$$

$$\langle r^2_{\nu_e} \rangle_{SM} = -8.2 \times 10^{-33}\ \mathrm{cm}^2$$

$$\langle r^2_{\nu_\mu} \rangle_{SM} = -4.8 \times 10^{-33}\ \mathrm{cm}^2$$

$$\langle r^2_{\nu_\tau} \rangle_{SM} = -3.0 \times 10^{-33}\ \mathrm{cm}^2$$

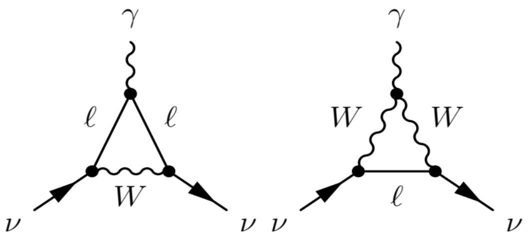

R. L. Workman et al. (Particle Data Group), "Review of Particle Physics," PTEP **2022**, 083C01 (2022).

VALUE (10^{-32} cm^2)	*CL%*	*DOCUMENT ID*		*TECN*	*COMMENT*
−2.1 to 3.3	90	[1] DENIZ	2010	TEXO	Reactor $\bar{\nu}_e e$
• • We do not use the following data for averages, fits, limits, etc. • •					
−27.5 to 3	90	[2] CADEDDU	2018		ν_μ coherent scat. on CsI
−0.53 to 0.68	90	[3] HIRSCH	2003		$\nu_\mu e$ scat.

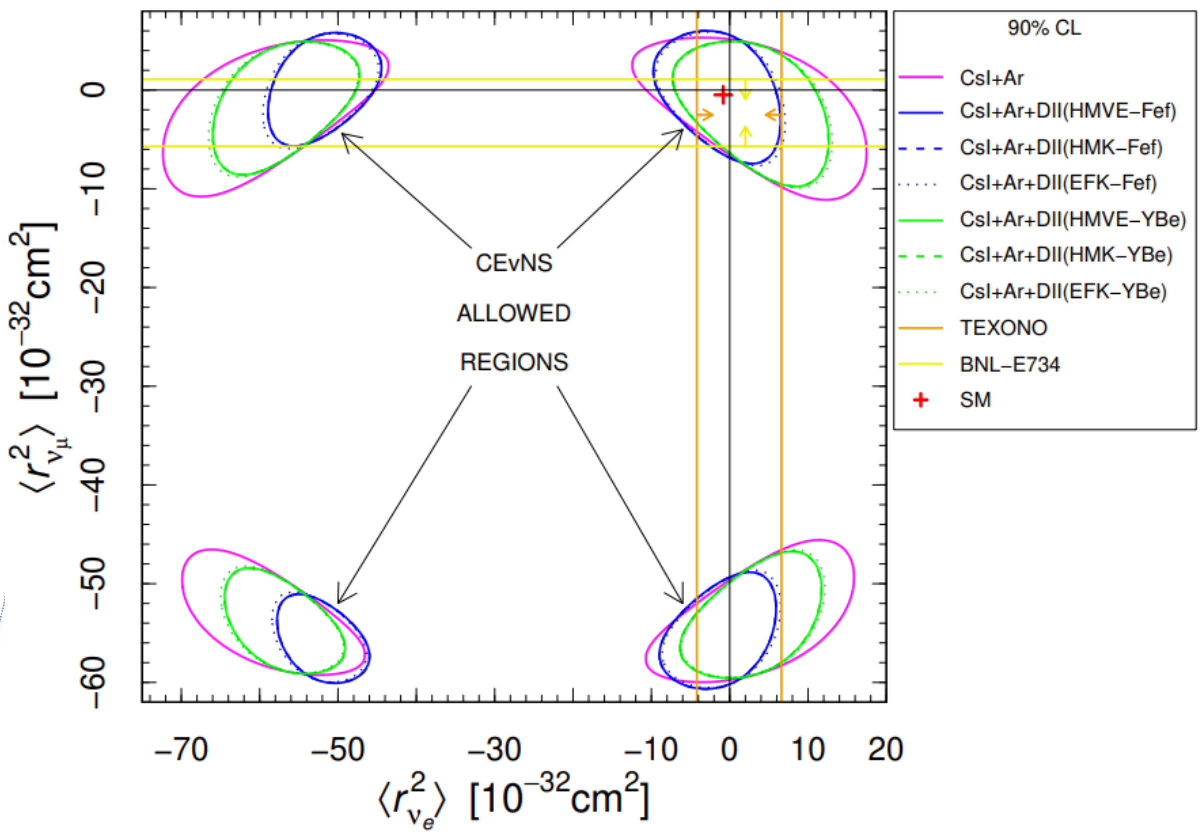

$$-7.1 < \langle r^2_{\nu_e} \rangle [10^{-32}\ \mathrm{cm}^2] < 5 \quad @\ 90\%\ \mathrm{CL}$$

M. Atzori Corona et al. **JHEP** 09 (2022) 164, arXiv:2205.09484

Current best limits:
accelerator $\nu_{e/\mu} - e$ scattering

- **TEXONO** $-4.2 < \langle r^2_{\nu_e} \rangle < \mathbf{6.6}\ [10^{-32}\mathrm{cm}^2]$
- **BNL-E734** $-5.7 < \langle r^2_{\nu_\mu} \rangle < 1.1\ [10^{-32}\mathrm{cm}^2]$ @90% CL

Constraints on light mediators from COHERENT data

M. Atzori Corona et al. JHEP 05 (2022)109, arXiv:2202.11002

New light scalar boson mediator that is assumed, for simplicity, to have universal coupling with quarks and leptons

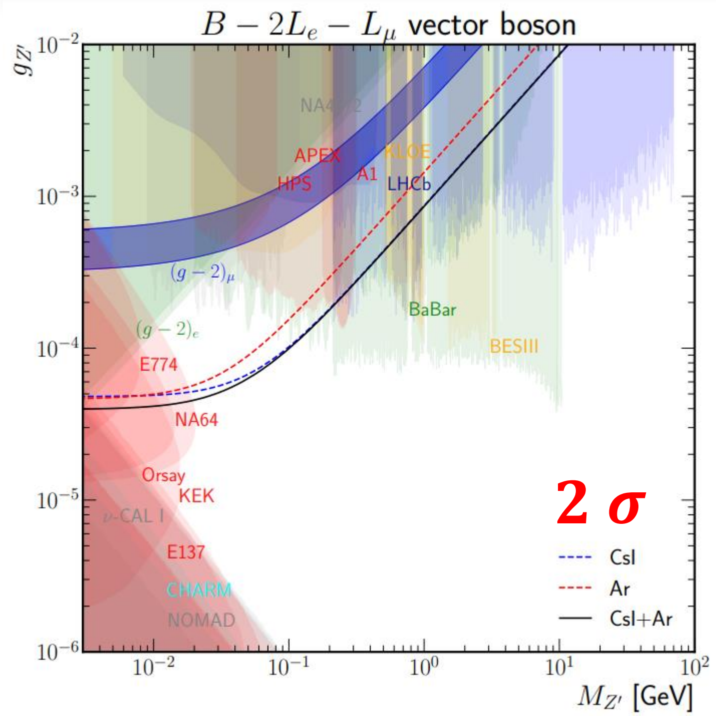

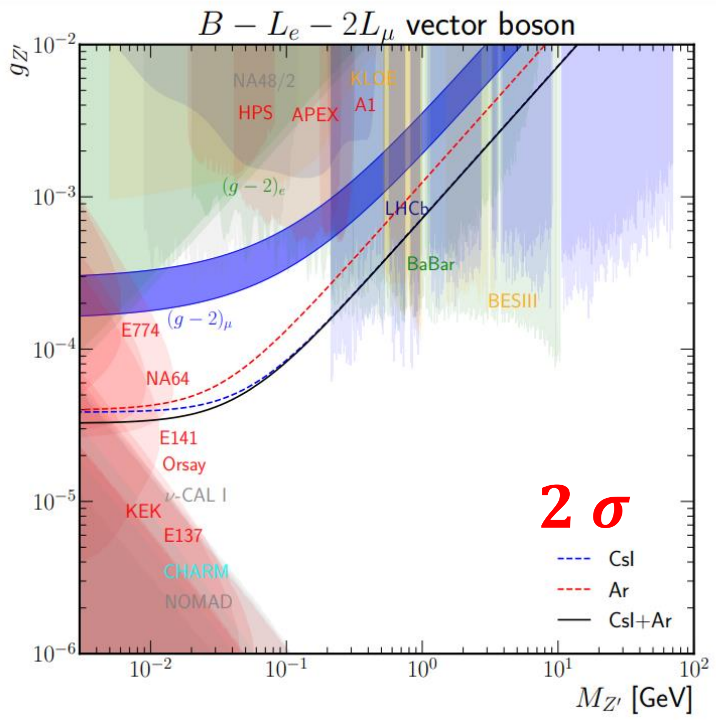

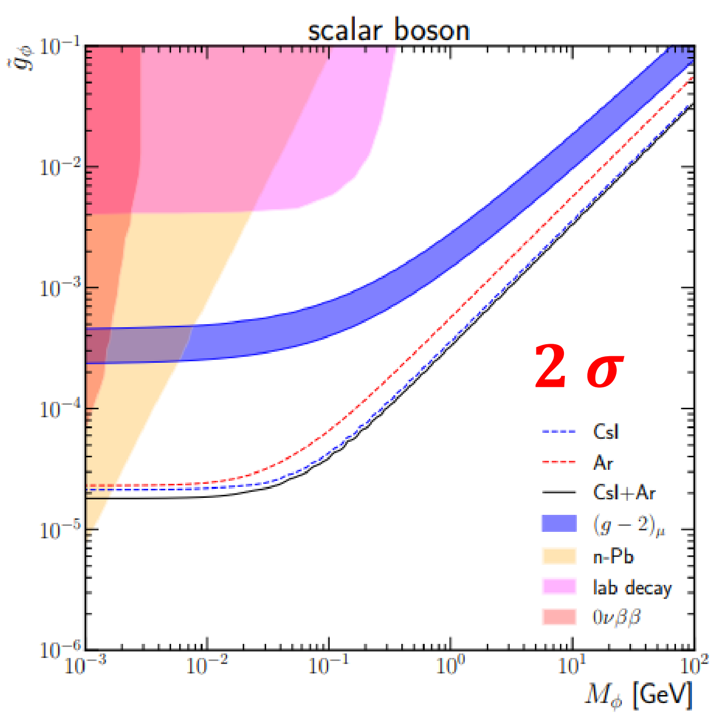

$B - 2L_e - L_\mu$

- $Q_q = 1/3$; $Q_e = -2$; $Q_\mu = -1$
- Improved constraints for $10 < M_{Z'} < 100$ MeV and $5 \times 10^{-5} < g_{Z'} < 2 \times 10^{-4}$
- $(g-2)_\mu$ excluded

$B - L_e - 2L_\mu$

- Improved constraints for $20 < M_{Z'} < 200$ MeV and $3 \times 10^{-5} < g_{Z'} < 3 \times 10^{-4}$
- $(g-2)_\mu$ excluded

Scalar mediator

- Very strong limits with CEνNS for $M_\phi > 2$ MeV
- $(g-2)_\mu$ excluded

The $L_\mu - L_\tau$ scenario

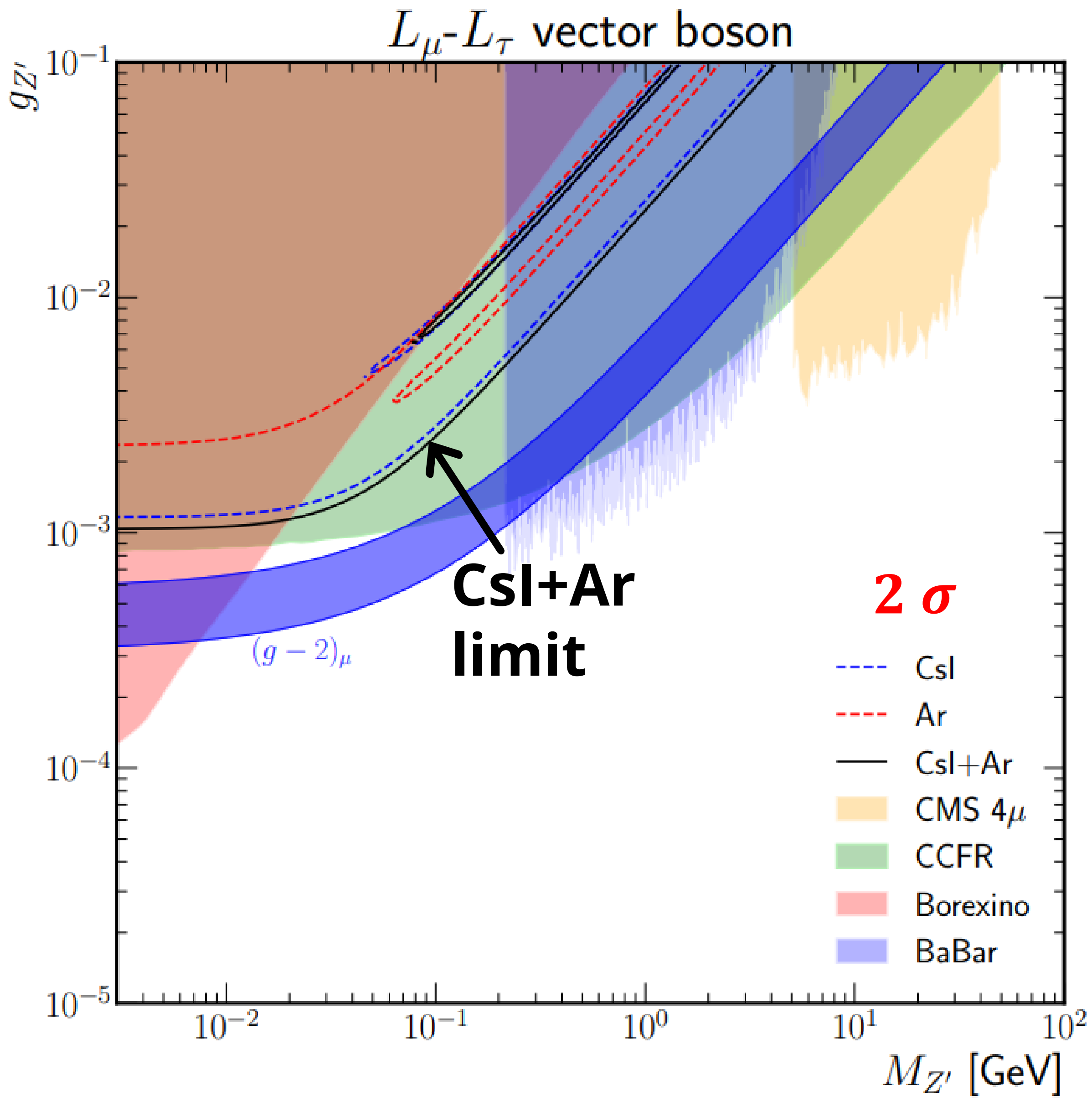

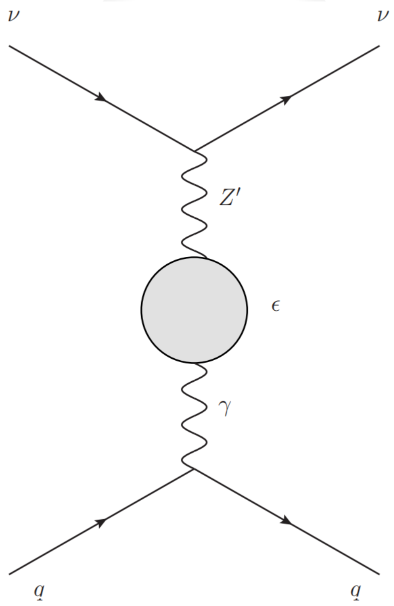

- As for all the $L_\alpha - L_\beta$ models the constraints that we can obtain from CEvNS data are weaker than those in the previous models, because the **interaction with quarks occurs only at loop level**, and hence it is weaker

- Coupling only to μ and τ flavor $Q_\mu = 1; Q_\tau = -1$
- One of the most popular model because $(\boldsymbol{g-2})_\mu$ band **is not excluded.**
- At the moment CEνNS limits are not competitive!

The $L_\mu - L_\tau$ scenario

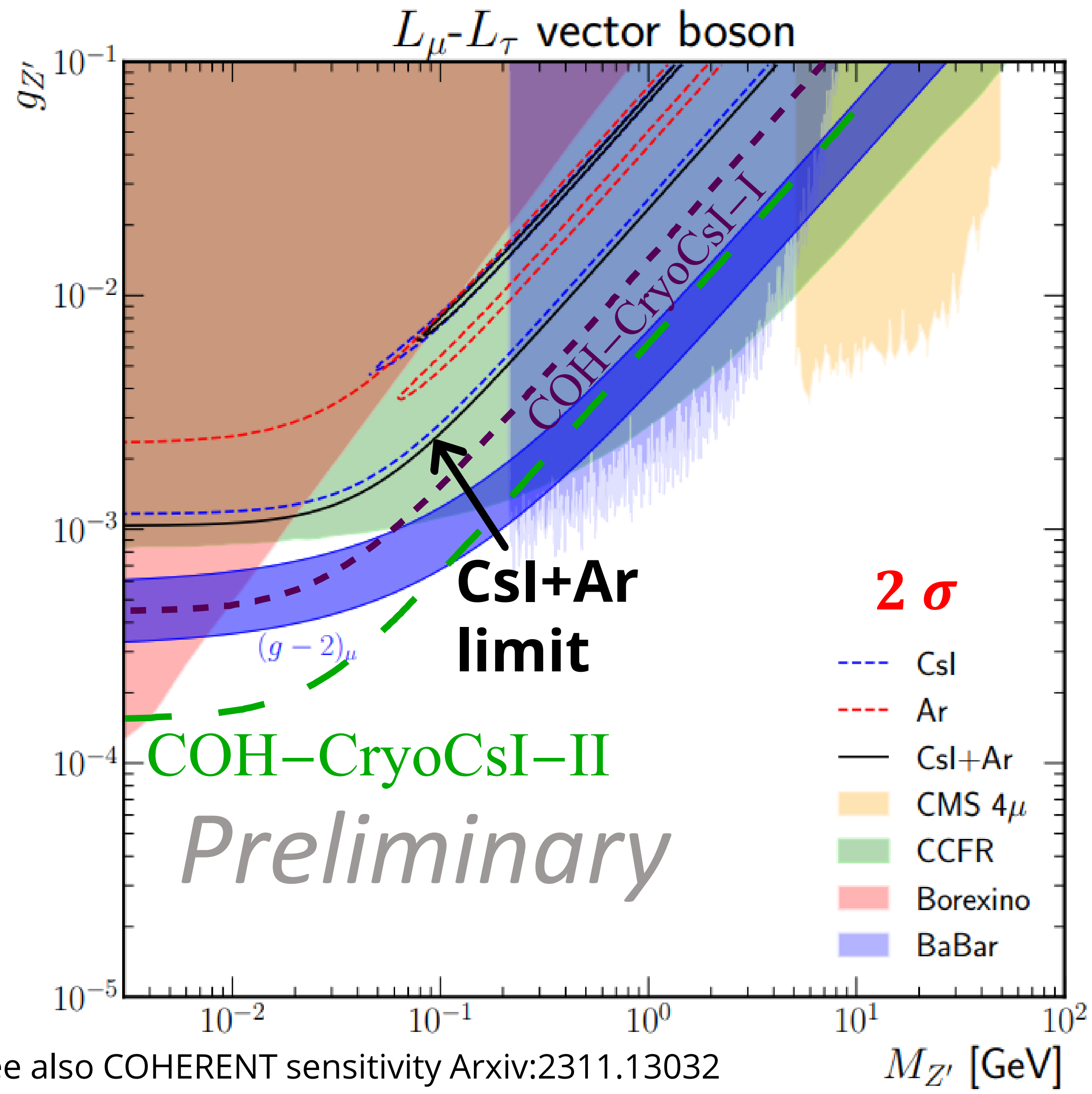

See also COHERENT sensitivity Arxiv:2311.13032

- The **situation will change** in the future thanks to the **COH-Cryo-CsI-I** and **COH-Cryo-CsI-II** detectors (See "The COHERENT Experimental Program" arXiv:2204.04575)
- ~10 kg (COH-CryoCsI-1) and a ~700 kg (COH-CryoCsI-2) cryogenic CsI detector with two target stations.

➢ The $(g-2)_\mu$ band needs to be updated after the recent result by the g-2 Collaboration @Fermilab and the new results on the hadronic vacuum polarzation contribution from lattice. See Arxiv:2308.06230

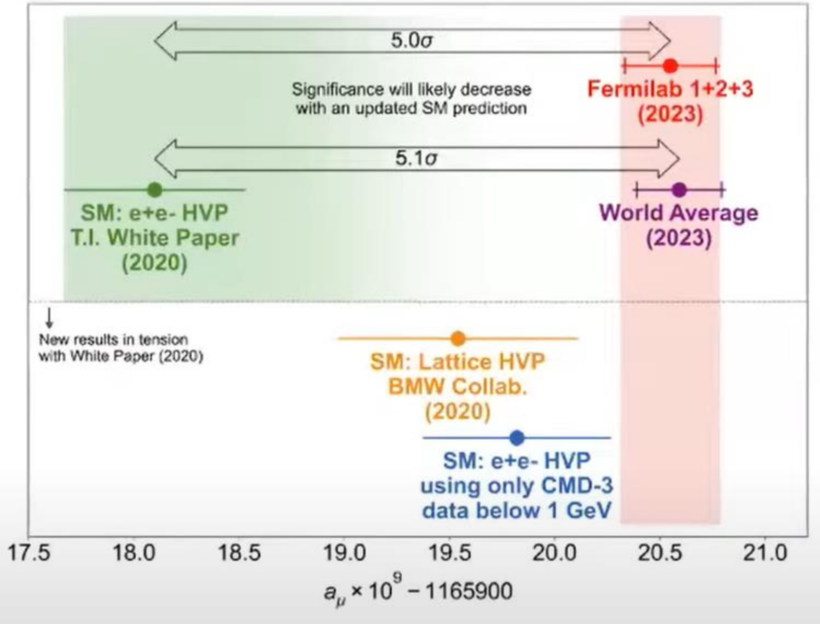

Combined 2D fit with COHERENT and APV(Cs)

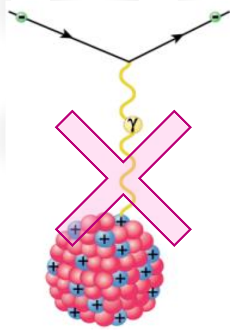

Mediated by photons. Sensitive to the charge (proton) distribution

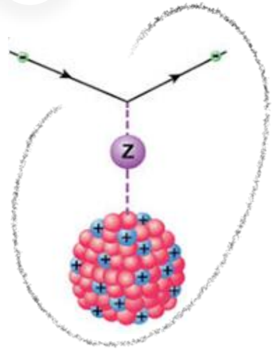

Mediated by the Z. Mostly sensitive to the weak (neutron) distribution.

M. Cadeddu and F. Dordei, PRD 99, 033010 (2019), arXiv:1808.10202

+ Atomic Parity Violation APV(Cs) and CEνNS depends both on the **weak charge** and thus on R_n(Cs) and $\sin^2\vartheta_W$

$$Q_W^{SM} \approx Z\left(1 - 4\sin^2\theta_W^{SM}\right) - N$$

+ We can combine APV(Cs) and COHERENT(CsI) to obtain a fully data driven measurement of the WMA in the low energy regime!

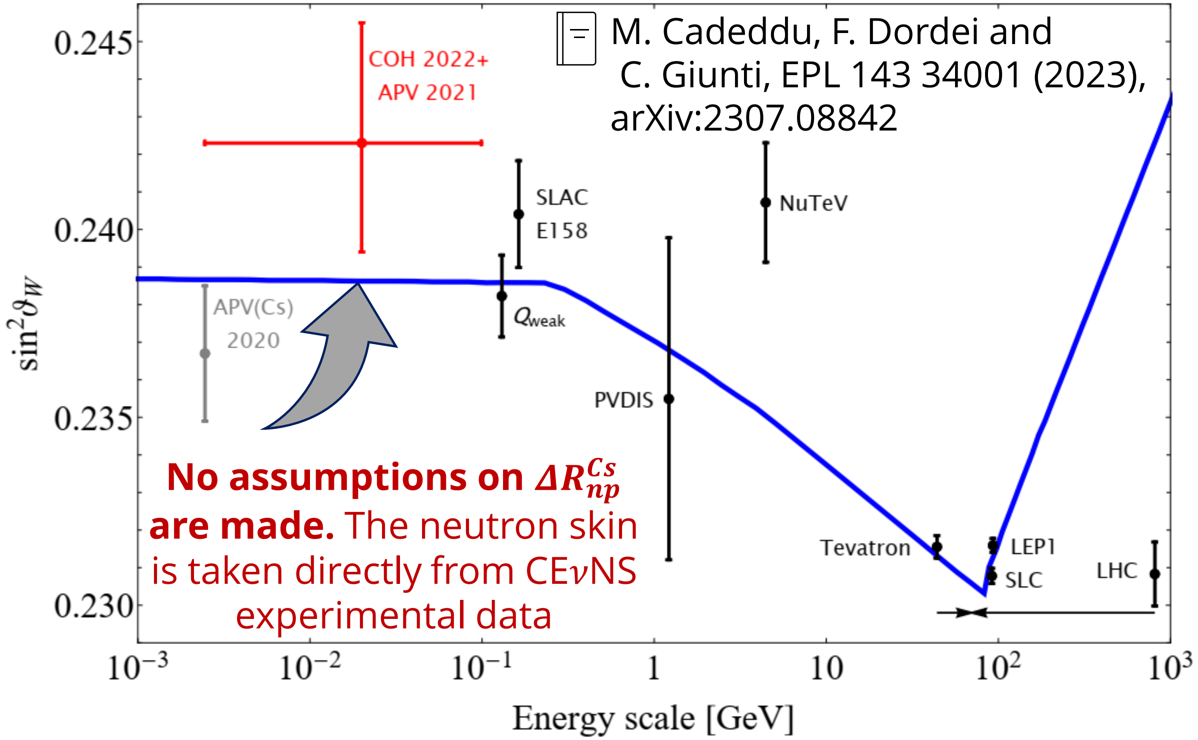

M. Cadeddu, F. Dordei and C. Giunti, EPL 143 34001 (2023), arXiv:2307.08842

No assumptions on ΔR_{np}^{Cs} are made. The neutron skin is taken directly from CEνNS experimental data

Measuring the WMA at low energies could reveal the presence of light dark Z bosons that would appear as a deviation of the SM prediction of the running depending on the value of the new mediator mass and kinetic mixing.

M. Cadeddu, N. Cargioli, F. Dordei, C. Giunti, E Picciau PRD 104, 011701 (2021), Arxiv:2104.03280

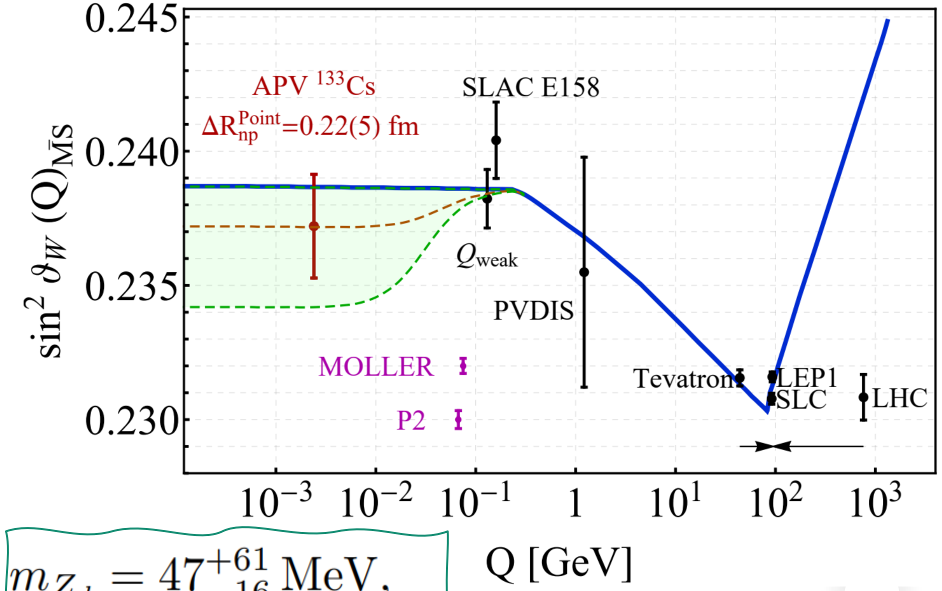

$$m_{Z_d} = 47^{+61}_{-16}\ \mathrm{MeV},$$
$$\varepsilon = 2.3^{+1.1}_{-0.4} \times 10^{-3}$$

Neutron nuclear radius in argon

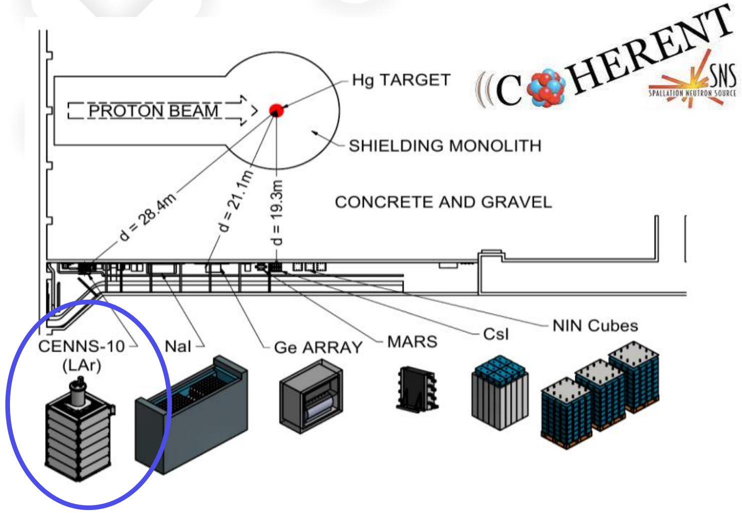

Combined fit in (time, energy, PSP) space suggest >3σ CEvNS detection significance

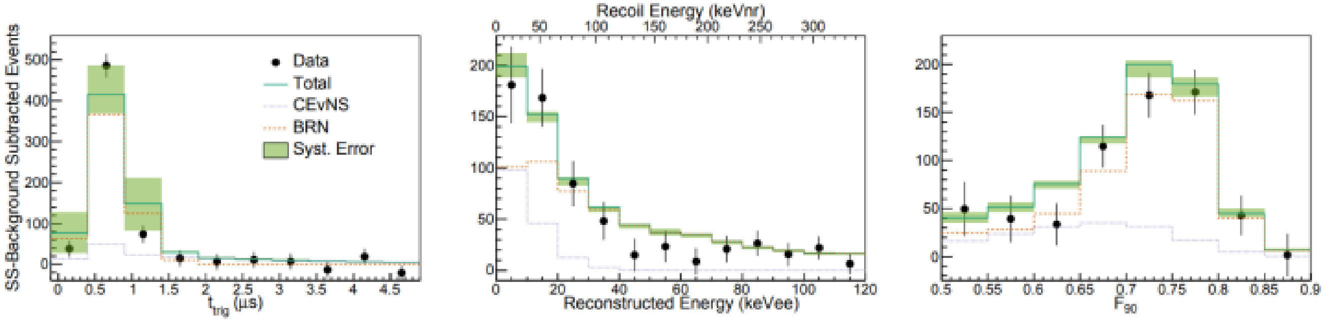

Dominant backgrounds:

1. ^{39}Ar beta decay
2. Beam related neutrons

Akimov et al, COHERENT Coll. PRL 126, 01002 (2021)

Cadeddu et al., PRD 102, 015030 (2020)

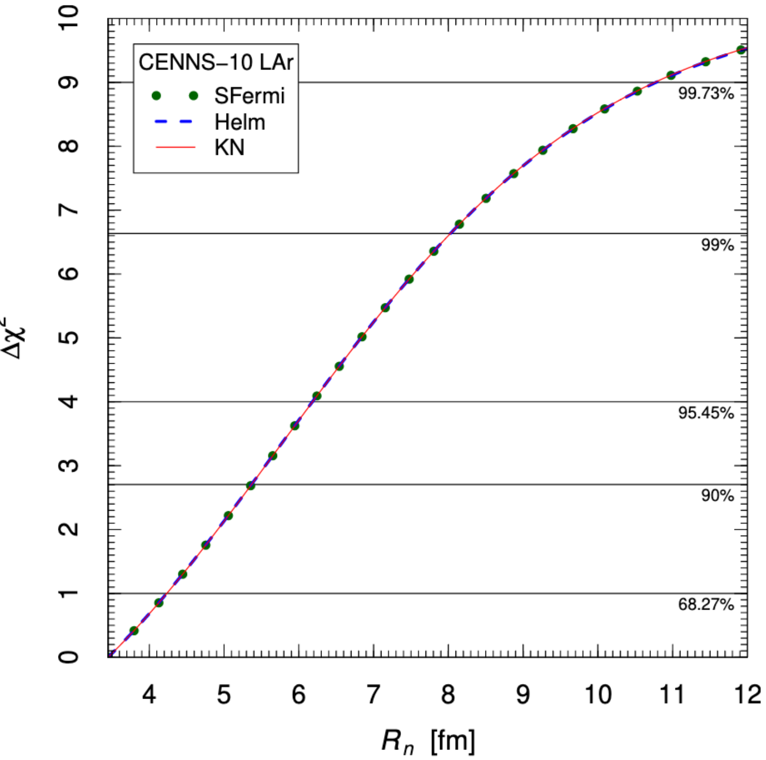

COHERENT Argon

$$R_n(^{40}\mathrm{Ar}) < 4.2 \text{ fm}$$

More statistics needed.

Theoretical values

Interaction	R_p^{point}	R_n^{point}
Sky3D		
SkI3 [37]	3.33	3.43
SkI4 [37]	3.31	3.41
Sly4 [38]	3.38	3.46
Sly5 [38]	3.37	3.45
Sly6 [38]	3.36	3.44
Sly4d [39]	3.35	3.44
SV-bas [40]	3.33	3.42
UNEDF0 [41]	3.37	3.47
UNEDF1 [42]	3.33	3.43
SkM* [43]	3.37	3.45
SkP [44]	3.40	3.48

See also:
Payne et al.,
PRC 100, 061304 (2019)

See also:
Miranda et al.,
JHEP 05 (2020) 130

COHERENT future argon: "COH-Ar-750"
LAr based detector for precision CEνNS

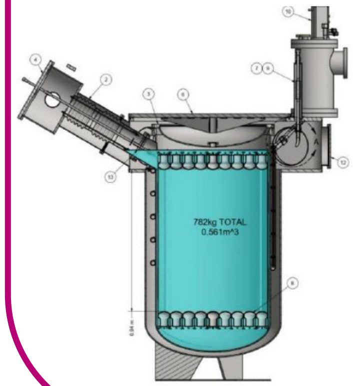

- Single phase, scintillation only, 750 kg total (610 kg fiducial)
- 3000 CEνNS/year

First average CsI neutron radius measurement (2018)

+ Using the first CsI dataset from D. Akimov et al. **Science** 357.6356 (2017)

M. Cadeddu, C. Giunti, Y.F. Li, Y.Y. Zhang, PRL 120 072501, (**2018**), arXiv:1710.02730

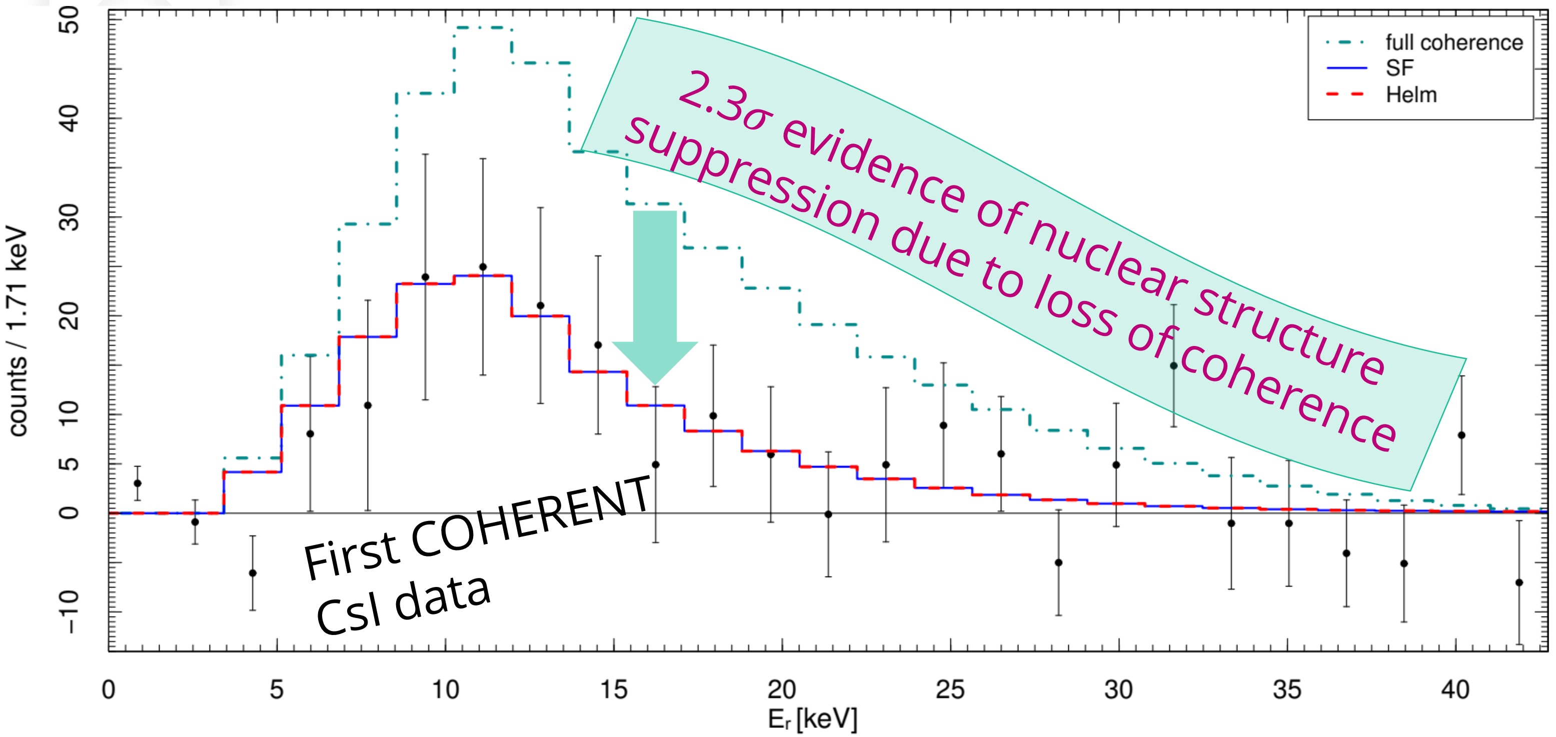

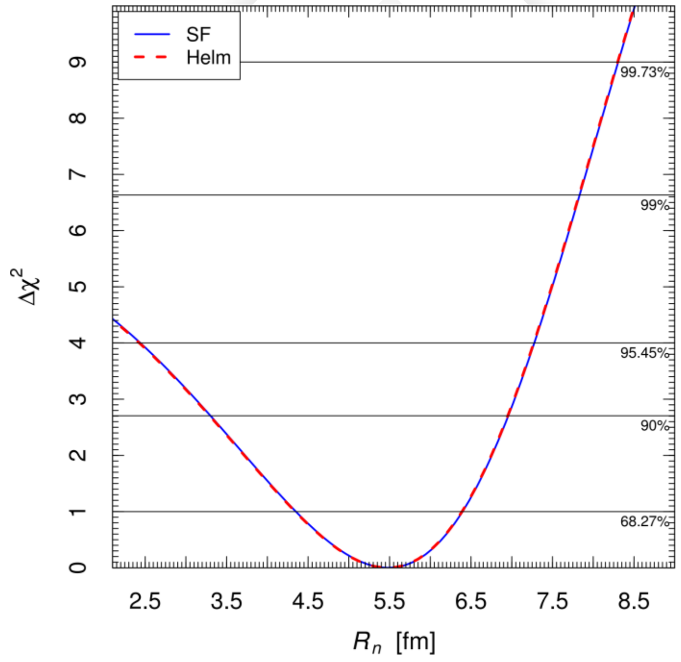

$$R_n^{CsI} = 5.5^{+0.9}_{-1.1}\ \mathrm{fm}$$

- We first compared the data with the predictions in the case of full coherence, i.e. all nuclear form factors equal to unity: the corresponding histogram does not fit the data.
- We fitted the COHERENT data in order to get information on the value of the neutron rms radius R_n, which is determined by the minimization of the χ^2 using the symmetrized Fermi (t=2.3 fm) and Helm form factors (s=0.9 fm).

✓ Only energy information used
x No energy resolution
x No time information
x Small dataset and big syst. uncer.

Improvements with the latest CsI dataset

+ New quenching factor

$$E_{ee} = f(E_{nr}) = aE_{nr} + bE_{nr}^2 + cE_{nr}^3 + dE_{nr}^4.$$

a=0.05546, b=4.307, c= -111.7, d=840.4

Akimov et al. (COHERENT Coll), arXiv:2111.02477, JINST 17 P10034 (2022)

+ 2D fit, arrival time information included

$$N_{ij}^{\mathrm{CE}\nu\mathrm{NS}} = (N_i^{\mathrm{CE}\nu\mathrm{NS}})_{\nu_\mu} P_j^{(\nu_\mu)} + (N_i^{\mathrm{CE}\nu\mathrm{NS}})_{\nu_e,\bar{\nu}_\mu} P_j^{(\nu_e,\bar{\nu}_\mu)}$$

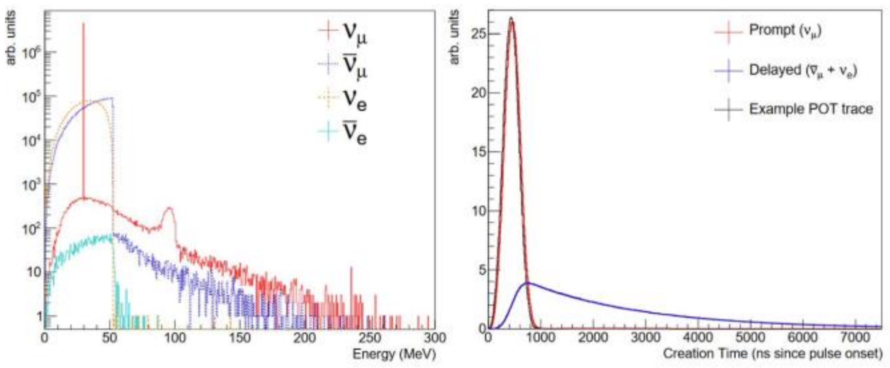

+ Doubled the statistics and reduced syst. uncertainties

$$\sigma_{\mathrm{CE}\nu\mathrm{NS}} = 13\%, \sigma_{\mathrm{BRN}} = 0.9\%,$$
$$\text{and } \sigma_{\mathrm{SS}} = 3\%$$

➢ Theoretical number of CEvNS events

$$N_i^{\mathrm{CE}\nu\mathrm{NS}} = N(\mathrm{CsI}) \int_{T_{\mathrm{nr}}^i}^{T_{\mathrm{nr}}^{i+1}} dT_{\mathrm{nr}}\, A(T_{\mathrm{nr}}) \int_0^{T'^{\max}_{\mathrm{nr}}} dT'_{\mathrm{nr}}\, R(T_{\mathrm{nr}}, T'_{\mathrm{nr}}) \int_{E_{\min}(T'_{\mathrm{nr}})}^{E_{\max}} dE \times \sum_{\nu=\nu_e,\nu_\mu,\bar{\nu}_\mu} \frac{dN_\nu}{dE}(E) \frac{d\sigma_{\nu\text{-CsI}}}{dT'_{\mathrm{nr}}}(E, T'_{\mathrm{nr}}),$$

➢ With the inclusion of energy resolution

$$R(N_{\mathrm{PE}}, N'_{\mathrm{PE}}) = \frac{[a_R(1+b_R)]^{1+b_R}}{\Gamma(1+b_R)} N_{\mathrm{PE}}^{b_R}\, e^{-a_R(1+b_R)N_{\mathrm{PE}}}$$

✓ Analysis with a Gaussian least-square function

$$\chi^2_{\mathrm{C}} = \sum_{i=2}^{9} \sum_{j=1}^{11} \left(\frac{N_{ij}^{\exp} - \sum_{z=1}^{3} (1+\eta_z) N_{ij}^z}{\sigma_{ij}} \right)^2 + \sum_{z=1}^{3} \left(\frac{\eta_z}{\sigma_z} \right)^2,$$

Cadeddu et al., PRC 104, 065502 (2021), arXiv:2102.06153

Analysis updated in this talk using a Poissonian least-square function after the COHERENT data release!

arXiv:2303.09360

Atomic Parity Violation in cesium APV(Cs)

M. Cadeddu and F. Dordei, PRD 99, 033010 (2019), arXiv:1808.10202

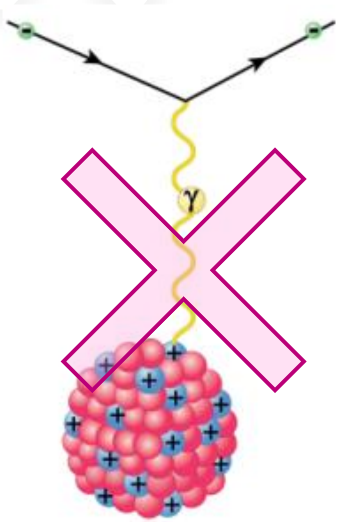

Interaction mediated by the photon and so mostly sensitive to the charge (proton) distribution

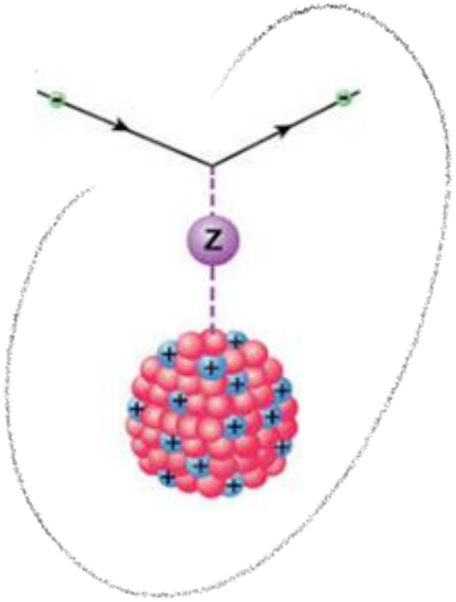

Interaction mediated by the Z boson and so mostly sensitive to the weak (neutron) distribution.

+ Parity violation in an atomic system can be observed as an **electric dipole transition amplitude between two atomic states with the same parity**, such as the $6S$ and $7S$ states in cesium.

   - Indeed, a transition between two atomic states with same parity is forbidden by the parity selection rule and cannot happen with the exchange of a photon.

   - ✓ However, an electric dipole transition amplitude can be induced by a Z boson exchange between atomic electrons and nucleons → Atomic Parity Violation (APV) or Parity Non Conserving (PNC).

+ The quantity that is measured is the usual **weak charge**

$$Q_W^{SM} \approx Z\left(1 - 4\sin^2\theta_W^{SM}\right) - N$$

Extracting the weak charge from APV

$$Q_W = N\left(\frac{\mathrm{Im}\,E_{\mathrm{PNC}}}{\beta}\right)_{\mathrm{exp.}}\left(\frac{Q_W}{N\,\mathrm{Im}\,E_{\mathrm{PNC}}}\right)_{\mathrm{th.}}\beta_{\mathrm{exp.+th.}}$$

+ Experimental value of electric dipole transition amplitude between 6S and 7S states in Cs

C. S. Wood et al., Science **275**, 1759 (1997)

J. Guena, et al., PRA **71**, 042108 (2005)

PDG2020 average

$$\mathrm{Im}\left(\frac{E_{\mathrm{PNC}}}{\beta}\right) = -\,1.5924(55)\ \mathrm{mV/cm}$$

✓ Theoretical amplitude of the electric dipole transition

$$E_{\mathrm{PNC}} = \sum_n \left[\frac{\langle 6s|H_{\mathrm{PNC}}|np_{1/2}\rangle\langle np_{1/2}|\mathbf{d}|7s\rangle}{E_{6s}-E_{np_{1/2}}} + \frac{\langle 6s|\mathbf{d}|np_{1/2}\rangle\langle np_{1/2}|H_{\mathrm{PNC}}|7s\rangle}{E_{7s}-E_{np_{1/2}}}\right],$$

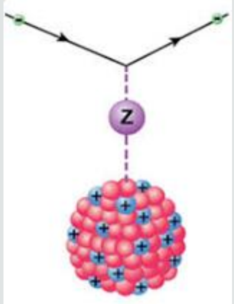

- where ***d*** is the electric dipole operator, and

$$H_{\mathrm{PNC}} = -\frac{G_F}{2\sqrt{2}} Q_W \gamma_5 \rho(\mathbf{r})$$

Value of ImE_{PNC} used by PDG (V. Dzuba *et al.*, PRL 109, 203003 (2012))

$$\mathrm{Im}\,E_{\mathrm{PNC}} = (0.8977 \pm 0.0040)\times 10^{-11}|e|\,a_B\,Q_W/N$$

see also

nuclear Hamiltonian describing the **electron-nucleus weak interaction**

$\rho(\mathbf{r}) = \rho_p(\mathbf{r}) = \rho_n(\mathbf{r}) \rightarrow$ **neutron skin correction** needed

β: tensor transition polarizability

It characterizes the size of the Stark mixing induced electric dipole amplitude (external electric field)

Bennet & Wieman, PRL 82, 2484 (1999)
Dzuba & Flambaum, PRA 62 052101 (2000)

PDG2020 average

β = 27.064 (33) a_B^3

NEW result on ImE_{PNC} !

- I will refer with APV2021 when usign Im E_{PNC} from B. K. Sahoo et al. PRD 103, L111303 (2021)

Weak mixing angle from APV(Cs)

Historically APV(Cs) has been used to estract the lowest energy determination of the weak mixing angle.

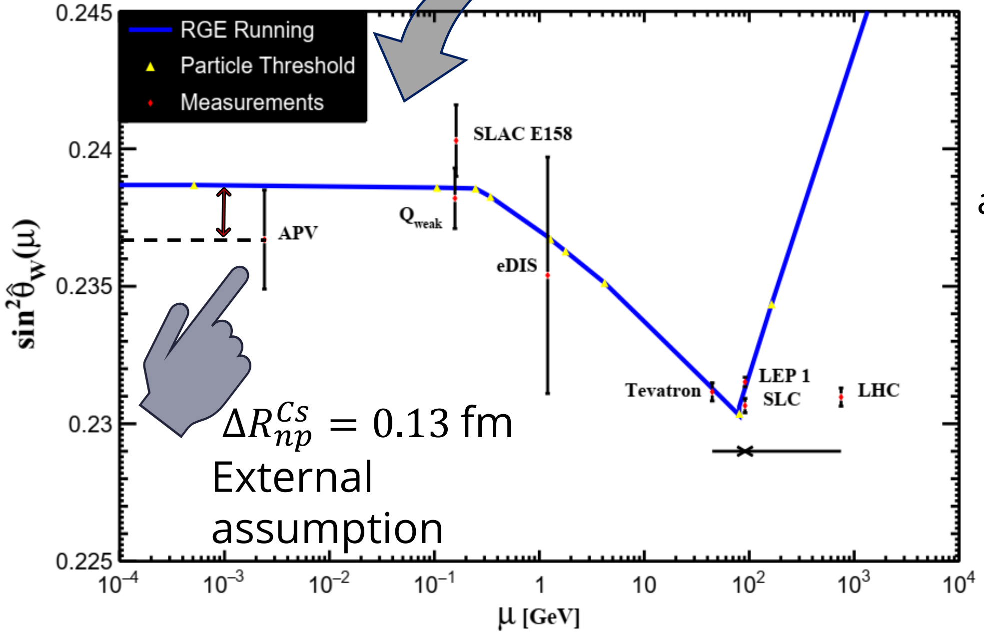

R. L. Workman et al. (Particle Data Group), "Review of Particle Physics," PTEP **2022**, 083C01 (2022).

However R_n(Cs) (or the neutron skin) has been taken from **indirect measurements** using antiprotonic atoms, which are known to be affected by considerable model dependencies

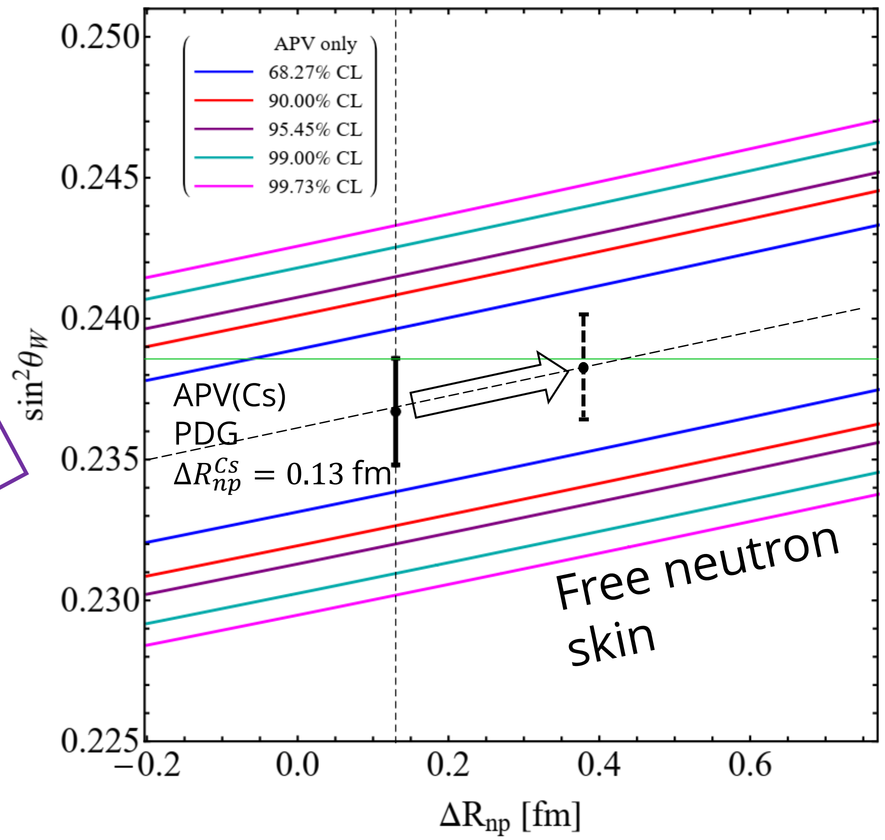

\+ In order to measure R_n one has to subtract to the so-called "neutron skin" correction in order to obtain

$$\delta E_{\rm PNC}^{\rm n.s.}(R_n) = \left[({\rm N}/Q_W)\left(1 - (q_n(R_n)/q_p)\right) E_{\rm PNC}^{\rm w.n.s.} \right]$$

$$q_{p,n} = 4\pi \int_0^\infty \rho_{p,n}(r) f(r) r^2 {\rm d}r$$

Where **ρ(r) are the proton and neutron densities** in the nucleus.

✓ The theoretical PNC amplitude of the electric dipole transition is calculated from atomic theory to be

$$\mathrm{Im}\, E_{\rm PNC} = (0.8977 \pm 0.0040) \times 10^{-11} |e|\, a_B\, Q_W / N$$

Value of ImE_{PNC} used by PDG (V. Dzuba *et al.*, PRL 109, 203003 (2012))
I will refer to it with "APV PDG".

But, we also use

NEW result on ImE_{PNC} !

- I will refer with APV 2021 when usign Im E_{PNC} from B. K. Sahoo et al. PRD 103, L111303 (2021)

Atomic Parity Violation for weak mixing angle measurements

✓ Weak charge in the SM including radiative corrections

Using SM prediction at low energy
$\sin^2\hat{\theta}_W(0) = 0.23857(5)$

$$Q_W^{SM+\text{r.c.}} \equiv -2[Z(g_{AV}^{ep} + 0.00005) + N(g_{AV}^{en} + 0.00006)]\left(1 - \frac{\alpha}{2\pi}\right) \approx Z(1 - 4\sin^2\theta_W^{SM}) - N$$

Theoretically

$$Q_W^{SM\ \text{th}}({}^{133}_{55}Cs) = -73.23(1)$$

1σ difference

Experimentally

$$Q_W^{\text{exp.}}({}^{133}_{55}Cs) = -72.82(42)$$

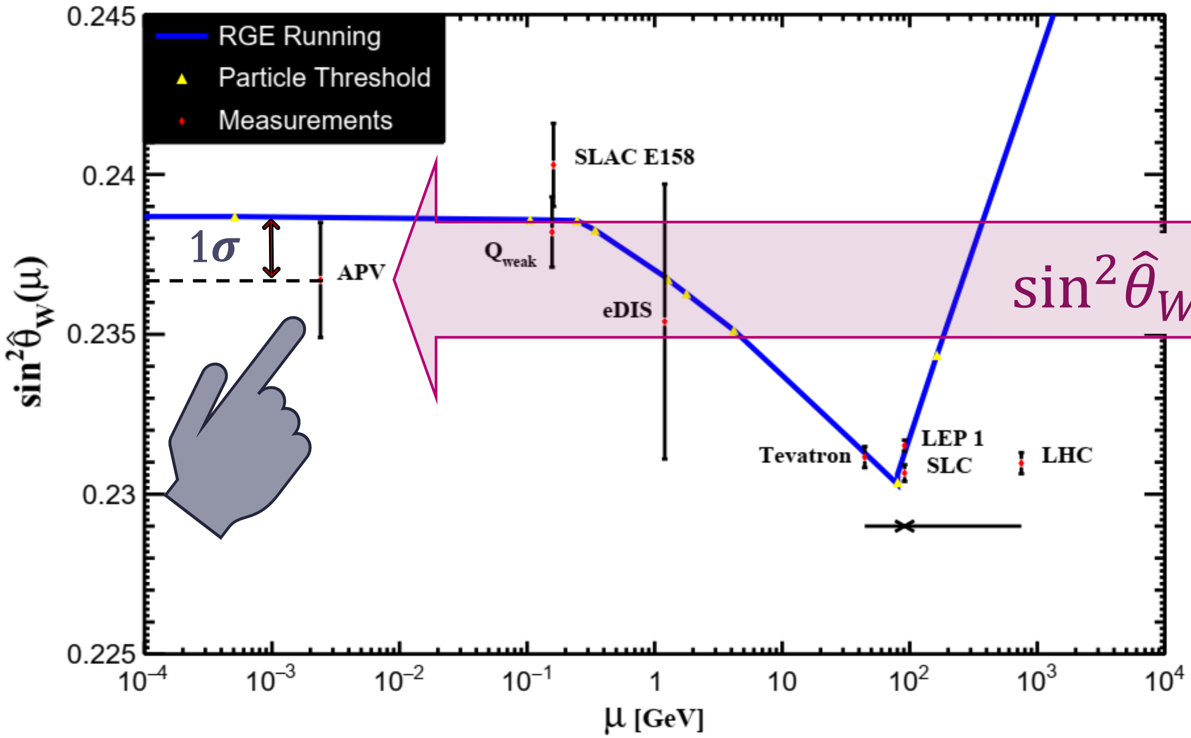

$\sin^2\hat{\theta}_W(2.4\ \text{MeV})=0.2367\pm0.0018$

But which Cs neutron skin correction is used?

R. L. Workman et al. (Particle Data Group), "Review of Particle Physics," PTEP **2022**, 083C01 (2022).

The dilemma

APV (Cs)

- Sensitive to the weak mixing angle
- Similarly sensitive to the neutron skin

COHERENT (CsI)

- CEνNS is sensitive to the neutron skin
- But less sensitive to the weak mixing angle

$$\sin^2\vartheta_W(\mathrm{COH-CsI}) = 0.231^{+0.027}_{-0.024}(1\sigma)^{+0.046}_{-0.039}(90\%\mathrm{CL})^{+0.058}_{-0.047}(2\sigma)$$

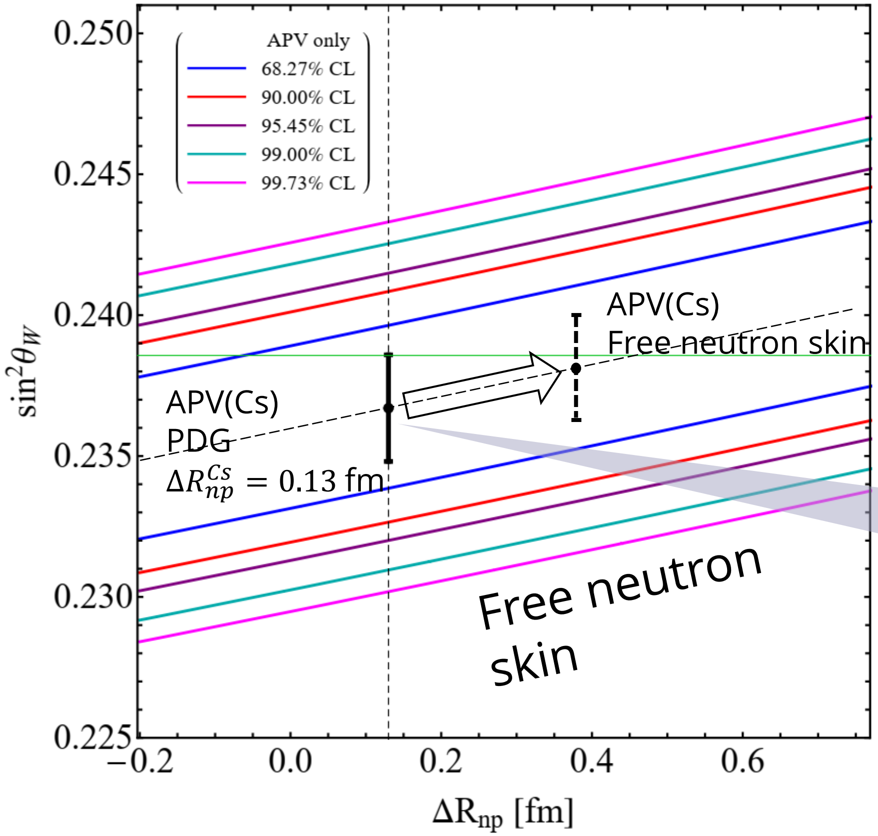

APV(Cs) PDG corresponds to $\Delta R_{np}^{Cs}(\mathrm{Extr.}) = 0.13$ fm

Extrapolated from antiprotonic atoms…

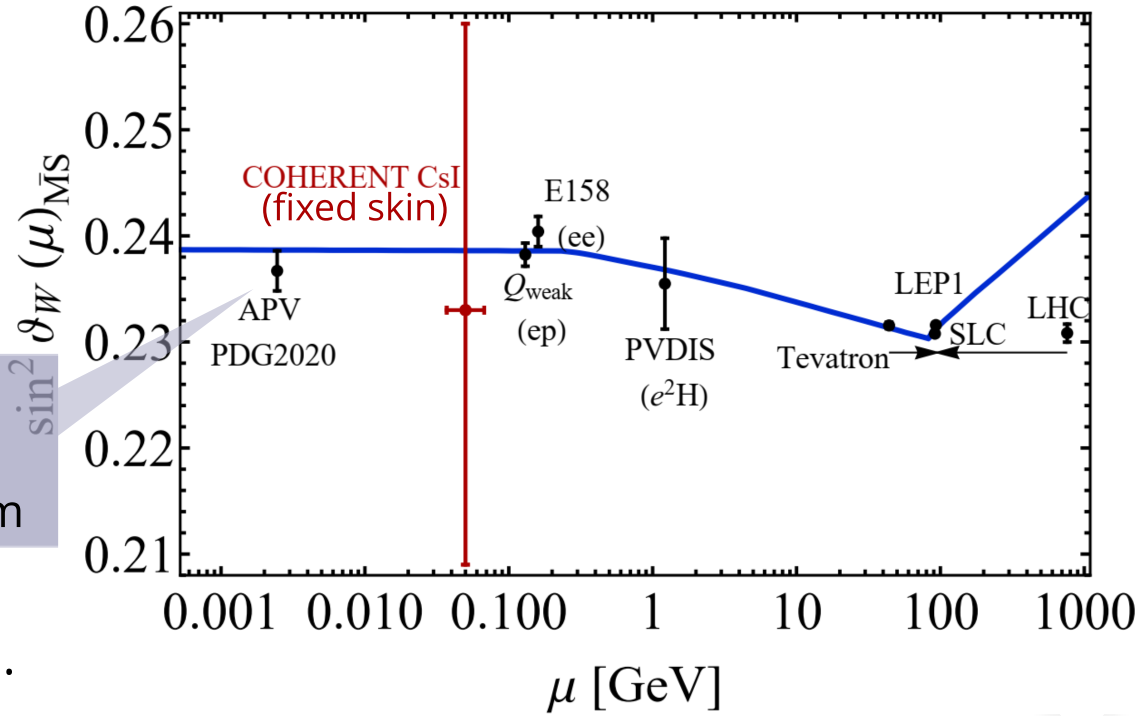

Extrapolated value of ΔR_{np}^{Cs}

+ Neutron-skin of a variety of nuclei as extracted from **antiprotonic data** as a function of the asymmetry parameter, I.

✓ From this **linear fit** one obtains the relation for the neutron skin for every nuclei

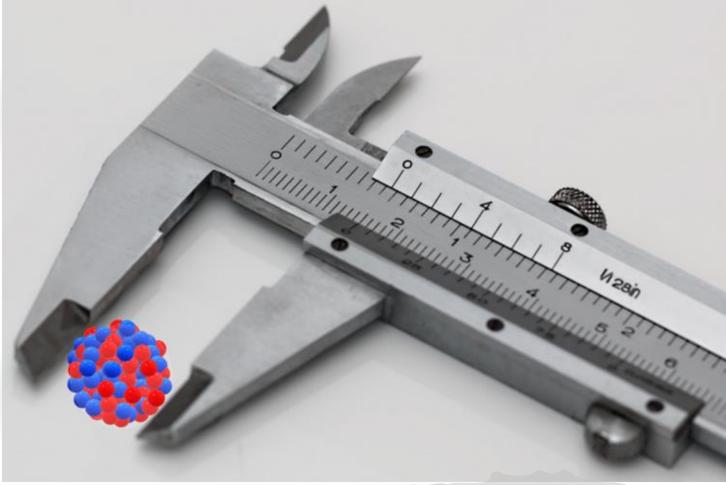

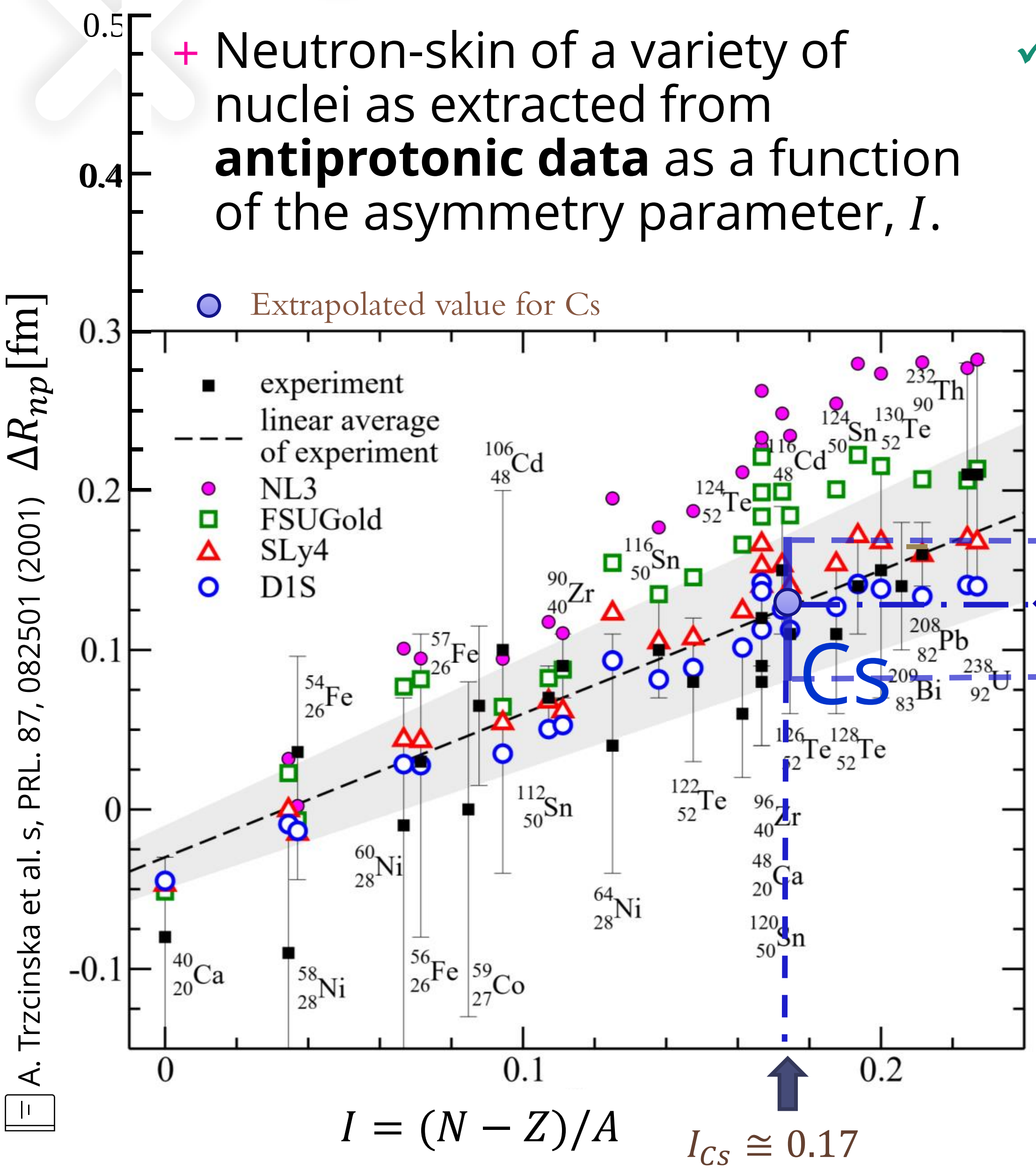

$$\Delta R_{np}[\mathrm{fm}] = -(0.04 \pm 0.03) + (1.01 \pm 0.15)\frac{N-Z}{A}$$

For cesium it gives

$$\Delta R_{np}^{Cs}(\mathrm{extrap}) \cong 0.13 \pm 0.04\ \mathrm{fm}$$

Extrapolated (not measured) value for cesium! ⚠

Antiprotonic data: radiochemical and the other based on x-ray data constraining the neutron distribution at the nuclear periphery

M. Thiel et al., Journal of Physics G, 46, 9 (2019), arXiv:1904.12269v1

Extrapolated value of ΔR_{np}^{Cs}

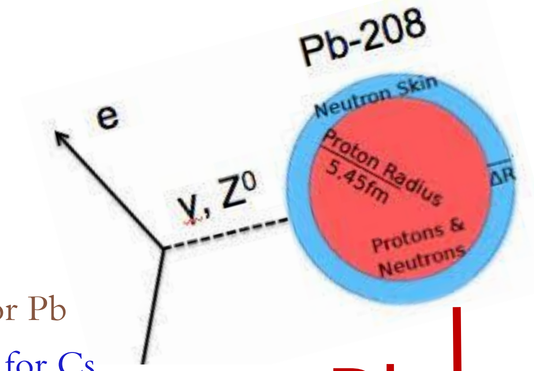

PREX-I & PREX-II

$\Delta R_{np}^{Pb} = 0.283 \pm 0.071$ fm

D. Adhikari *et al.* PRL 126, 172502 (2021)

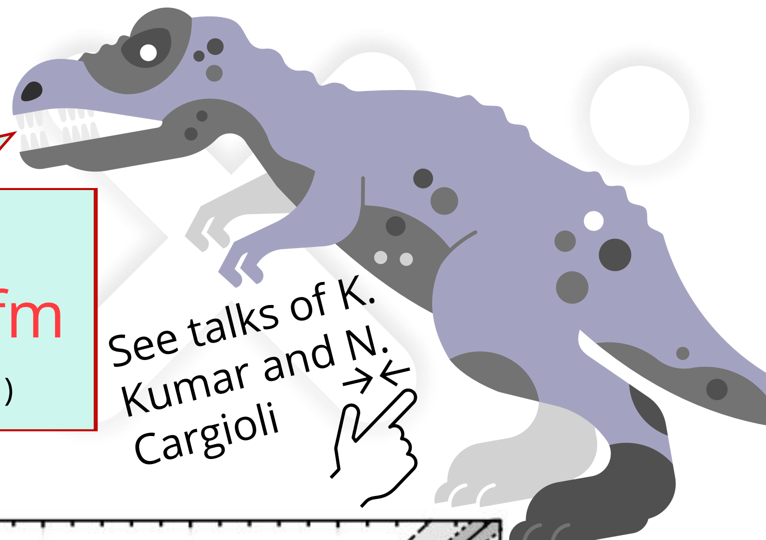

See talks of K. Kumar and N. Cargioli

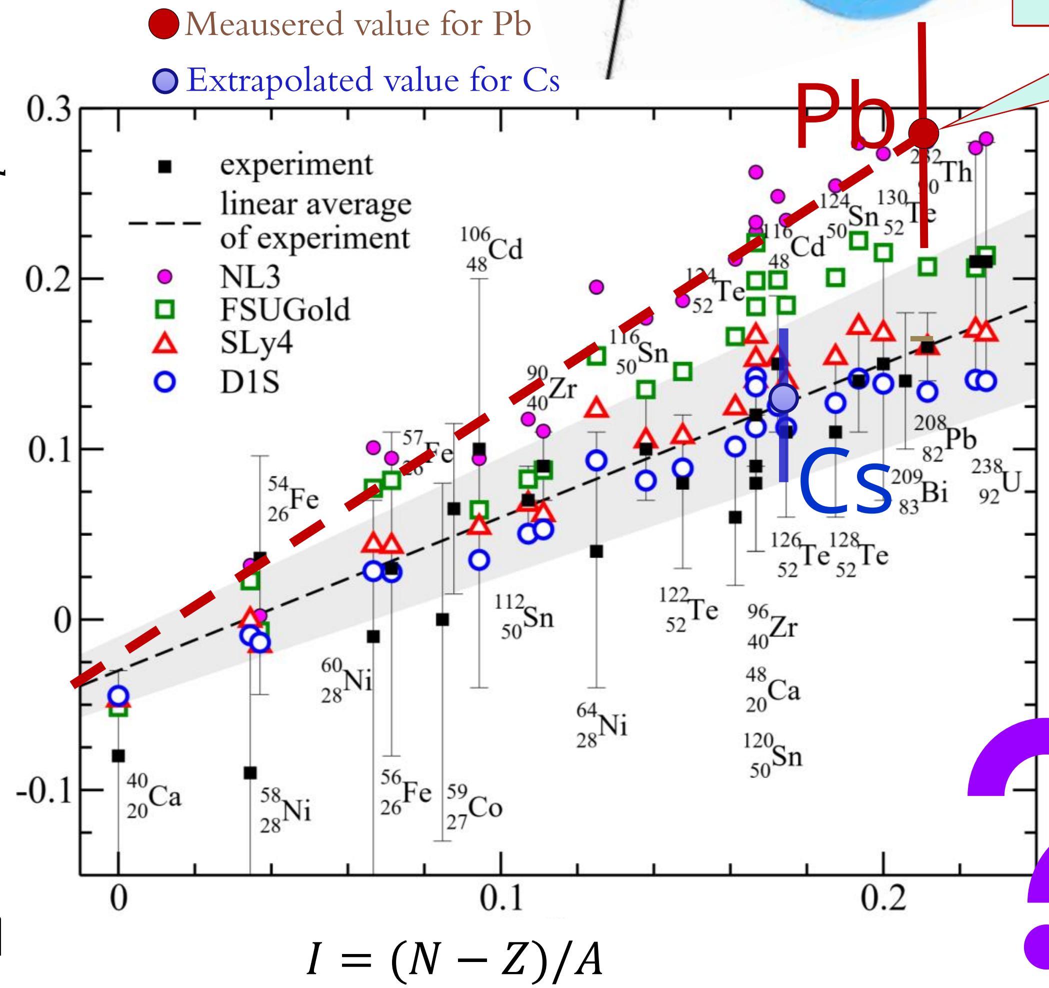

A. Trzcinska et al. s, PRL. 87, 082501 (2001

?

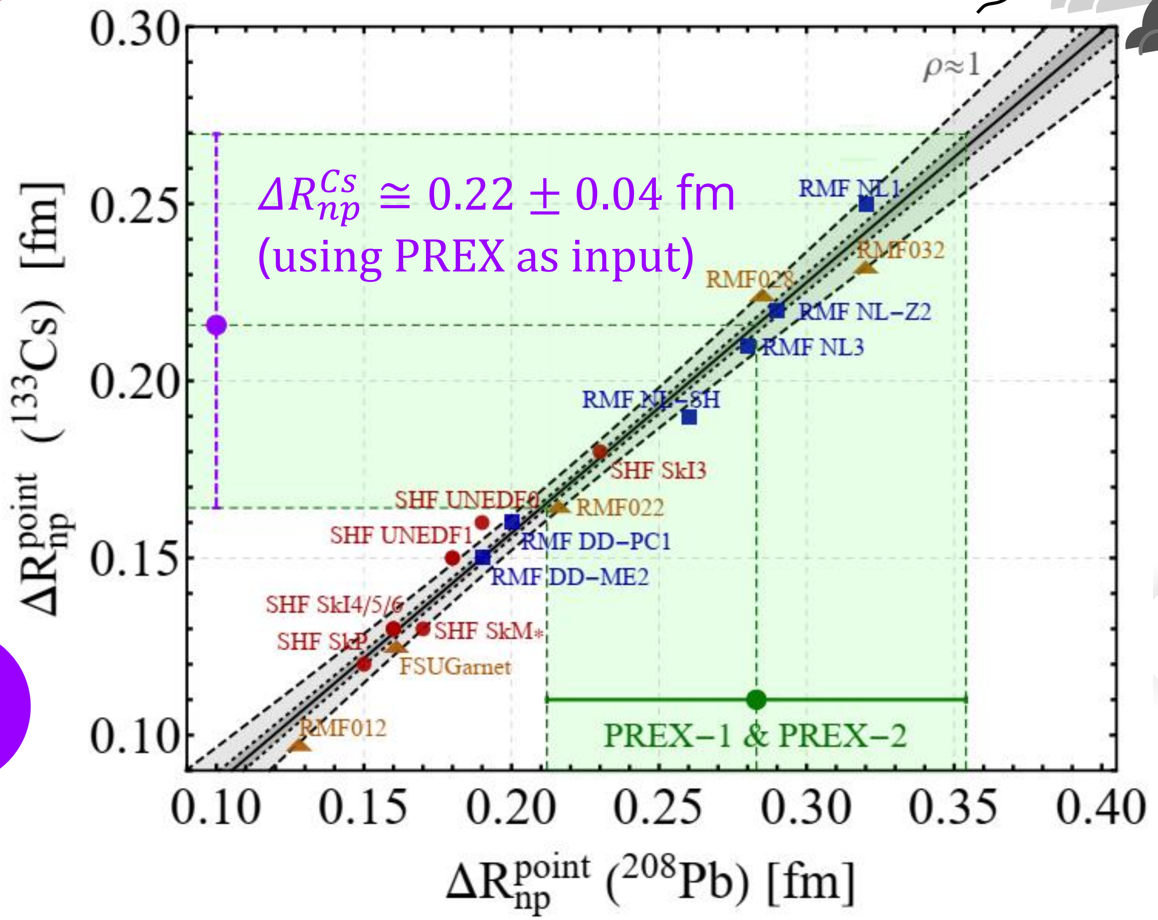

M. Cadeddu et al. PRD 104, L011701 (2021), arXiv:2104.03280

The past, present and future of R_n measurements with CEνNS and PVES

See details in **D. Akimov et al., arXiv:2204.04575 (2022)**

- **COH-CryoCsI-I**: 10 kg, cryogenic temperature ($\sim 40K$), twice the light yield of present CsI crystal at 300K
- **COH-CryoCsI-II**: 700 kg undoped CsI detector. Both lower energy threshold of 1.4 keVnr while keeping the shape of the energy efficiency of the present COHERENT CsI.

COHERENT future argon: "COH-LAr-750"
LAr based detector for precision CEνNS

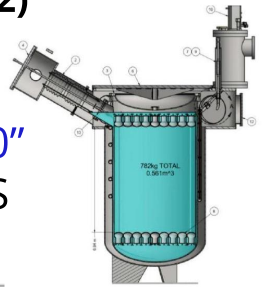

Single phase, scintillation only, 750 kg total (610 kg fiducial)
✓ 3000 CEνNS/year

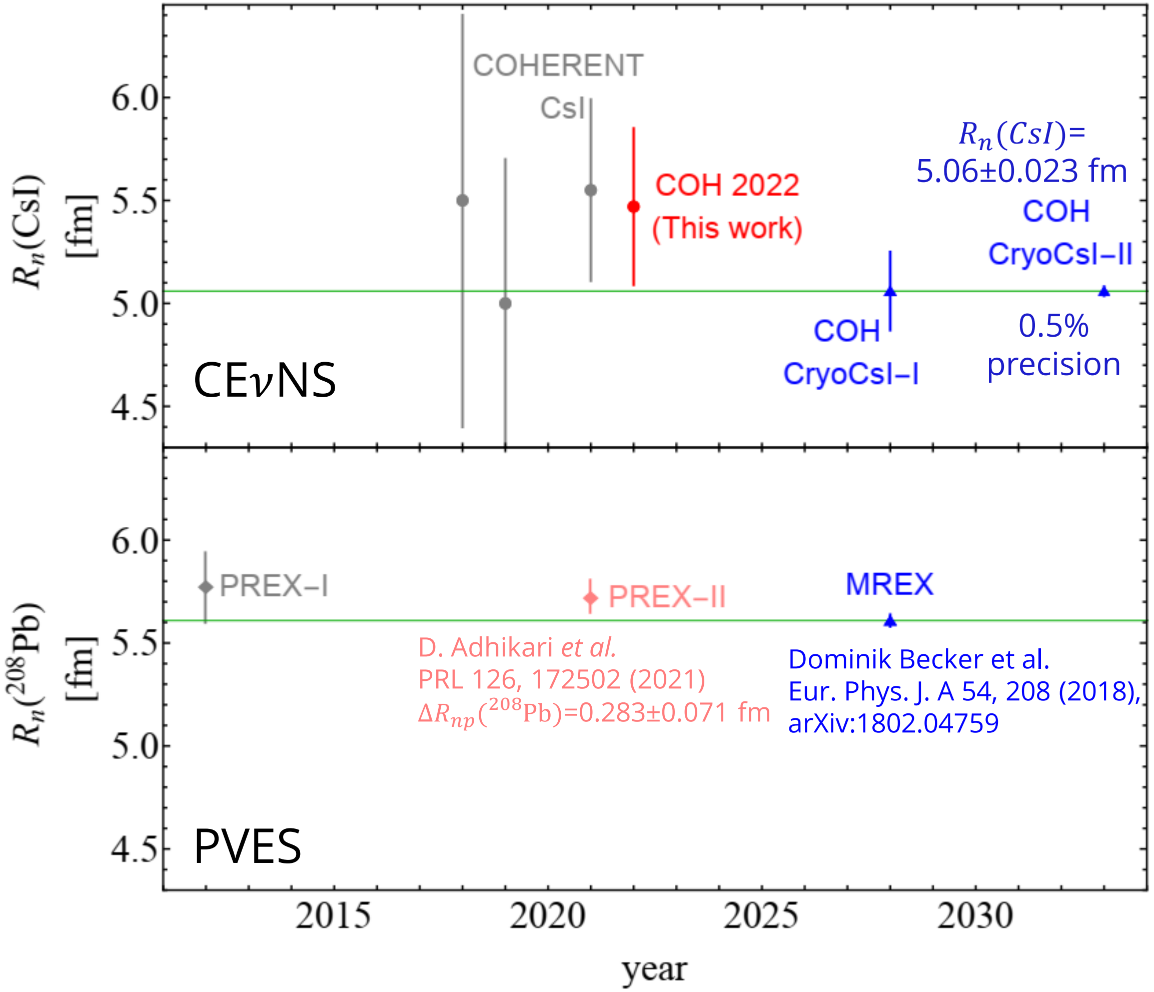

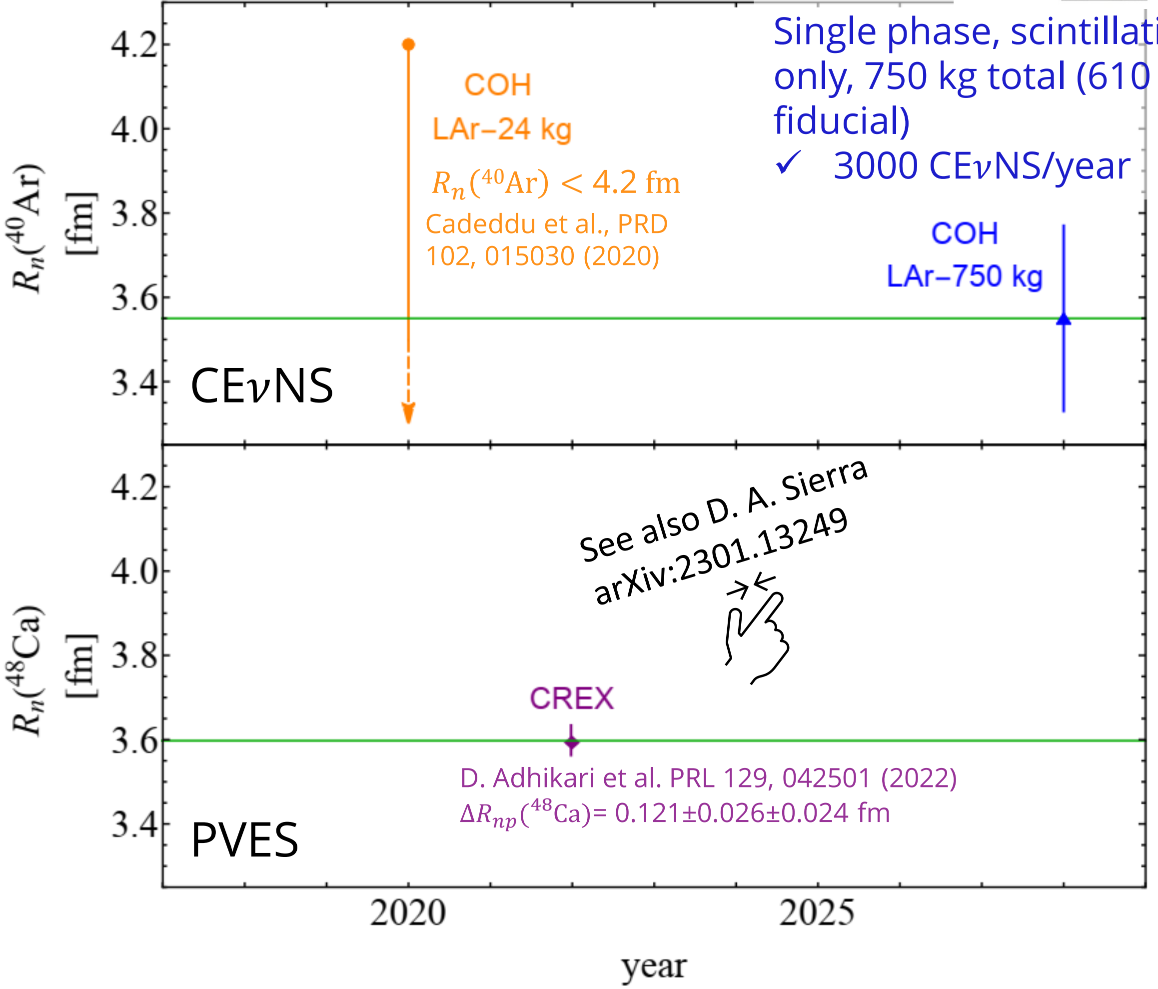

The past, present and future of $\sin^2\vartheta_W$ with CEνNS and APV

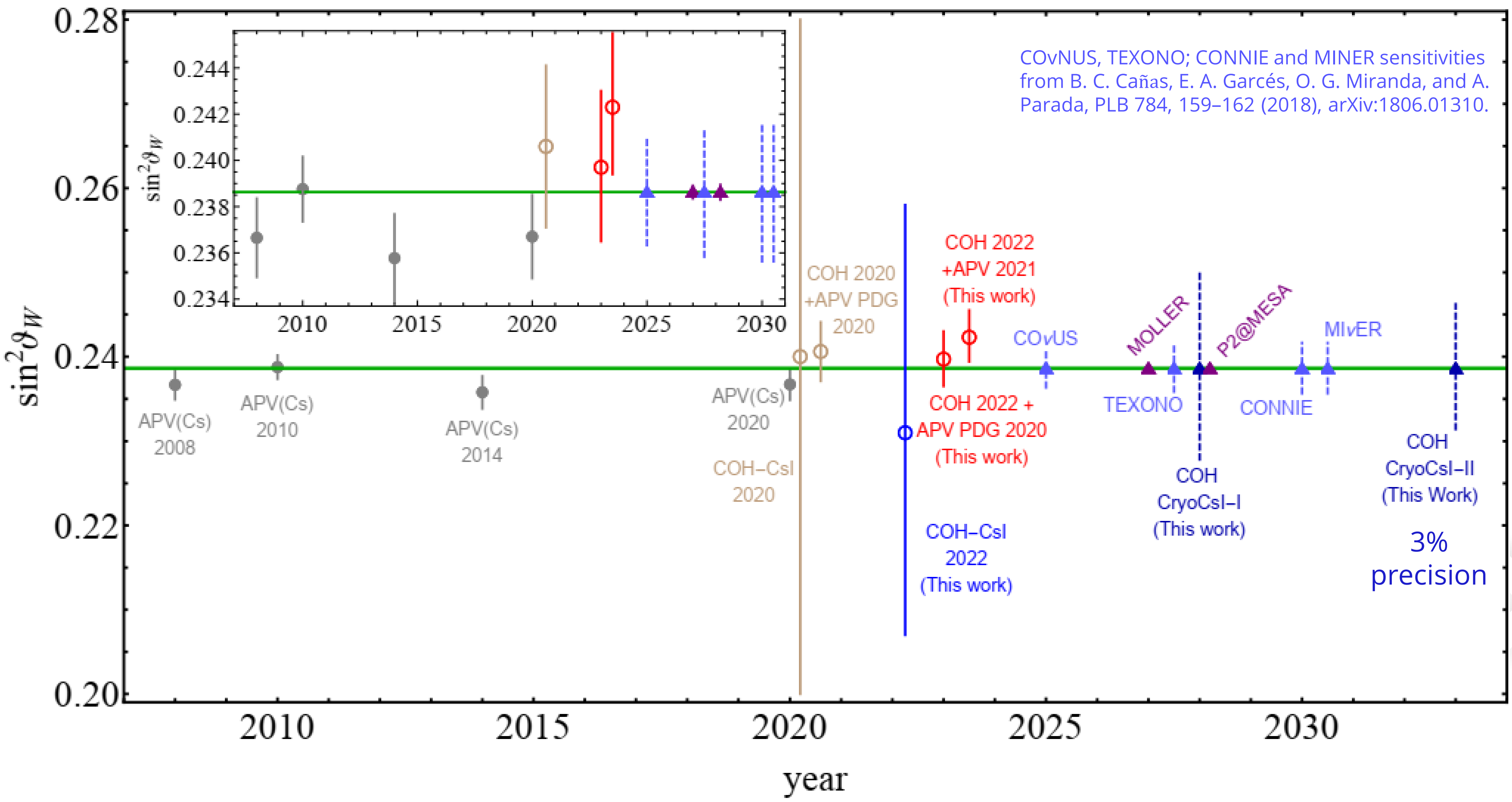

$R_n(\mathrm{Cs})=5.3^{+1.3}_{-1.2}$ fm $R_n(\mathrm{I})=5.6^{+1.6}_{-1.2}$ fm $\chi^2{}_{\min}= 85.2$

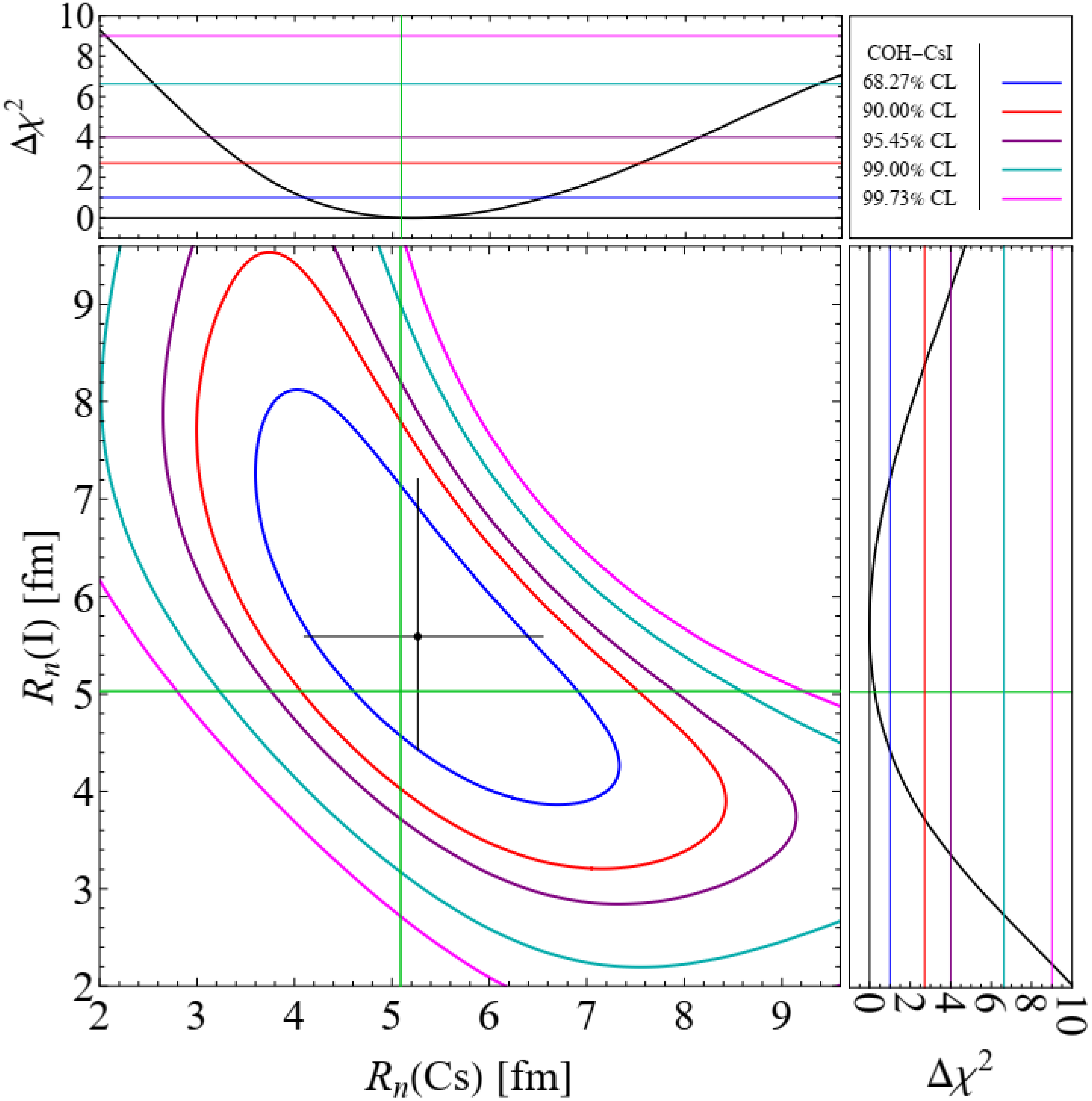

Leptophilic models

In the $\boldsymbol{L_\alpha - L_\beta}$ (where α and β are two leptons flavors) models there is **no direct coupling** between a $L_\alpha - L_\beta$ gauge boson and quarks

$$\left(\frac{d\sigma}{dT_{\rm nr}}\right)^{\nu_\ell-\mathcal{N}}_{L_\alpha-L_\beta}(E,T_{\rm nr}) = \frac{G_F^2 M}{\pi}\left(1-\frac{MT_{\rm nr}}{2E^2}\right) \times \left\{\left[g_V^p\left(\nu_\ell\right) + \frac{\sqrt{2}\alpha_{\rm EM}g_{Z'}^2\left(\delta_{\ell\alpha}\varepsilon_{\beta\alpha}(|\vec{q}|)+\delta_{\ell\beta}\varepsilon_{\alpha\beta}(|\vec{q}|)\right)}{\pi G_F\left(|\vec{q}|^2+M_{Z'}^2\right)}\right] Z F_Z(|\vec{q}|^2) + g_V^n N F_N(|\vec{q}|^2)\right\}^2$$

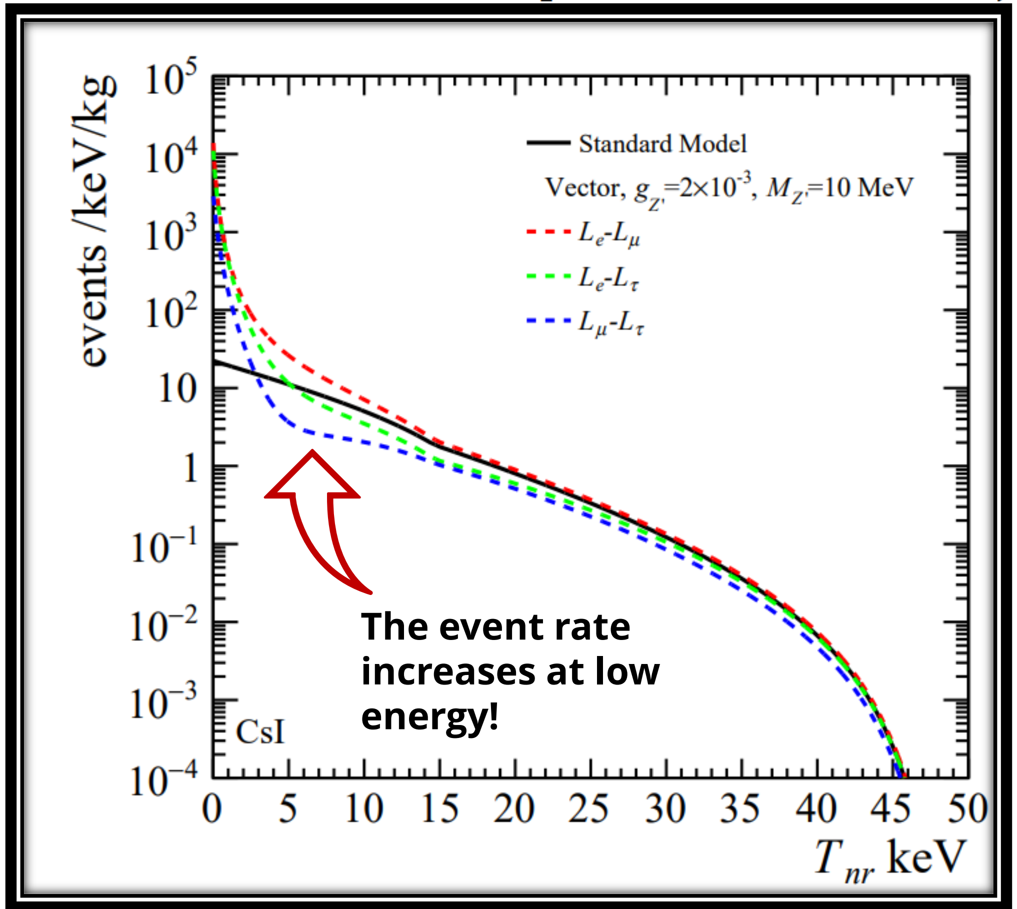

The coupling between neutrinos and quark is due to 1-loop effects

Phys. Rev. D 104, 015015

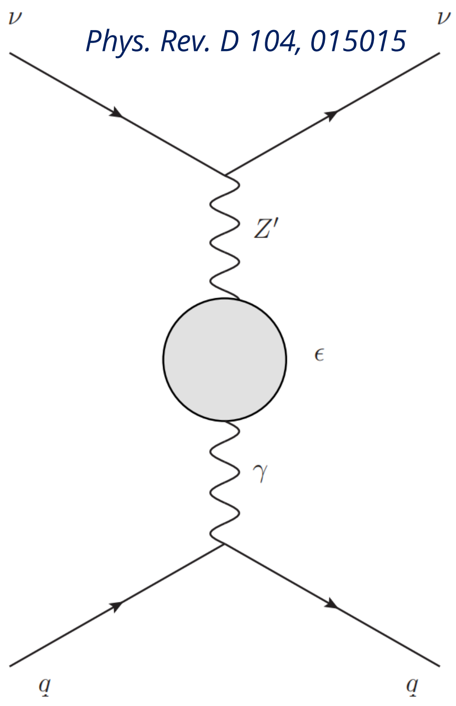

The scalar mediator case

+ The interaction can be mediated by a scalar field ϕ
+ We assume a scalar boson with $g_\phi^d = g_\phi^u \doteq g_\phi^q$ and $g_\phi^{\nu_e} = g_\phi^{\nu_\mu} \doteq g_\phi^{\nu_\ell}$
+ The contribution of the scalar boson to CEνNS is incoherent

JHEP 05 (2018) 066

$$\frac{d\sigma_{\nu_\ell\text{-}\mathcal{N}}}{dT_{\rm nr}} = \left(\frac{d\sigma_{\nu_\ell\text{-}\mathcal{N}}}{dT_{\rm nr}}\right)_{\rm SM} + \left(\frac{d\sigma_{\nu_\ell\text{-}\mathcal{N}}}{dT_{\rm nr}}\right)_{\rm scalar}$$

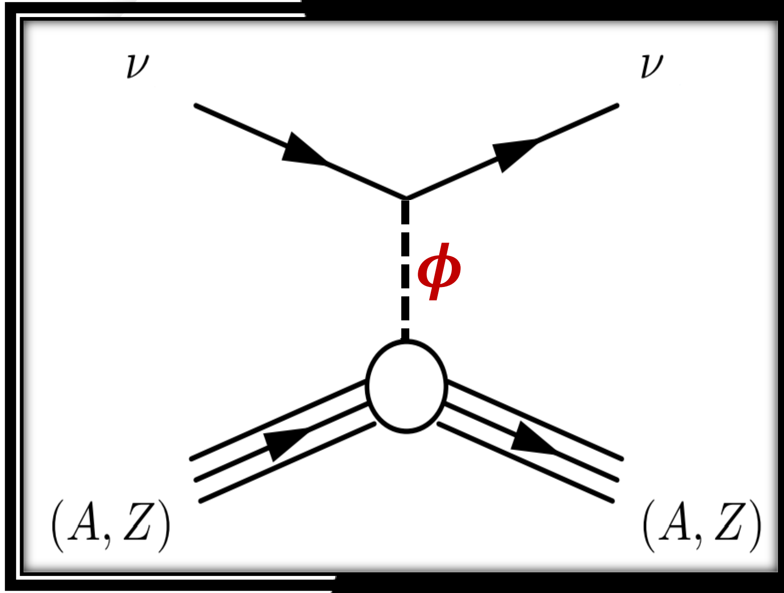

$$\left(\frac{d\sigma_{\nu_\ell\text{-}\mathcal{N}}}{dT_{\rm nr}}\right)_{\rm scalar} = \frac{M^2 T_{\rm nr}}{4\pi E^2} \frac{\boxed{\tilde{g}_\phi^4}}{(|\vec{q}|^2 + \boxed{M_\phi^2})^2} \boxed{\left(\frac{\sigma_{\pi N}}{m_{ud}}\right)_{\rm ref}^2} \left[Z F_Z(|\vec{q}|^2) + N F_N(|\vec{q}|^2)\right]^2$$

Reference value of $\sim$ 17,3 *Phys. Rev. Lett. 115, 092301* *Particle Data Group, PTEP 2022, 083C01 (2022)*

Radiative corrections

$F_N\left(|\vec{q}|^2\right)$. Thus, in this paper, we calculated the couplings taking into account the radiative corrections in the $\overline{\mathrm{MS}}$ scheme following Refs. [51, 62]

$$
\begin{aligned}
g_V^{\nu_\ell\, p} &= \rho\left(\frac{1}{2} - 2\sin^2\vartheta_{\mathrm{W}}\right) + 2\text{⧖}_{WW} + \Box_{WW} - 2\varnothing_{\nu_\ell W} + \rho(2\boxtimes^{uL}_{ZZ} + \boxtimes^{dL}_{ZZ} - 2\boxtimes^{uR}_{ZZ} - \boxtimes^{dR}_{ZZ}), \\
g_V^{\nu_\ell\, n} &= -\frac{\rho}{2} + 2\Box_{WW} + \text{⧖}_{WW} + \rho(2\boxtimes^{dL}_{ZZ} + \boxtimes^{uL}_{ZZ} - 2\boxtimes^{dR}_{ZZ} - \boxtimes^{uR}_{ZZ}).
\end{aligned}
\tag{2}
$$

The quantities in Eq. (2), $\Box_{WW}, \text{⧖}_{WW}$ and $\boxtimes^{fX}_{ZZ}$, with $f \in \{u, d\}$ and $X \in \{L, R\}$, are the radiative corrections associated with the WW box diagram, the WW crossed-box and the ZZ box respectively, while $\rho = 1.00063$ is a parameter of electroweak interactions. Moreover, $\varnothing_{\nu_\ell W}$ describes the neutrino charge radius contribution and introduces a dependence on the neutrino flavour ℓ (see Ref. [62] or the appendix B of Ref. [63] for further information on such quantities). Numerically, the values of these couplings correspond to $g_V^p(\nu_e) = 0.0382$, $g_V^p(\nu_\mu) = 0.0300$, and $g_V^n = -0.5117$.

M. Atzori Corona et al., EPJC 83 (2023) 7, 683, arXiv:2303:09360

COHERENT CsI χ^2

+ Poissonian least-square function:

+ Since in some energy-time bins the number of events is zero, we used the Poissonian least-squares function

$$\chi^2_{\mathrm{CsI}} = 2\sum_{i=1}^{9}\sum_{j=1}^{11}\left[\sum_{z=1}^{4}(1+\eta_z)N_{ij}^{z} - N_{ij}^{\mathrm{exp}} + N_{ij}^{\mathrm{exp}}\ln\left(\frac{N_{ij}^{\mathrm{exp}}}{\sum_{z=1}^{4}(1+\eta_z)N_{ij}^{z}}\right)\right] + \sum_{z=1}^{4}\left(\frac{\eta_z}{\sigma_z}\right)^2, \qquad (10)$$

where the indices i, j represent the nuclear-recoil energy and arrival time bin, respectively, while the indices $z = 1, 2, 3, 4$ for N_{ij}^{z} stand, respectively, for CEνNS, ($N_{ij}^{1} = N_{ij}^{\mathrm{CE}\nu\mathrm{NS}}$), beam-related neutron ($N_{ij}^{2} = N_{ij}^{\mathrm{BRN}}$), neutrino-induced neutron ($N_{ij}^{3} = N_{ij}^{\mathrm{NIN}}$) and steady-state ($N_{ij}^{4} = N_{ij}^{\mathrm{SS}}$) backgrounds obtained from the anti-coincidence data. In our notation, N_{ij}^{exp} is the experimental event number obtained from coincidence data and $N_{ij}^{\mathrm{CE}\nu\mathrm{NS}}$ is the predicted number of CEνNS events that depends on the physics model under consideration, according to the cross-section in Eq. (1), as well as on the neutrino flux, energy resolution, detector efficiency, number of target atoms and the CsI quenching factor [16]. We take into account the systematic uncertainties with the nuisance parameters η_z and the corresponding uncertainties $\sigma_{\mathrm{CE}\nu\mathrm{NS}} = 0.12$, $\sigma_{\mathrm{BRN}} = 0.25$, $\sigma_{\mathrm{NIN}} = 0.35$ and $\sigma_{\mathrm{SS}} = 0.021$ as explained in Refs. [6, 16].

Neutrino charge radius

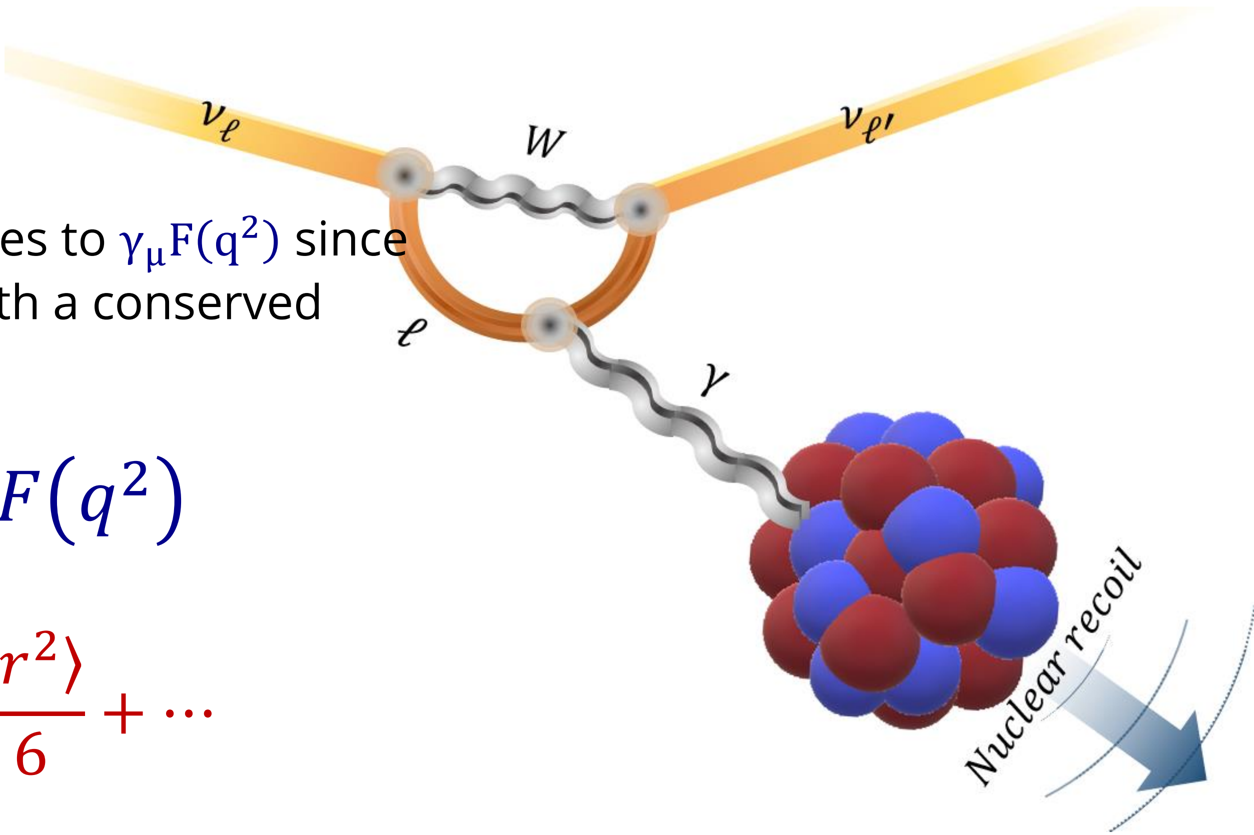

- In the Standard Model (SM) the effective vertex reduces to $\gamma_\mu F(q^2)$ since the contribution $q_\mu \gamma^\mu q_\mu / q^2$ vanishes in the coupling with a conserved current

$$\Lambda_\mu(q) = \left(\gamma_\mu - q_\mu \gamma^\mu q_\mu / q^2\right) F(q^2) \cong \gamma_\mu F\left(q^2\right)$$

$$F(q^2) = \cancel{F(0)} + q^2 \left.\frac{\mathrm{d}F(q^2)}{\mathrm{d}q^2}\right|_{q^2=0} + \cdots = q^2 \frac{\langle r^2 \rangle}{6} + \cdots$$

- In the Standard Model $\langle r^2_{\nu_\ell} \rangle_{SM} = -\frac{G_F}{2\sqrt{2}\pi^2}\left[3 - 2\log\left(\frac{m_\ell^2}{m_W^2}\right)\right]$

$$\langle r^2_{\nu_e} \rangle_{SM} = -8.2 \times 10^{-33}\ cm^2$$
$$\langle r^2_{\nu_\mu} \rangle_{SM} = -4.8 \times 10^{-33}\ cm^2$$
$$\langle r^2_{\nu_\tau} \rangle_{SM} = -3.0 \times 10^{-33}\ cm^2$$

"A charge radius that is gauge-independent, finite is achieved by including additional diagrams in the calculation of $F(q^2)$"

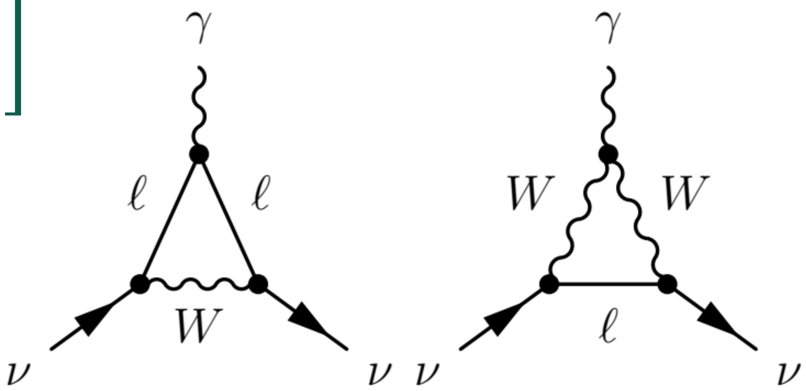

[Bernabeu et al, PRD 62 (2000) 113012, NPB 680 (2004) 450]

Dresden-II weak mixing angle results

M. Atzori Corona et al., JHEP **09**, 164 (2022), arXiv:2205.09484

- + Insensitive to $R_n(\mathrm{Ge})$
- + Insensitive to the antineutrino flux parametrization

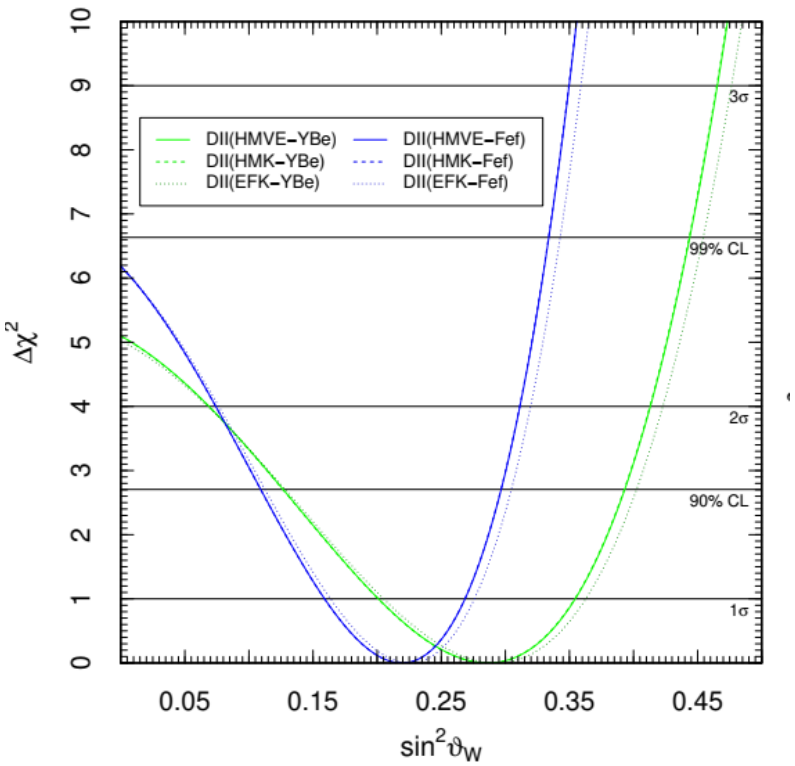

- + Very sensitive to the Ge quenching factor parametrization

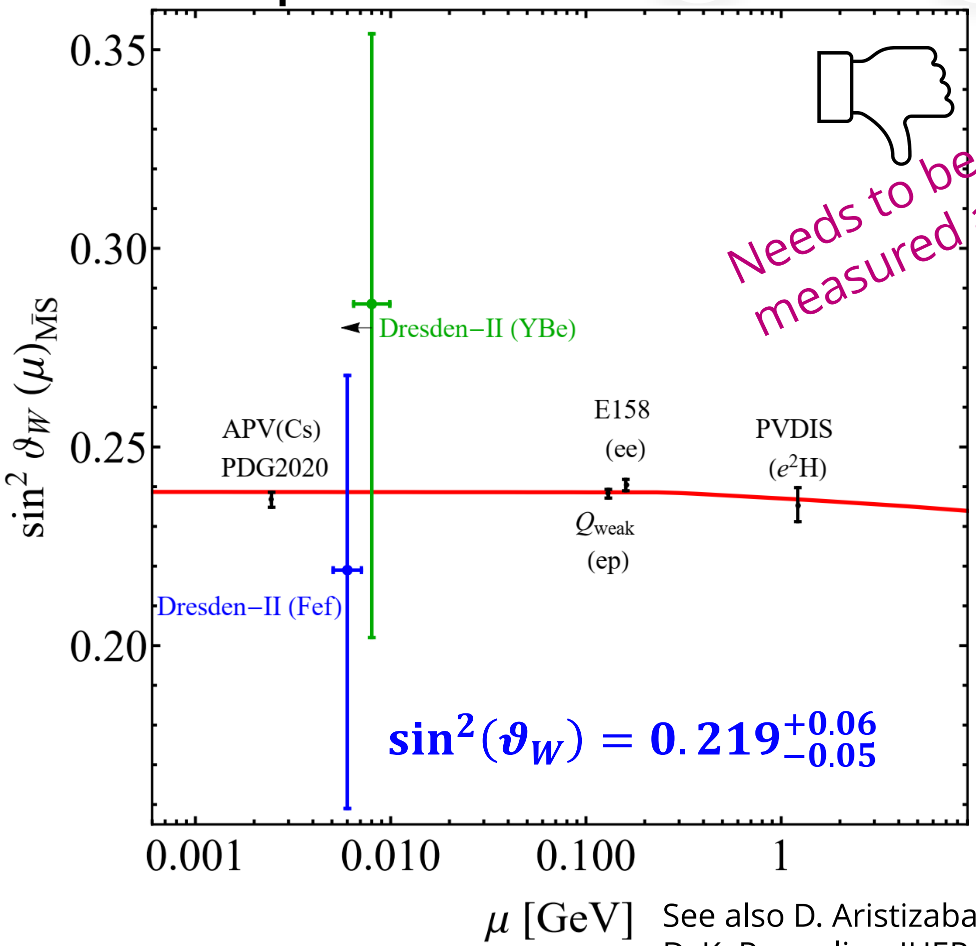

Needs to be accurately measured at low energies

See also D. Aristizabal Sierra, V. De Romeri, and D. K. Papoulias, JHEP **09**, 076 (2022)

THE NUCLEAR FORM FACTOR

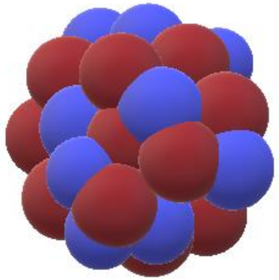

- The nuclear form factor, F(q), is taken to be the **Fourier transform** of a spherically symmetric ground state **mass distribution (both proton and neutrons)** normalized so that **F(0) = 1**:

Helm R. Phys. Rev. **104**, 1466 (1956)

For a weak interaction like for CEvNS you deal with the **weak form factor**: the Fourier transform of the weak charge distribution (neutron + proton distribution weighted by the weak mixing angle)

$$\frac{d\sigma}{dE_r} \cong \frac{G_F^2\, m_N}{4\pi}\left(1-\frac{m_N E_r}{2E_\nu^2}\right) Q_w^2 \times |F_{weak}(E_r)|^2$$

Weak charge × weak form factor

$$\left[g_V^p Z F_Z(E_r, R_p) + g_V^n N F_N(E_r, R_n)\right]^2$$

Proton + Neutron from factor

Extensively studied
Huge bibliography

Poorly known…

It is convenient to have an analytic expression like the **Helm form factor**

$$\boxed{F_N^{\text{Helm}}(q^2) = 3\,\frac{j_1(qR_0)}{qR_0}\, e^{-q^2 s^2/2}}$$

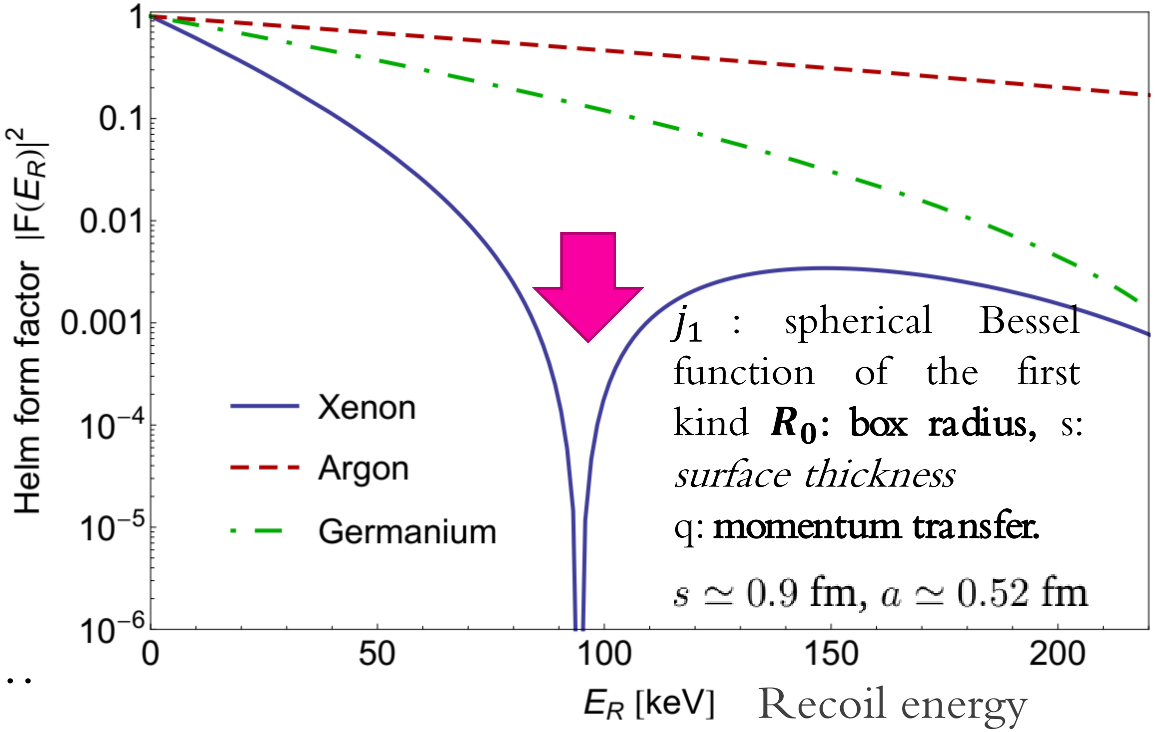

j_1 : spherical Bessel function of the first kind $\boldsymbol{R_0}$**: box radius,** s: *surface thickness*

q: **momentum transfer.**

$s \simeq 0.9$ fm, $a \simeq 0.52$ fm

Recoil energy

FITTING THE COHERENT CsI DATA FOR THE NEUTRON RADIUS

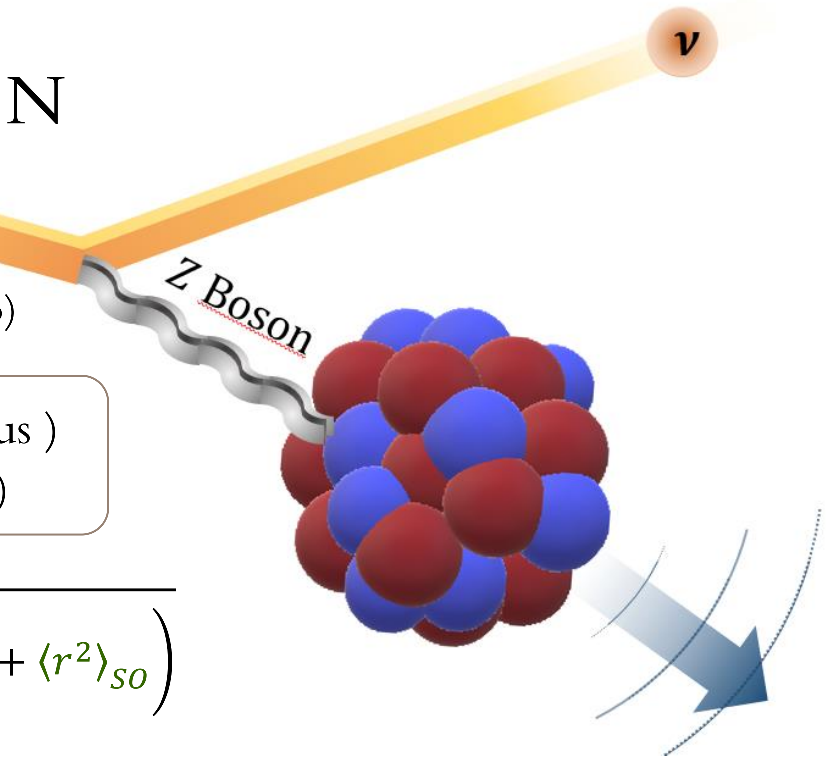

G. Fricke et al., Atom. Data Nucl. Data Tabl. **60**, 177 (1995)

✓ From muonic X-rays data we have
(For fixed $t = 2.3$ fm)

$R_{ch}^{Cs} = 4.804$ fm (Cesium charge rms radius)
$R_{ch}^{I} = 4.749$ fm (Iodine charge rms radius)

$$R_p^{\mathrm{rms}} = \sqrt{R_{\mathrm{ch}}^2 - \left(\frac{N}{Z}\langle r_{\mathrm{n}}^2\rangle + \frac{3}{4M^2} + \langle r^2\rangle_{SO}\right)}$$

$$\underbrace{\begin{array}{l} R_p^{Cs} = 4.821 \pm 0.005 \text{ fm (Cesium rms proton radius)} \\ R_p^{I} = 4.766 \pm 0.008 \text{ fm (Iodine rms-proton radius)} \end{array}}$$

$$\frac{d\sigma}{dE_r} \cong \frac{G_F^2\, m_N}{4\pi}\left(1 - \frac{m_N E_r}{2E_\nu^2}\right)\left[g_V^p Z F_Z\left(E_r, R_p^{Cs/I}\right) + g_V^n N F_N\left(E_r, R_n^{CsI}\right)\right]^2$$

R_n^{Cs} & R_n^{I} very well known so we fitted COHERENT CsI data looking for R_n^{CsI} …

FROM THE CHARGE TO THE PROTON RADIUS

One need to take into account finite size of both protons and neutrons plus other corrections

$$R_{ch}^2 = R_{\mathrm{point}}^2 + \langle r_{\mathrm{p}}^2 \rangle + \frac{N}{Z}\langle r_{\mathrm{n}}^2 \rangle + \frac{3}{4M^2} + \langle r^2 \rangle_{SO}$$

Charge radius

Point-proton radius

Mean squared charge radius of a single proton

$\langle r_{\mathrm{p}}^2 \rangle = 0.7071\ \mathrm{fm}^2$

Mean squared charge radius of a single neutron

$\langle r_{\mathrm{n}}^2 \rangle = -0.1161\ \mathrm{fm}^2$

Relativistic Darwin-Foldy correction

$\sim 0.033\ \mathrm{fm}^2$

Spin-orbit correction

$\sim 0.09\ \mathrm{fm}^2$ for $^{48}\mathrm{Ca}$

$\sim 0.028\ \mathrm{fm}^2$ for $^{208}\mathrm{Pb}$

G. Hagen et al. *Nature Physics* **12**, 186–190 (2016), Arxiv: 1509.07169

M. Cadeddu et al. PRD 102, 015030 (2020), Arxiv: 2005.01645

$$R_p^{\mathrm{rms}} = \sqrt{R_{\mathrm{point}}^2 + \langle r_{\mathrm{p}}^2 \rangle} =$$

$$= \sqrt{R_{ch}^2 - \left(\frac{N}{Z}\langle r_{\mathrm{n}}^2 \rangle + \frac{3}{4M^2} + \langle r^2 \rangle_{SO}\right)}$$

RMS proton distribution radius

COHERENT+APV compared to PREX

$\Delta R_{np}(^{133}\mathrm{Cs}) = 0.45^{+0.33}_{-0.33}$ fm

@fixed $\sin^2\hat{\theta}_W$

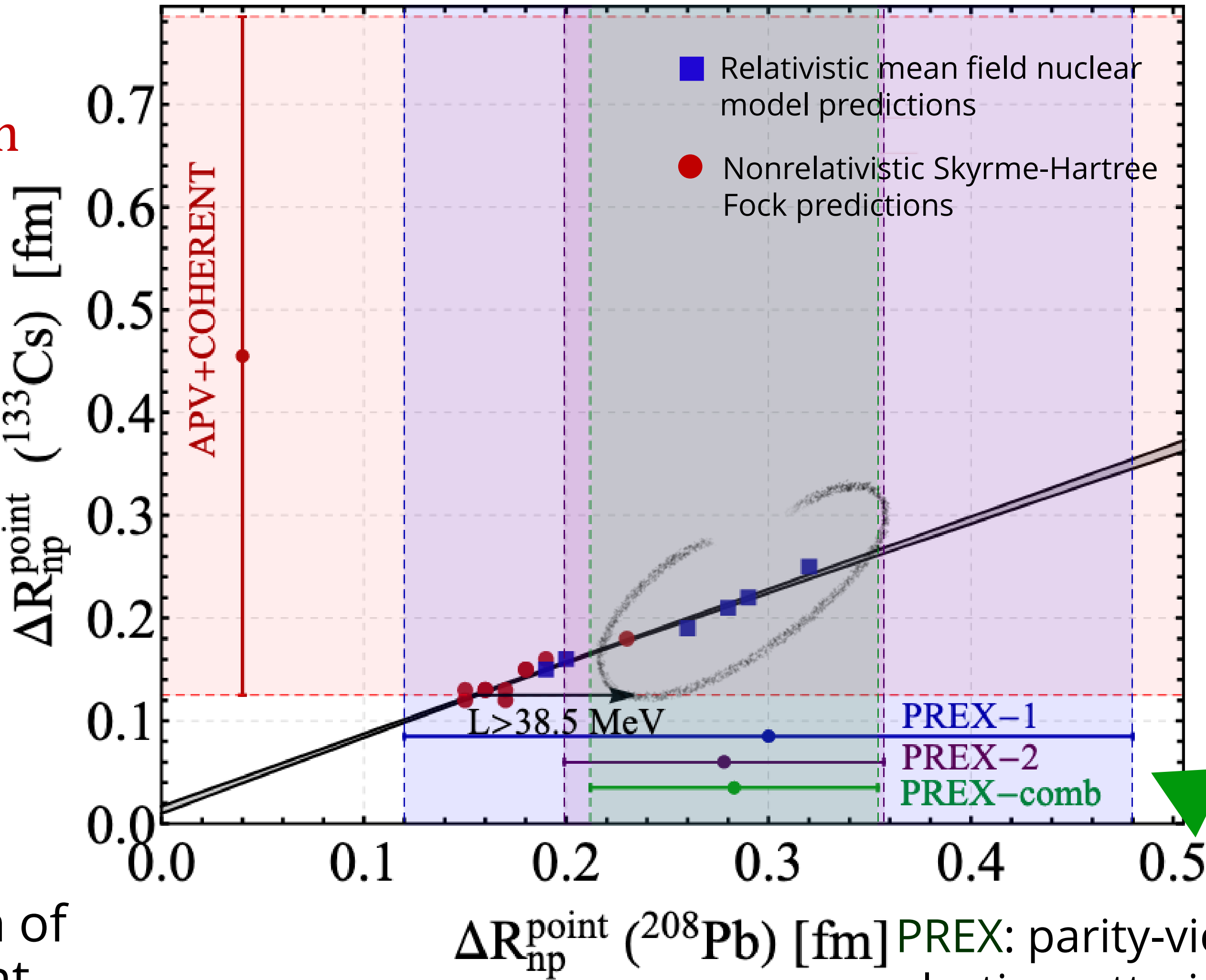

Cadeddu et al., PRC 104, 065502
arXiv:2102.06153

@fixed $\sin^2\hat{\theta}_W$

+ Strong linear correlation between the neutron skin of Cs and Pb among different nuclear model predictions

PREX: parity-violating asymmetry in the elastic scattering of longitudinally polarized electrons on ^{208}Pb

PREX, PRL 126, 172502 (2021)

$$A_{\mathrm{PV}} = \frac{\sigma_R - \sigma_L}{\sigma_R + \sigma_L} \approx \frac{G_F Q^2 |Q_W|}{4\sqrt{2}\pi\alpha Z} \frac{F_{\mathrm{W}}(Q^2)}{F_{\mathrm{ch}}(Q^2)}$$

The proton form factor

$$\frac{d\sigma_{\nu-CsI}}{dT} = \frac{G_F^2 M}{4\pi}\left(1 - \frac{MT}{2E_\nu^2}\right)\left[N\, F_N(T, R_n) - \varepsilon Z\, F_Z(T, R_p)\right]^2$$

The proton structures of $^{133}_{55}Cs$ $(N = 78)$ and $^{127}_{53}I$ $(N = 74)$ have been studied with muonic spectroscopy and the data were fitted with **two-parameter Fermi density distributions** of the form

$$\rho_F(r) = \frac{\rho_0}{1 + e^{(r-c)/a}}$$

Where, the **half-density radius c** is related to the **rms radius** and the a parameter quantifies the **surface thickness** $t = 4\,a\,\ln 3$
(in the analysis fixed to 2.30 fm).

- Fitting the data they obtained

$R_{ch}^{Cs} = 4.804$ fm (Caesium proton rms radius)
$R_{ch}^{I} = 4.749$ fm (Iodine proton rms radius)

[G. Fricke et al., Atom. Data Nucl. Data Tabl. **60**, 177 (1995)]

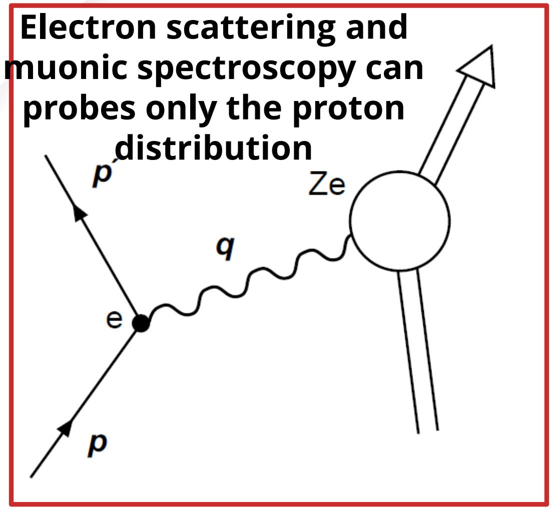

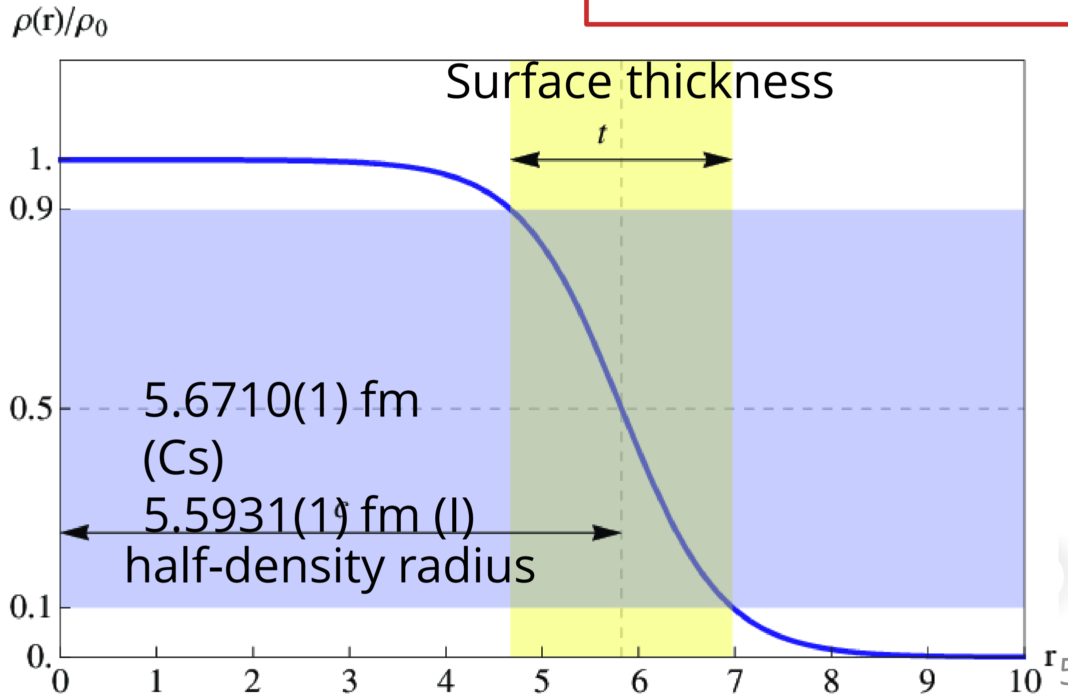

Weak mixing angle (WMA)

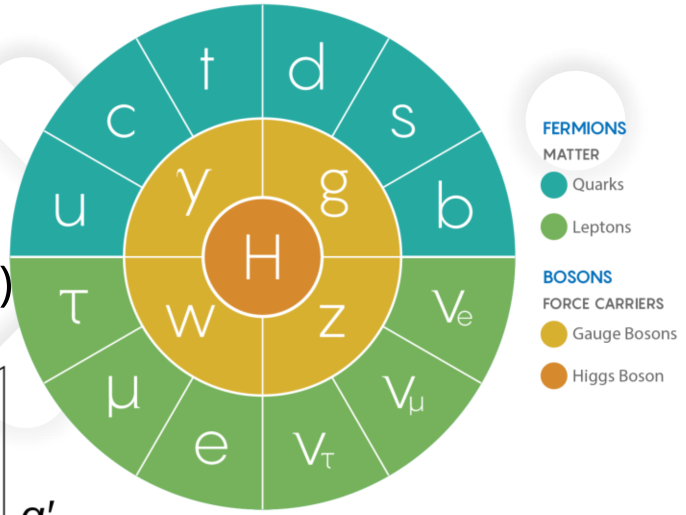

+ The Weinberg angle, θ_W is a fundamental parameter of the **electroweak** (EW) theory of the Standard Model (SM), usually expressed as $\sin^2\theta_W$
+ WMA determines the relative strength of the weak neutral current (NC) vs. electromagnetic interaction

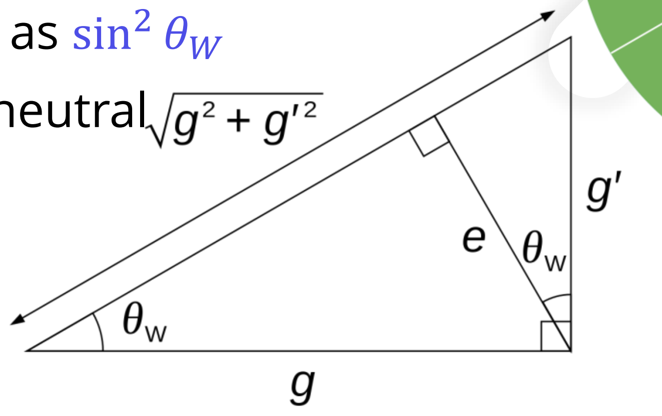

$$e = g\sin\theta_W$$
$$e = g'\cos\theta_W$$

➢ **Tree-level** $\sin^2\theta_W = 1 - \frac{M_W^2}{M_Z^2} = \frac{g'^2}{g^2+g'^2}$

+ The **on-shell scheme** promotes the tree-level formula to a definition of the renormalized $\sin^2\theta_W$ to all orders in perturbation theory (quite sensitive to the top mass)

  ➢ $\sin^2\theta_W \rightarrow s_W^2 \equiv 1 - \frac{M_W^2}{M_Z^2} = 0.22343 \pm 0.00007$ (on−shell)

+ **Minimal subtraction scheme** ($\overline{\text{MS}}$) $\sin^2\hat{\theta}_W(\mu) = \frac{\hat{g}'^2(\mu)}{\hat{g}^2(\mu)+\hat{g}'^2(\mu)}$ where the couplings are defined in the $\overline{\text{MS}}$ and the energy scale μ is conveniently chosen to be M_Z for many EW processes (less sensitive to the top mass)

  ➢ $\sin^2\hat{\theta}_W(M_Z) \equiv \hat{s}_Z^2 = 0.23122 \pm 0.00003$ ($\overline{\text{MS}}$)

Scale dependent→ running of WMA

- The value of $\sin^2\hat{\theta}_W$ varies as a function of the momentum transfer or energy scale («running»).
- Working in the $\overline{\text{MS}}$, the main idea is to relate the case of the WMA to that of the electromagnetic coupling $\hat{\alpha}$
- The vacuum polarization contributions are crucial

Allows precision tests of the Standard Model!

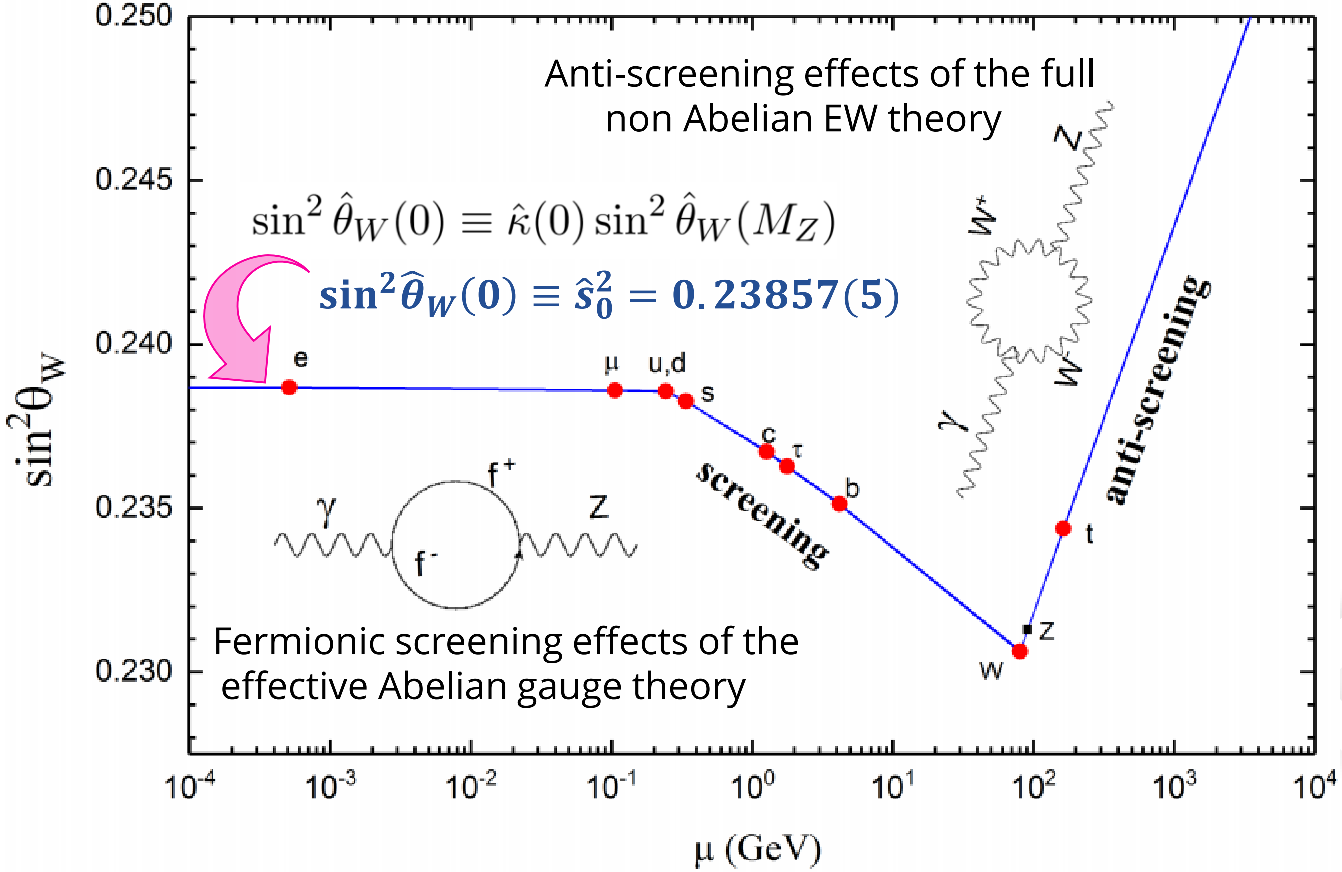

[Erler et al. JHEP 03 (2018) 196, ArXiv:1712.09146]

The «running» function changes sign at $\mu = M_W$ where the fermionic screening effects are overcompensated by the anti-screening effects

Neutrino electromagnetic properties

For ν the electric charge is zero and there are no electromagnetic interactions at tree level. However, such interactions can arise at the quantum level from loop diagrams at higher order of the perturbative expansion of the interaction.

- In the SM the ν charge radius is

$$\langle r^2_{\nu_\ell}\rangle_{SM} = -\frac{G_F}{2\sqrt{2}\pi^2}\left[3 - 2\log\left(\frac{m_\ell^2}{m_W^2}\right)\right]$$

$$\langle r^2_{\nu_e}\rangle_{SM} = -8.2\times 10^{-33}\ \mathrm{cm}^2$$
$$\langle r^2_{\nu_\mu}\rangle_{SM} = -4.8\times 10^{-33}\ \mathrm{cm}^2$$
$$\langle r^2_{\nu_\tau}\rangle_{SM} = -3.0\times 10^{-33}\ \mathrm{cm}^2$$

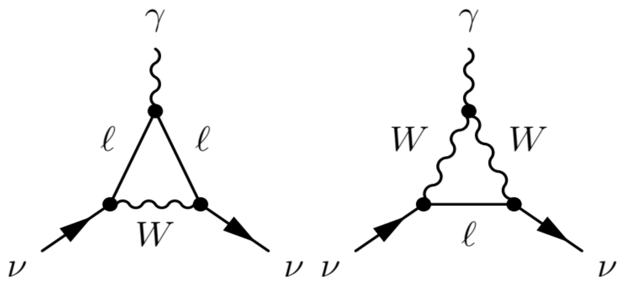

- The charge radius contributes as a correction to the neutrino-proton coupling

- In the minimally extended SM the ν magnetic moment

$$\mu_\nu = \frac{3eG_F}{8\sqrt{2}\pi^2}m_\nu \simeq 3.2\times 10^{-19}\left(\frac{m_\nu}{\mathrm{eV}}\right)\mu_B$$

- In CEνNS $\frac{d\sigma_{\nu_\alpha\text{-}\mathcal{N}}}{dT}(E_\nu, T) = \frac{G_F^2 M}{\pi}\left(1 - \frac{MT}{2E_\nu^2}\right)\left[g_V^n N F_N(|\vec{q}|) + g_V^p Z F_Z(|\vec{q}|)\right]^2$

$$+\frac{\pi\alpha^2}{m_e^2}\left(\frac{1}{T} - \frac{1}{E_\nu}\right) Z^2 F_Z^2(|\vec{q}|)\frac{\mu_{\nu_\alpha}^2}{\mu_B^2}$$

- Neutrino-electron scattering in the SM is negligible

$$\frac{d\sigma^{\mathrm{ES}}_{\nu_\alpha-\mathcal{A}}}{dT_e}(E, T_e) = Z^{\mathcal{A}}_{\mathrm{eff}}(T_e)\frac{G_F^2 m_e}{2\pi}\left[\left(g_V^{\nu_\alpha} + g_A^{\nu_\alpha}\right)^2 + \left(g_V^{\nu_\alpha} - g_A^{\nu_\alpha}\right)^2\left(1 - \frac{T_e}{E}\right)^2 - \left((g_V^{\nu_\alpha})^2 - (g_A^{\nu_\alpha})^2\right)\frac{m_e T_e}{E^2}\right]$$

- Significant neutrino magnetic moment contribution for small T_e:

$$\frac{d\sigma^{\mathrm{ES,\ MM}}_{\nu_\alpha\text{-}\mathcal{A}}}{dT_e}(E, T_e) = Z^{\mathcal{A}}_{\mathrm{eff}}(T_e)\frac{\pi\alpha^2}{m_e^2}\left(\frac{1}{T_e} - \frac{1}{E}\right)\left|\frac{\mu_{\nu_\alpha}}{\mu_B}\right|^2$$

Neutrino charge radius limits

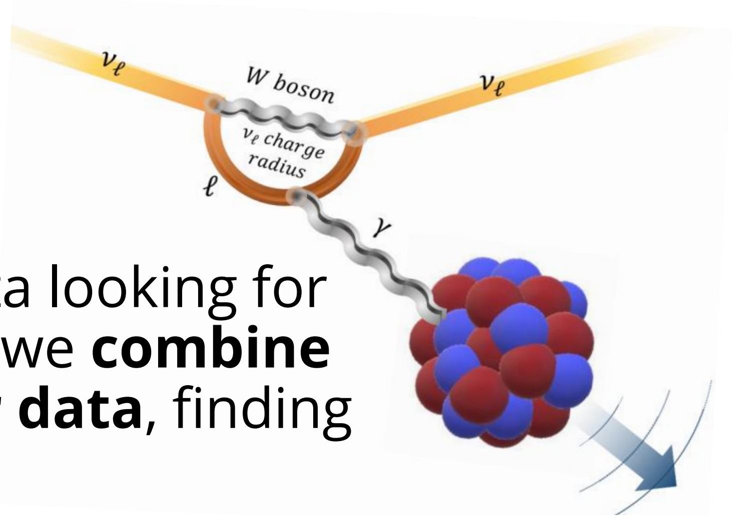

+ We fitted the **Dresden-II** data looking for neutrino EM properties and we **combine with COHERENT CsI and Ar data**, finding very interesting results.

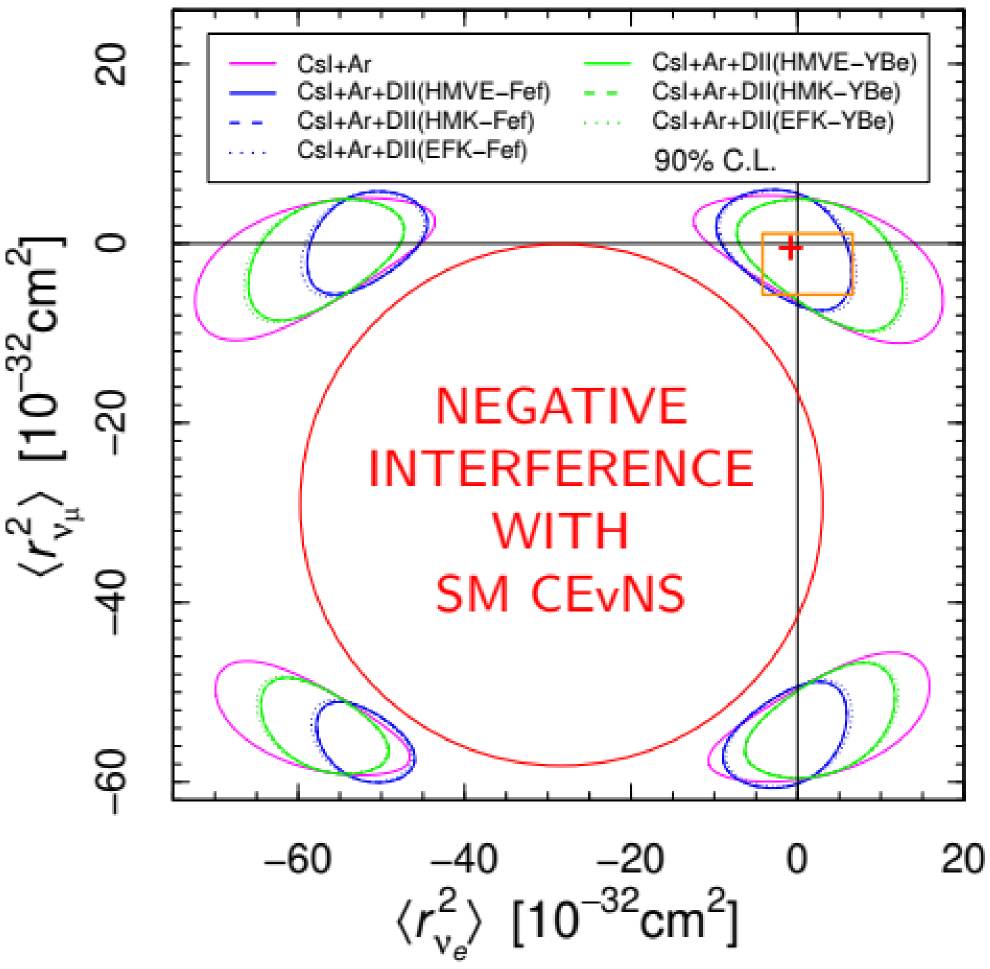

Method	Experiment	Limit [10^{-32} cm^2]	C.L.	Year
Reactor $\bar{\nu}_e\, e^-$	Krasnoyarsk	$\lvert\langle r^2_{\nu_e}\rangle\rvert < 7.3$	90%	1992
	TEXONO	$-4.2 < \langle r^2_{\nu_e}\rangle < 6.6^a$	90%	2009
Accelerator $\nu_e\, e^-$	LAMPF	$-7.12 < \langle r^2_{\nu_e}\rangle < 10.88^a$	90%	1992
	LSND	$-5.94 < \langle r^2_{\nu_e}\rangle < 8.28^a$	90%	2001
Accelerator $\nu_\mu\, e^-$	BNL-E734	$-5.7 < \langle r^2_{\nu_\mu}\rangle < 1.1^{a,b}$	90%	1990
	CHARM-II	$\lvert\langle r^2_{\nu_\mu}\rangle\rvert < 1.2^a$	90%	1994
CEvNS [arXiv:2205.09484]	COHERENT + Dresden-II	$-7.1 < \langle r^2_{\nu_e}\rangle < 11.2$ $-8.1 < \langle r^2_{\nu_\mu}\rangle < 4.3$	90%	2022

a Corrected by a factor of two due to a different convention.
b Corrected in Hirsch, Nardi, Restrepo, hep-ph/0210137.

M. Atzori Corona et al, arXiv:2205.09484

Most stringent upper limit on the electron neutrino charge radius when using the Fef quenching factor for germanium data

Neutrino magnetic moment limits

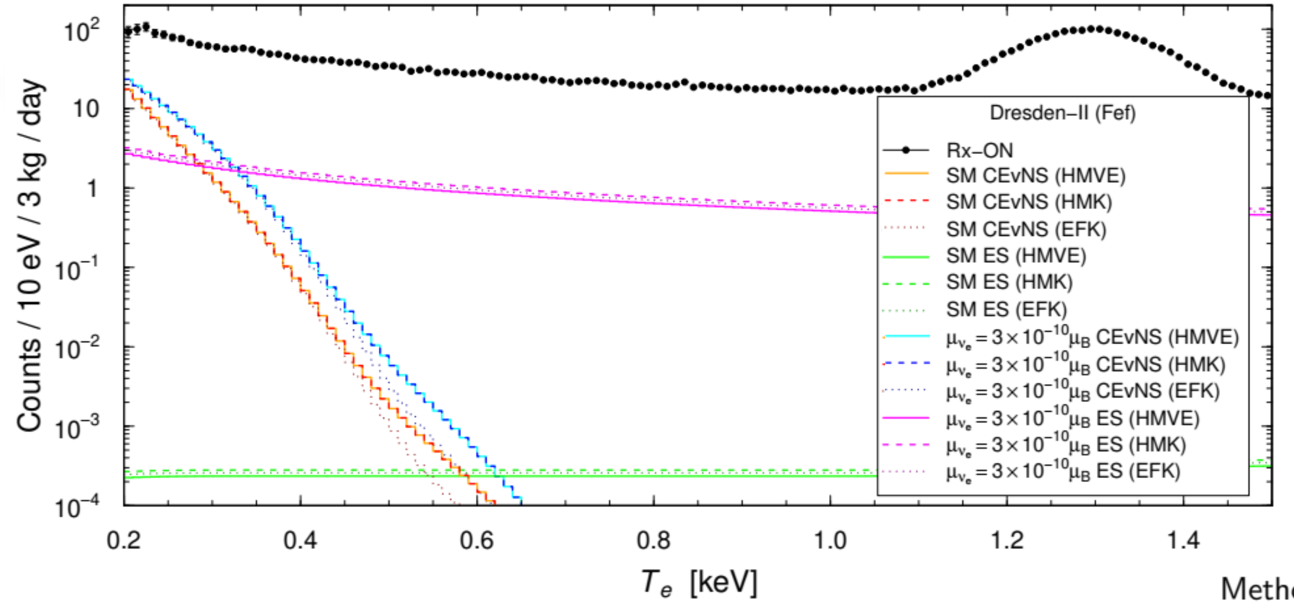

- SM ES are practically negligible
- The ES with magnetic moment are not negligible.
- Moreover ES is sensitive to the low energy antineutrino reactor flux:
  - **HMVE**: Huber-Mueller (2011) + Vogel-Engel (1989) ($E_\nu < 2$ MeV)
  - **HMK**: Huber-Mueller + Kopeikin (2012) ($E_\nu < 2$ MeV)
  - **EFK**: Estienne-Fallot (2019) + Kopeikin (2012) ($E_\nu < 0.44$ MeV)

Limits on ν magnetic moment @ 90% CL

$$|\mu_{\nu_e}| < 2.13 \times 10^{-10}\,\mu_B \quad \text{Dresden}-\text{II}\,(\text{CE}\nu\text{NS}+\text{ES}),$$
$$|\mu_{\nu_\mu}| < 18 \times 10^{-10}\,\mu_B \quad \text{CsI}\,(\text{CE}\nu\text{NS}+\text{ES})+\text{Ar}\,(\text{CE}\nu\text{NS}),$$

Using the Fef quenching factor for germanium data

M. Atzori Corona et al, arXiv:2205.09484

These limits are still less stringent than the bounds obtained in other reactor and accelerator neutrino experiments, but the strategy looks promising.

Method	Experiment	Limit [μ_B]	CL	Year
Reactor ES ($\bar{\nu}_e\, e^-$)	Krasnoyarsk	$|\mu_{\nu_e}| < 2.4 \times 10^{-10}$	90%	1992
	Rovno	$|\mu_{\nu_e}| < 1.9 \times 10^{-10}$	95%	1993
	MUNU	$|\mu_{\nu_e}| < 9 \times 10^{-11}$	90%	2005
	TEXONO	$|\mu_{\nu_e}| < 7.4 \times 10^{-11}$	90%	2006
	GEMMA	$|\mu_{\nu_e}| < 2.9 \times 10^{-11}$	90%	2012
Reactor CEvNS+ES	Dresden-II [Coloma et al, arXiv:2202.10829] [Atzori Corona et al, arXiv:2205.09484]	$|\mu_{\nu_e}| < 3.3 \times 10^{-10}$	90%	2022
Accelerator ES ($\nu_\mu\, e^-$)	BNL-E734	$|\mu_{\nu_\mu}| < 8.5 \times 10^{-10}$	90%	1990
	LAMPF	$|\mu_{\nu_\mu}| < 7.4 \times 10^{-10}$	90%	1992
	LSND	$|\mu_{\nu_\mu}| < 6.8 \times 10^{-10}$	90%	2001
Accelerator CEvNS+ES	COHERENT [Coloma et al, arXiv:2202.10829] [Atzori Corona et al, arXiv:2205.09484]	$|\mu_{\nu_\mu}| < 2 \times 10^{-9}$	90%	2022

New constraint on neutrino magnetic moment from LZ dark matter search results

M. Atzori Corona,[1,2,a] W. Bonivento,[2,b] M. Cadeddu,[2,c] N. Cargioli,[1,2,d] and F. Dordei[2,e]

J. Aalbers et al., First Dark Matter Search Results from the LUX-ZEPLIN (LZ) Experiment (2022), arXiv:2207.03764

- LZ @the Sanford Underground Research Facility in South Dakota.
- Dual-phase TPC filled with about 10 t of LXe, of which 7 (5.5) t of the active (fiducial) region.

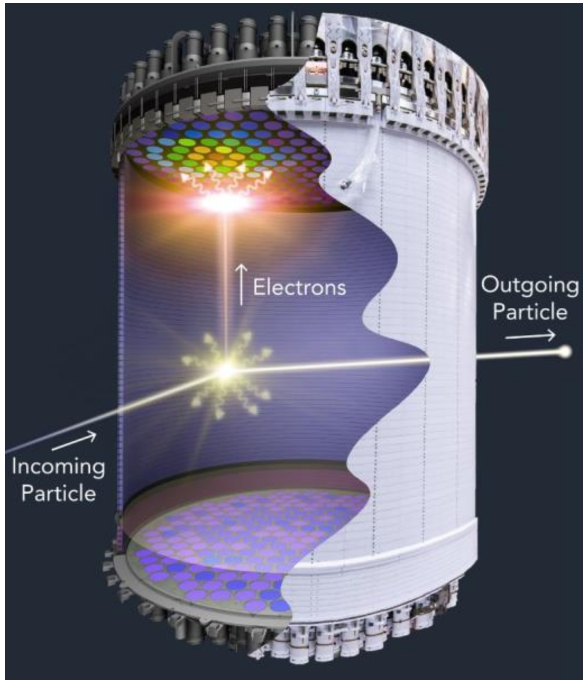

- The new LZ data allows us to set the **most stringent limit on the ν magnetic moment**
- It supersedes the previous best limit set by Borexino by almost a factor of 5
- It rejects by more than 5σ the hint of a possible ν magnetic moment found by the XENON1T Collaboration

M. Atzori Corona et al. arXiv:2207.05036v2 (2022)

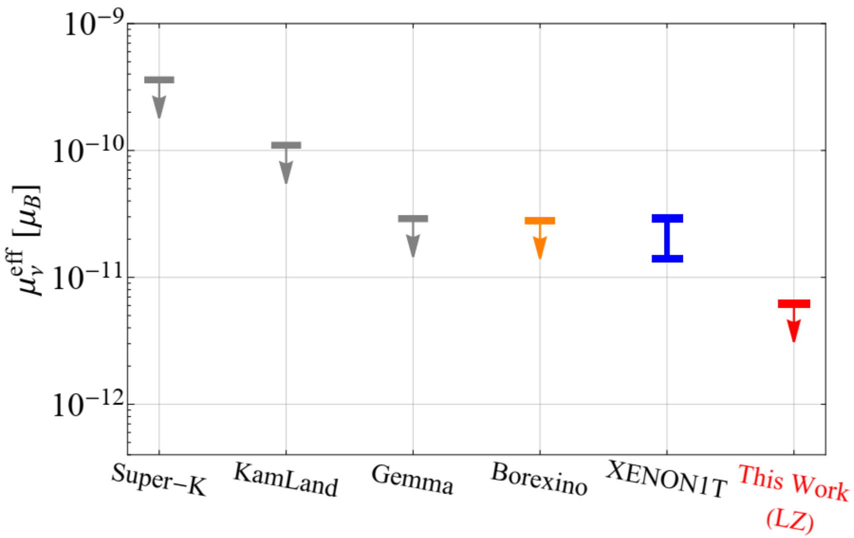

$\mu_\nu^{eff} < 6.2 \times 10^{-12} \mu_B$ @ 90% CL $\quad \chi^2_{min} = 106.2$

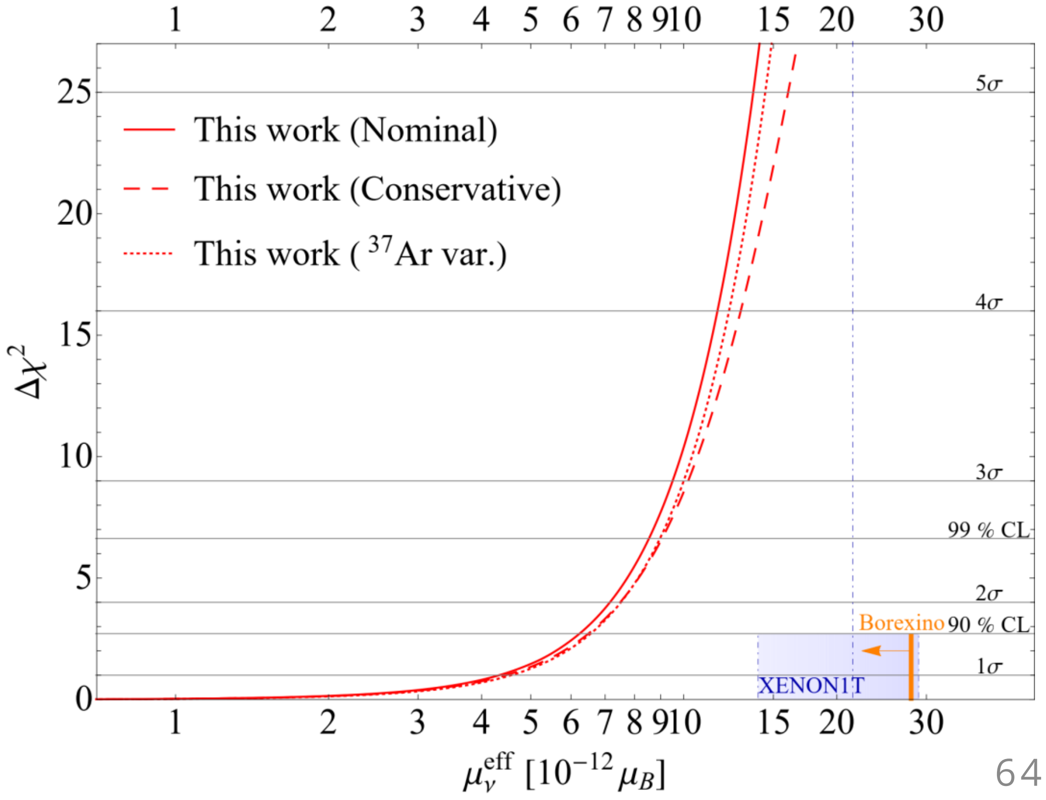

New constraint on neutrino magnetic moment from LZ dark matter search results

M. Atzori Corona,[1,2,a] W. Bonivento,[2,b] M. Cadeddu,[2,c] N. Cargioli,[1,2,d] and F. Dordei[2,e]

[1] *Dipartimento di Fisica, Università degli Studi di Cagliari, Complesso Universitario di Monserrato - S.P. per Sestu Km 0.700, 09042 Monserrato (Cagliari), Italy*
[2] *Istituto Nazionale di Fisica Nucleare (INFN), Sezione di Cagliari, Complesso Universitario di Monserrato - S.P. per Sestu Km 0.700, 09042 Monserrato (Cagliari), Italy*

Elastic neutrino-electron scattering represents a powerful tool to investigate key neutrino properties. In view of the recent results released by the LUX-ZEPLIN Collaboration, we provide a first determination of the limits achievable on the neutrino magnetic moment, whose effect becomes non-negligible in some beyond the Standard Model theories. Interestingly, we are able to show that the new LUX-ZEPLIN data allows us to set the most stringent limit on the neutrino magnetic moment when compared to the other laboratory bounds, namely $\mu_\nu^{\mathrm{eff}} < 6.2 \times 10^{-12}\,\mu_B$ at 90% C.L.. This limit supersedes the previous best one set by the Borexino Collaboration by almost a factor of 5 and it rejects by more than 5σ the hint of a possible neutrino magnetic moment found by the XENON1T Collaboration.

arXiv:2207.05036v2